LARGE REINFORCING BARS SPLICED IN ULTRA-HIGH PERFORMANCE CONCRETE

FLORIDA DEPARTMENT OF TRANSPORTATION
M. H. ANSLEY STRUCTURES RESEARCH CENTER
PRINCIPAL INVESTIGATOR: CHRISTINA FREEMAN, P.E.
REVIEWED BY: WILLIAM POTTER, P.E.
MARCH 2023

Acknowledgements

This project was made possible due to the contributions of many people. Credit for most of the testing documented herein is due to Justin Robertson, who installed instrumentation and administered loading during the reinforcing bar splice tests. Several other members of the FDOT Structures Research Center team were key contributors to the construction and testing of specimens, including Paul Tighe, Miguel Ramirez, Benjamin Allen, Stephen Eudy, and Michael Waters. For their tireless work processing and seeking to understand data from this project, many thanks go to Samuel Adeniji, Ariana Morales Rapallo, and Nathan Schaffer. For secondary report review, thank you to Steven Nolan. Conclusions from this work would have been invalid without careful material testing, and credit for that goes to Richard DeLorenzo, Patrick Carlton, and Nelson Diaz from the FDOT State Materials Office and Eduardo Torres from the University of Florida. For their help with understanding fiber dispersion in the UHPC test specimens, thank you to Daniel Alabi, Megan Voss, Kyle Riding, and Christopher Ferraro from the University of Florida. Finally, for their technical expertise and guidance, thank you to Zachary Haber, Benjamin Graybeal, and Andrew Ross.

Executive Summary

There is potential for construction time savings through replacement of cast-in-place substructure columns and/or piers with prefabricated bridge elements and systems. Typical cast-in-place substructure construction requires forming, placing steel, and pouring concrete at the construction site. Further work cannot progress until the concrete reaches a specified strength. Using prefabricated elements would decrease the extent of work required at the site and potentially reduce required concrete curing time. This research furthers the effort to use ultra-high performance concrete (UHPC) as a joining material for prefabricated bridge substructure elements. UHPC has a high early strength, requires less development or splice length than conventional concrete, and has been used previously for accelerated construction projects such as bridge deck replacement with precast units. UHPC also has a discontinuous pore structure that reduces liquid ingress, significantly enhancing durability compared to conventional concrete.

Although UHPC has been researched extensively, previous research for reinforcing bar splice and development lengths have focused on #9 and smaller diameter bars. Typically, larger diameter bars are used for substructures. This research determined the required splice lengths for large diameter steel deformed reinforcing bars embedded in UHPC based on 127 individual reinforcing bar tests. Two primary variables were included in the testing matrix: bar size and concrete cover. To achieve at least 75-ksi reinforcing bar stress in UHPC with 14-ksi strength, the required embedment length ranges from 8 to 13 times the bar diameter, depending on the bar size and concrete cover. The corresponding splice length varies from 6 to 11 times the bar diameter, again depending on the bar size and concrete cover. This research provides a hypothesis to explain the behavior of spliced bars in UHPC. Additionally, this research observed no apparent difference in spliced bond strength when UHPC was placed at one end of a connection and allowed to flow along the connection or when UHPC was placed randomly at multiple locations along the connection.

In conclusion, this research determined that UHPC is a suitable material for joining prefabricated substructure elements. Specific connections which can benefit from the use of prefabricated elements joined with UHPC are connections for a drilled shaft to bent cap, footing to column, and beam to beam. A connection between a pile and footing is not ideal for the use of UHPC.

Substructure connections would require UHPC cast between two concrete surfaces. For top-formed UHPC, voids and air bubbles commonly form on the top surface of the finished product. Future research work can be done to evaluate the bond between the two materials and determine the extent of slope on the bottom surface of a precast concrete component required to minimize voids. Future work can also be completed to determine constructability requirements for these details, including the minimum UHPC depth between two precast components and the required head pressure for successful casting. It may also be appropriate to conduct full-scale connection testing before implementation of the connection detail. A single readily available propriety UHPC mix with 2% steel fiber by volume was used for this research. Future evaluation on the use of a performance-based specification for projects with UHPC may be required to ensure alternative products have similar performance to the product tested.

Table of Contents

List of Figures

List of Tables

Chapter 1. Introduction

Increasing the use of Prefabricated Bridge Elements & Systems (PBES) is a design innovation goal set by the Florida Department of Transportation (FDOT). The goal is supported by FHWA's Every Day Counts initiative, which encourages accelerated project delivery. FDOT recognizes the potential of PBES to be an economical way to increase quality, reduce costs and construction time, and support safety.

There is potential for construction time savings through replacement of cast-in-place substructure columns and/or piers with PBES. Typical cast-in-place substructure construction requires forming, placing steel, and pouring concrete at the construction site. Further work cannot progress until the concrete reaches a specified strength. Use of precast elements would decrease the extent of work required at the site and potentially reduce required on-site concrete curing time.

This research furthers the effort to use ultra-high performance concrete as a joining material for prefabricated bridge substructure elements. Ultra-high performance concrete has a high early strength, requires less development or splice length than conventional concrete and has been used previously for accelerated construction projects, such as bridge deck replacement with precast units. UHPC also has a discontinuous pore structure that reduces liquid ingress and chloride ion diffusion, significantly enhancing durability compared to conventional concrete (FHWA, 2014). For construction in the marine environment along the coastline of Florida, using UHPC for substructures is more appropriate than for superstructures. Generally, in Florida, substructures have a higher risk of chloride exposure than superstructures. Durability would be enhanced at connections due to the use of UHPC and elsewhere in the substructure due to the use of PBES components, which are cast in a controlled environment.

Connection designs for prefabricated substructure elements have already been developed and used. Two examples are the foundation-to-column, column-to-column and column-to-cap connection for the Edison Bridge in Lee County and the precast bent cap-to-column connection for the US-90 bridges over Little River west of Tallahassee. The Edison Bridge used grouted reinforcing splice couplers for the connections between various substructure elements. Depending on the manufacturer and bar size, grouted reinforcing splice couplers allow a very limited construction tolerance. For instance, a proprietary coupler for a #11 bar allows only 0.3825 in., or 0.23 d_b, of tolerance in any direction, where d_b is defined as the bar diameter. The connection used for the US-90 project consisted of a 4-in. corrugated metal duct with #9 reinforcing bars. For that detail, the typical construction tolerance was reduced to 1.3 d_b in any lateral direction. However, the contractor still experienced fit-up problems for that connection. Potential assembly problems should be carefully avoided for projects with an accelerated schedule. UHPC connections could increase allowable construction tolerances, limiting the potential for problems during construction.

Although UHPC has been researched extensively, previous research for reinforcing bar splice and development lengths have focused on #9 and smaller diameter bars. Typically, larger diameter bars are used for substructures. Some research has been conducted for splice length of #11 bars, but the number of tests is limited, with only nine tests by Lagier et al. (2015), eight tests by McMullen and Haber (2019), and nine tests by Dagenais and Massicotte (2015). The extent of research is not sufficient to clearly define the required reinforcing bar splice length for the large bars typical in substructure construction.

This research addresses single bar splice capacity for a range of variables, including bar size, splice length, concrete cover, and construction tolerances. The bar sizes to be considered are #8, #9, #10 and #11 bars. Splice and development length in UHPC for these large bar sizes have not previously been sufficiently researched. The considered bar sizes are typical for substructure construction and include the maximum size permitted by the FDOT Structures Manual (2021), Volume 2, Table 4.3.11, for footings, pier columns, piers and bent caps. Lap splices are not allowed for bar sizes larger than a #11 bar, per AASHTO LRFD (2014) 5.11.5.2.1, therefore research on lap splices for bar sizes larger than #11 is a low priority. The tested splice length was varied to determine the appropriate splice length for future designs.

A variable not considered in this research was the UHPC mix design. A single readily available propriety UHPC mix with 2% steel fiber by volume was used for this research. Future evaluation on the use of a performance-based specification for projects with UHPC may be required to ensure alternative products have similar performance to the product tested.

Chapter 2. Literature Review

Construction time savings can be achieved through the replacement of cast-in-place substructure columns or piers with prefabricated components. Typical cast-in-place substructure construction requires forming, placing steel, and pouring concrete at the construction site. Work cannot progress until the concrete reaches a specified strength. The use of prefabricated elements decreases the extent of work required at the site and can accelerate construction schedules.

Ultra-high performance concrete (UHPC) has proven to be an excellent material to join prefabricated bridge superstructure elements, such as precast deck panels and approach slabs. UHPC has a high early strength, requires less reinforcing bar development or splice length than conventional concrete and has often been used to accelerate construction projects. UHPC also has a discontinuous pore structure that reduces liquid ingress and chloride ion diffusion, significantly enhancing durability compared to conventional concrete (FHWA, 2014). For construction in the marine environment along the coastline of Florida, where substructures have a higher risk of chloride exposure than superstructures, use of UHPC for substructures has potential for improved durability.

Typically, large diameter bars are used for substructures. For construction in Florida, #11 bars are the largest size reinforcing bar allowed for pier columns, piers and bent caps. Examples provided by FDOT (2021) show #6 and #8 bars for bent cap examples and #10 and #11 main reinforcing bars for pier and pier column examples. UHPC connections for prefabricated components have been researched extensively, but previous research related to reinforcing bar splice and development length has focused on #8 and smaller diameter bars. Some splice length research has been completed for #11 size bars, but the number of tests is limited.

Required Splice Length

This research project focused on splice length testing for bar sizes commonly used for bridge substructures - #8, #9, #10 and #11 bars. Research on splice length for #8 bars and limited work on #11 bars had already been completed by others but was repeated during this study to verify consistent results were achieved. Because information on splice length for large diameter bars was limited, previous research on both small and large diameter bars was reviewed. The findings were used for detailing preliminary UHPC connections and planning a test matrix.

The most extensive work on bond behavior of reinforcing steel in UHPC was completed at FHWA by Yuan and Graybeal (2014), with over 200 direct tension pullout tests. A conventional concrete slab was constructed with protruding bars. The protruding bar was spliced in a layer of UHPC, and the splice bar was tensioned. Various bar types were considered, including ASTM A615 Grade 60 uncoated #5 bars, epoxy coated #5 and #8 bars and ASTM A1035 Grade 120 #4, #5 and #7 bars. Other variables considered in the testing regimen included UHPC compressive strength, embedment length, concrete side cover and bar spacing.

Yuan and Graybeal (2014) recommended connections have a minimum embedment length of $8d_b$ and a minimum side cover of $3d_b$. The splice length was specified as 75 percent of the embedment length for bar sizes between #4 and #8, resulting in a required splice length of $6d_b$. The recommended limits assure the bar reaches the lesser of the bar yield strength or 75 ksi at bond failure, when the UHPC strength reaches 14 ksi compressive strength, which can be achieved one day after the UHPC is cast with some high-early strength mix designs. For reduced concrete cover or high strength reinforcing, splice length requirements increased. For reinforcing bar yield strengths up to 100 ksi, the recommended embedment length was $10d_b$, with a corresponding splice length of $7.5d_b$. The minimum embedment length was also increased by $2d_b$ if a reduced concrete cover of $2d_b$ was used instead of $3d_b$.

McMullen and Haber (2019) documented the results of splice testing for #11 bars completed by FHWA. Grade 120 bars were tested in the configuration described in (Yuan & Graybeal, 2014). For embedment lengths of $6d_b$ and $8d_b$, the peak stress at bond failure varied from approximately 70 to 100 ksi. They determined larger diameter bars developed lower peak stresses than the smaller diameter bars which revealed a "size effect" that may indicate refinements for required splice and embedment lengths are appropriate for #8 and larger bar sizes.

Ronanki et al. (2016) completed sixteen direct tension UHPC lap splice tests and six tests of bar splices in four-point beam bending. Their findings agree with Yuan and Graybeal (2014), except that a different threshold of developed bar stress was used. Ronanki et al. concludes that, to develop a stress of 60 ksi, the minimum embedment length is $8d_b$ with a minimum concrete cover of $3d_b$, the same values as Yuan and Graybeal. The minimum bar stress of 60 ksi is less than the 75 ksi bar stress that Yuan and Graybeal recommend can be achieved with the same embedment length and cover.

Kim et al. (2016) completed 43 reinforcing bar pull-out tests and 18 flexural tests for bar sizes ranging from 9.5 mm (#3) to 22.2 mm (#7). Pull out tests consisted of a single bar cast into a UHPC cube. The assembly was tested in a 100-ton universal testing machine. The flexural test specimens consisted of UHPC beams 2 m (6.6 ft) long. Two sets of reinforcing bar splices were cast in the tension face of the beams. Cover depth and bond length were varied for both the pull-out and flexural tests to determine the correlation between the two variables and evaluate the requirements of the Korea Concrete Institute Design Guidelines for K-UHPC, which required a lap splice length of $5.5d_b$. Kim et al. determined that $2.2d_b$ would be sufficient to ensure load carrying capacity and ductile behavior but did not recommend a lesser value than $5.5d_b$. They acknowledged that the value of $5.5d_b$ required by the Design Guidelines provided a rational and sufficient safety margin. $5.5d_b$ was only slightly less than the $6d_b$ value recommended by Yuan and Graybeal (2014) and Ronanki et al. (2016). Therefore, Kim et al. substantially agreed with the previous two references discussed.

Dagenais and Massicotte (2015) tested a total of eighteen full-scale beam specimens with two deformed bars spliced at mid-span. The splice region consisted of a small closure pour with UHPFRC material, while the remainder of the beam was constructed with conventional concrete. Their work investigated two different bar diameters, 25 mm (#8) and 35 mm (#11), splice lengths ranging from $6d_b$ to $18d_b$, UHPFRC repair depths of zero, $1d_b$ and $2d_b$, and both contact and offset bars. Their work differs from the beam tests documented in Ronanki et al. (2016) and Kim et al. (2016) in that UHPFRC was only used in the splice region and not the entire beam. The scale of the specimen was also larger. Dagenais and Massicotte tested beams which were 5,660 mm (18 ft) long, while Ronanki et al. tested beams which were 40 in. long and Kim et al. tested beams which were 2 m (6.6 ft) long.

The bar sizes tested by Dagenais and Massicotte (2015) were of interest to this research project. Both #8 and #11 bars were tested, which are two of the bar sizes tested in this project. However, the concrete cover used was much less than investigated by this project. A concrete cover of only 30 mm (approximately 1.2 in.) was considered. Although FDOT (2021) does not specifically address required cover for UHPC, typical cover for formed substructure components ranges from 3 to 4.5 in. for conventional concrete. Recommendations from Yuan and Graybeal (2014) would require 3 in. and 4.125 in. for the #8 and #11 bars tested, respectively. Another difference is the material used. The UHPFRC material used by Dagenais and Massicotte (2015) was developed at Ecole Polytechnique of Montreal and contains 3% by volume of steel fibers. In contrast, the material used in this project contains 2% steel fibers. UHPC used for Yuan & Graybeal, Ronanki et al. (2016) and Kim et al. (2016) also contained steel fibers at a rate of 2% by volume.

Dagenais and Massicotte (2015) recommended the same splice lengths as the previously discussed references for #8 bars and a longer splice length for #11 bars, with reduced cover requirements. To reach yielding, a bar lap splice of $6d_b$ was required for the 25 mm (#8) bar, exactly matching Yuan and Graybeal (2014) and Ronanki et al. (2016). A longer splice length of $12d_b$ was required for the 35 mm (#11) bar with 1.2 in. concrete cover. Intervals between $6d_b$ and $12d_b$ were not investigated.

In contrast, Lagier et al. (2015) recommended a much longer splice length than the other references. Specimens consisted of a pair of spliced bars, tested in direct tension. Both 25 mm (#8) and 35 mm (#11) bars were considered, with a constant $1.2d_b$ cover. Three different fiber volumes were considered – 1%, 2% and 4%. All mixes had a constant water to binder ratio, with increased sand content for the lower fiber volume mixes. Higher fiber volume mixes had a lower compressive strength, but a higher tensile strength. Five different lap splices were considered: 5, 8, 10, 12, and 18 times d_b. The test results indicated that a splice length of $14d_b$ was required for 2% fiber volume UHPC, for both bar sizes. A higher fiber volume required a slightly shorter splice length compared to UHPC with a lower fiber volume.

Influence of Concrete Cover and Compressive Strength

Yuan and Graybeal (2014) noted that by increasing embedment length, side cover or UHPC compressive strength, the required splice length was reduced. Tests conducted on #5 ASTM A1035 bars with $3d_b$ side cover and 13.9 ksi UHPC compressive strength had bar stresses exceeding 75 ksi when only $6d_b$ embedment length was provided. For the same test parameters, except with a UHPC compressive strength of 19.6 ksi, bar stress at bond failure was even higher. Ronanki et al. (2016) agreed with Yuan and Graybeal in stating that if one variable is increased, other variables can be decreased with the bar still sufficiently spliced. For example, an embedment length of $10d_b$ was sufficient to achieve a 60 ksi bar stress when the cover was decreased from $3d_b$ to $1.8d_b$.

Kim et al. (2016) determined that the Korea Concrete Institute Design Guidelines for K-UHPC minimum required cover of 20 mm (0.8 in) was insufficient, regardless of the splice length used. They recommended the limit be increased to the maximum value of $1.5d_b$ and 25 mm (1 in.). If the recommendations of Yuan and Graybeal (2014) and Ronanki et al. (2016) are followed, a much higher cover of $3d_b$ is required, a value which results in cover exceeding 1 in. for all common bar sizes.

Lagier et al. (2015) used a concrete cover of $1.2d_b$, which is less than the other references. The typical failure mode during testing was gradual splitting on the face of the specimen, approximately along the bar. Increasing concrete cover would have mitigated splitting failure and, at some point, caused the bar splice to fail via pull-out (ACI, 2003). The relatively high splice length of $14d_b$ recommended by Lagier et al. may not be required if more concrete cover is provided.

Influence of Bar Spacing

Yuan and Graybeal (2014) determined that contact lap splices had lower bond strength than non-contact lap splices, probably due to decreased contact between the bar and UHPC materials. Therefore, they recommended the bar spacing to be at least $2d_b$. Conversely, bond strength was also reduced when the bar spacing was too high, at the point when induced diagonal cracks from the pullout force did not intersect with the adjacent bar. To address that case, Yuan and Graybeal also recommended that the bar spacing did not exceed the splice length.

Along the length of the bar, Dagenais and Massicotte (2015) recommended a minimum of one bar diameter of UHPC between the surface of the bar and the interface between the UHPC repair and conventional concrete. The spacing between lapped bars was determined to have no effect. Testing considered three configurations: lapped bars in contact, $0.5d_b$ between bars and $1d_b$ between bars. Their findings differed from Yuan and Graybeal (2014), who noted higher bond strengths for laps with a bar clear spacing between $2d_b$ and the splice length. Dagenais and Massicotte investigated only bar spacing less than the minimum recommended by Yuan and Graybeal.

Influence of Bar Size

Yuan and Graybeal's (2014) findings should not be applied to bar sizes larger than #8 both because they were not tested and because the results indicated that as the bar diameter increased, the bar stress at bond failure decreased. Higher bond strength was observed for the smaller bar diameters tested, with all other variables held constant. McMullen and Haber (2019) confirmed that larger diameter bars developed lower peak stresses than smaller diameter bars. Therefore, a longer splice length than their recommendation of $6d_b$ was considered.

The findings from Dagenais and Massicotte (2015) confirmed that longer lap lengths, in multiples of the bar diameter, were required for larger size bars. However, the cover was kept constant for each bar size, and was noted as a potential reason that a longer lap splice was required for the larger bar size.

In contrast, Lagier et al. (2015) noted only a negligible effect of bar size on bond strength for the 25 mm (#8) and 35 mm (#11) bars tested. However, that research considered a much lower concrete cover ($1.2d_b$) than the other references and the minimal cover may have controlled the failure mode.

Bond Behavior

ACI (2003) noted that the transfer of forces between concrete and reinforcing bar was essential for reinforced concrete construction, and previous research proved that the transfer of forces from the reinforcing bar to the surrounding concrete was achieved through chemical adhesion, frictional forces and/or bearing of the ribs against the concrete. After initial slip, most of the force is transferred by bearing forces, which act perpendicular to the bar deformations. The component of bearing force longitudinal to the bar resists the longitudinal forces and movement of the bar and is characterized as bond stress, as shown in Figure 1(a). The component of bearing force transverse to the bar generates tensile hoop stresses, as shown in Figure 1(b).

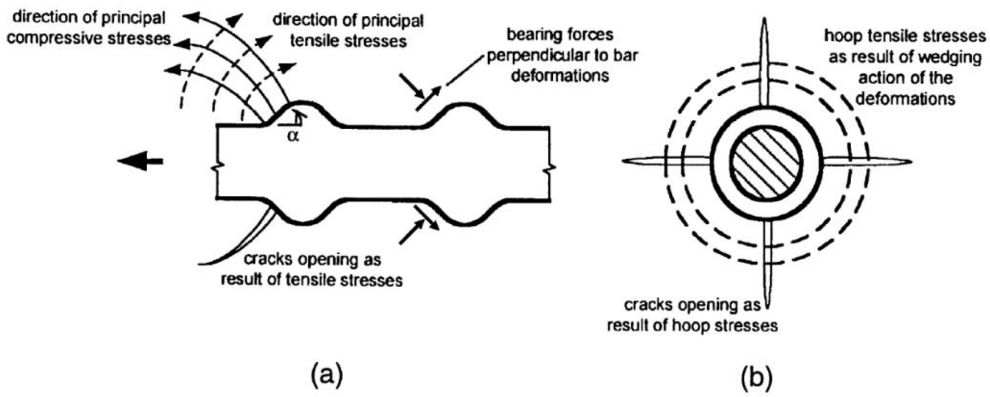

Figure 1: Cracking and damage mechanisms in bond, with (a) side view of a deformed bar with deformation face angle a showing formation of Goto (1971) cracks; (b) end view showing formation of splitting cracks parallel to the bar per ACI 408R-03 **(ACI, 2003)**

In normal strength concrete reinforced with deformed bars, the bond stress along a stressed reinforcing bar has been proven to be uniform along the length of the bar. Evidence of crushed concrete at each lug of the reinforcing bar at the conclusion of testing proved that behavioral assumption and was documented in Azizinamini et al. (1993). However, in high strength concrete, Azizinamini et al. determined that the bond stress was not uniform, specifically for high strength concretes with compressive strengths ranging from 10.9 ksi to 15.12 ksi. Azizinamini et al. presented a failure hypothesis explaining the observed behavior. The higher bearing capacity of the high strength concrete prevented crushing in the vicinity of the reinforcing bar and thus may have prevented all lugs from participating in resisting axial forces. The first few lugs contributed most to bond capacity and a splitting failure due to hoop tensile stresses may have occurred before the bond stress was uniform along the development length. When comparing normal and high strength concretes, splitting failure mode was more likely in high strength concrete because, as compressive strength increases, bearing strength increases at a faster rate than tensile strength. Azizinamini et al. (1999) advocated that placing minimum transverse reinforcement over the splice region was an efficient solution for improving bond in high strength concretes. ACI (2003) recognized that fibers such as are present in UHPC act as transverse reinforcement and should improve resistance to splitting cracks and mitigate the splitting mode of failure. The use of fibers together with transverse reinforcement was not recommended by Marchand et al. (2019), who noted that shear reinforcement can have negative effects on fiber orientation, which can result in cracking. Structural fibers in UHPC and the tensile properties of the composite material were found to be essential to the bond between it and deformed reinforcing bars, as noted by many researchers (FHWA, 2014; Dagenais & Massicotte, 2015; Lagier et al., 2015; Haber & Graybeal, 2018; Dagenais et al., 2018; Ronanki et al., 2018).

Lagier et al. (2012) compared UHPCs with three different fiber volume percentages: 1%, 2% and 4%, and found a consistent increase in the average bond stress reached at failure as the volume of fiber was increased in the mixes, due to the beneficial effects of both the high tensile strength of UHPC and its ability to offer ductile softening during macro-crack propagation. Haber et al. (2018) also investigated UHPCs with fiber volume percentages which varied from 1% to 4.5% in 0.5% increments. They observed that increasing fiber content tended to increase the peak reinforcing bar stress prior to bond failure and post-peak energy-dissipation capacity, while the initial slope of the stress-slip curve and the slope of the post peak curve were unaffected by the varied fiber content.

Lagier et al. (2015) and Dagenais and Massicotte (2015) examined the relationship between bar or bond stress and transverse strain in the test specimens they examined. Both proved that ductile behavior can be achieved with reinforcing bars spliced in UHPC. Lagier et al. characterized the overall transverse strain evolution in two stages, where the first stage corresponded to the elastic strain limit reached with direct tension tests on UHPC and the second stage consisted of large inelastic strains in UHPC until the maximum steel stress which could be achieved based on the test parameters was reached. In general, the behavior was found to be similar to what was observed in UHPC direct tension tests and indicated that the UHPC tensile properties counterbalanced the hoop stresses generated by the deformed reinforcing bar ribs.

The average bond stress along the splice length was defined by Azizinamini et al. (1993) and ACI (2003) as Equation 1, where f_s is the stress in the reinforcing bar, d_b is the diameter of the reinforcing bar and l_s is the splice length. Yuan and Graybeal (2014) presented the same definition for bond stress, except that embedment length, l_e, was substituted for splice length, l_s (Equation 2). Bond strength was defined as the maximum value of the bond stress recorded during a single test (Rolland et al., 2018), (FHWA, 2014).

Equation 1: Bond Stress using splice length

$$u = \frac{f_s \times d_b}{4 \times l_s}$$

Equation 2: Bond Stress using development length

$$\tau = \frac{f_s \times d_b}{4 \times l_e}$$

Assuming a uniform bond stress along the splice length, Dagenais and Massicotte (2015) and Dagenais et al. (2018) described a simple model for the bonding mechanism between deformed reinforcing bars and UHPC, as shown in Figure 2 and described by Equation 3, where α accounts for the bursting force magnification in the case of two bars contributing to the splitting force (with a suggested value of 0.53), d_b is the bar diameter, τ is the average bond stress tangential component, β is the angle of bond stress resultant with respect to the bar axis ($\tan\beta$ having a suggested value of 1.6), and b_e is the effective resisting width.

The bond model described by Dagenais and Massicotte (2015) and Dagenais et al. (2018) was based on the assumption that bond stress was uniform along the splice length of the reinforcing bar. Several studies have challenged that assumption. Lagier et al. (2015) noted a general trend that increased splice strength (defined as maximum bar stress) was not linearly proportional to the splice length. For tests on UHPC with 1% and 2% steel fibers, by volume, the average bond stress was significantly lower when a shorter splice length was tested. For UHPC with a higher fiber volume fraction, 4%, the bond stress differed only 5% between the two tested splice lengths. Ronanki et al. (2016) adhered strain gauges to the reinforcing test bars at half of the embedded length for the pull-out specimens which they tested. They observed that the bond stress did not reduce to 50% of the peak value at half of the embedment length, leading them to conclude that the bond stress distribution along the rebar embedded in UHPC was not uniform. Ronanki et al. (2018) described the testing of 12 beam specimens which had strain gauges adhered to the reinforcing bars at various locations along the embedded length. The beams had bar sizes ranging from #4 to #7, all with $8d_b$ splice length. Six beams had a single pair of bars, while the other six had two pairs of bars. The beams had width and heights ranging from 5 to 6 in., lengths ranging from 40 to 45 in. and concrete covers ranging from 0.8 to 1.5 in. One strain gauge was adhered to each bar, at locations ranging from $2d_b$ to $8d_b$, measured from the end of the reinforcing bar in the spliced region. Based on measurements from the foil strain gauges, Ronanki et al. concluded that the bond stress distribution along the rebar splice length was not uniform. Very high bond stresses were developed over a short length of $2.5d_b$ from the free end of the reinforcing bars, accounting for nearly 60% of the maximum stress developed in the bar. Evidence of their findings was presented in bond stress and reinforcing bar strain graphed versus the position along the reinforcing bar. The bond stress was determined based on Equation 1, with the reinforcing bar stress determined based on the measured reinforcing bar strain and the steel reinforcing bar's material characterization. Due to strain measurements only being available at discrete locations, the bond stress diagram was a stepped block shape. An important finding of their work was that pull-out tests provided a conservative lower bound estimate of the splice length required in UHPC, as compared to beam tests. Thus, pull-out tests with a configuration similar to those tested by Ronanki et al., should be considered valid for predicting the required splice length in members with bending or combined bending and axial loads.

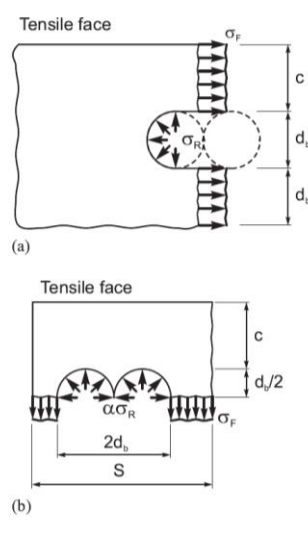

Figure 2: UHPC tensile stresses: (a) tensile stresses, and (b) side splitting, per Dagenais et al. **(2018)**

Equation 3: Required Plastic Tensile Stress, per Dagenais and Massicotte **(2015)**

$$\sigma_f = \frac{\alpha \times d_b \times \tau \times \tan \beta}{b_e}$$

Marchand et al. (2016) conducted development testing on #3, #4, and #5 bars in a commercially available UHPC with 2.5% steel fibers, by volume, and additional polypropylene fibers. For the #3 and #4 bars, concrete covers of 0.8 in. and 1.2 in. were tested, with development lengths of $4d_b$ and $8d_b$. For the #5 bars, the concrete cover was constant at 7.5 in., and the development lengths tested were $2.5d_b$ and $8d_b$. The test specimens consisted of single bars embedded in UHPC, with bond breakers applied at the top and bottom of the UHPC to generate the target embedment length. The bars were loaded with a hydraulic jack on a tripod or in a uniaxial testing machine with hold-down anchors. Fiber optic sensors were affixed to the reinforcing bar, in a groove machined into the bar's longitudinal rib. The fiber optic sensor measured strain along both the free and embedded portion of the reinforcing bar at approximately 0.04-in. increments. Displacement transducers were also used at the top and bottom of UHPC to measure the bar movement in comparison to the UHPC. Marchand et al. noted a linear strain profile along the reinforcing bars for tests with the shorter embedment length of $2.5d_b$ and $4d_b$. The linear profile indicates the bond between reinforcement and UHPC is effective in the whole embedment length, and there is uniform bond stress. In comparison, for tests with a longer embedment of $8d_b$, an exponential strain profile was evident, indicating a non-uniform bond stress. To determine the influence of concrete confinement on bond strength, the normalized bond strength was plotted versus the normalized cover thickness. The normalized bond strength is the maximum average bond stress observed during the test, divided by the square root of the concrete strength. The normalized cover thickness is the cover divided by the reinforcing bar diameter. The researchers additionally plotted results from literature, and the idealized curve is described in Equation 4, where τ_{max} is the bond strength (maximum average bond stress), f_c' is the concrete strength, c is the concrete cover, and $\emptyset$ is the reinforcing bar diameter.

Equation 4: Idealized Curve Corresponding to the Limit of Observed Debonding Failure, per Marchand et al. **(2016)**

$$\frac{\tau_{max}}{\sqrt{f_c'}} = \frac{3.5}{4}\frac{c}{\emptyset}\ (f_c'\ in\ MPa)\ or\ \frac{\tau_{max}}{\sqrt{f_c'}} = \frac{1}{3}\frac{c}{\emptyset}\ (f_c'\ in\ ksi)\ if\ \frac{c}{\emptyset} \leq 4$$

$$\frac{\tau_{max}}{\sqrt{f_c'}} = 3.5\ (f_c'\ in\ MPa)\ or \frac{\tau_{max}}{\sqrt{f_c'}} = 1.33\ (f_c'\ in\ ksi)\ if\ \frac{c}{\emptyset} \geq 4$$

Marchand et al. (2016) also developed a local bond stress-slip model based on their experimental results and compared the model to the *fib* Model Code (2013). They developed the model by determining the bond stress and local displacement at each gauge location along the bar. The bond stress was calculated using Equation 1, with the reinforcing bar stress equal to the incremental change in stress based on the strain measured by the fiber optic sensor at the given location and the material properties of the reinforcing bar. The local displacement at each corresponding location was determined based on the slip measured between the UHPC and bar at the surface of the UHPC and strain along the embedded portion of the bar. The method is described further in Figure 3. Strain measured by the fiber optic sensor exhibited "waving" along its measurement length corresponding to peak stresses at the spacing of the reinforcing bar ribs. The sensor measured strain close to the surface of the bar and was affected locally by the ribs. For that reason, smoothing was required for the strain measurements, using a 3rd order moving polynomial interpolation fitted on interval [x-dx, x+dx] with dx = 0.8 in.

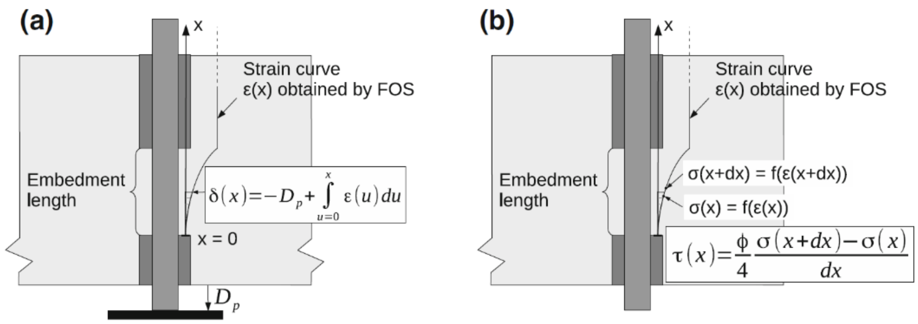

Figure 3: Method to obtain local "bond stress-slip", (a) determining $\boldsymbol{\delta(x)}$, and (b) determining $\boldsymbol{\tau(x)}$, per Marchand et al. (2016)

Marchand et al. (2016) determined that the local stress-slip curve could be characterized as having three phases. First, in the quasi-elastic phase, the UHPC surrounding the reinforcing bar behaved linearly under the pressure of the reinforcing bar ribs. Next, in the micro-cracking phase, the UHPC surrounding the rebar displayed micro-cracking which led to a decrease of stiffness. Finally, in the slipping/debonding phase, the bond stress was roughly constant while the rebar slipped in the UHPC, leading to a pull-out failure. The smoothed model is shown in Figure 4. The modified fib Model Code (2013) formula proposed by Marchand et al. is presented in Equation 5.

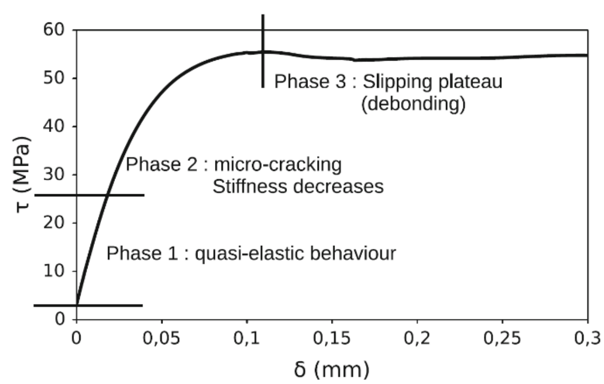

Figure 4: Bond stress-slip curve, per Marchand et al. (2016)

Equation 5: Stress-Slip Model, where $\boldsymbol{\delta_1 = 0.1\,mm}$, $\boldsymbol{\delta_2 = 0.6\,mm}$, and $\boldsymbol{f_{cm}}$ is the concrete strength, in MPa, per Marchand et al. (2016)

$$\tau_0 = \tau_{max}\left[1 - \left(\frac{\delta_1 - \delta}{\delta_1}\right)^3\right] for\ 0 \le \delta \le \delta_1$$

$$\tau_1 = \tau_{max}\ \ for\ \delta_1 \le \delta \le \delta_2$$

$$\tau_{max} = 3.9\sqrt{f_{cm}}\ (f_{cm}\ in\ MPa)\ or\ \tau_{max} = 1.485\sqrt{f_{cm}}\ (f_{cm}\ in\ ksi)$$

Chapter 3. Experimental Testing Program

Test Variables

Variables considered in the test matrix included splice length, embedment length, concrete cover and bar spacing. UHPC material age and strength were approximately consistent for all tests, with the target strength ranging from 10 ksi to 14 ksi, which was achieved at a material age of 2 or 3 days. A strength of 14 ksi corresponds to the strength which can be achieved with certain UHPC mix formulations with 1 day of curing. 14 ksi is also the concrete compressive strength targeted in the research by Yuan and Graybeal (2014) and specified in design guidance by FHWA (2014). Bar splice lengths considered ranged from $4.8d_b$ to $11.2d_b$ and were selected based on an iterative test matrix. The bar embedment length for all tests was approximately 2 in. plus the splice length. That matched the Yuan and Graybeal recommendations for #8 bars and for simplicity, was targeted for all bar sizes. Per the PCI Design Handbook (PCI, 2004), the recommended erection tolerance for interfaces of precast and cast-in-place members is 1 in., so 2 in. will exceed industry recommended tolerances.

In some cases, the UHPC connection will need to match the conventional concrete components being connected, therefore cover will be equivalent. Two different cover dimensions were primarily tested, 1.75 in. (1.25 – 1.5 d_b) and 3.75 in. (2.6 – 3.3 d_b). In addition, #11 bars were tested with a cover of 2.75 in. (2.0 d_b). The minimum of the cover dimensions, 1.75 in., corresponds to the minimum cover allowed by the FDOT Structures Manual (2021) for superstructures, with a 0.25 in. tolerance allowed by the FDOT Standard Specifications for Road and Bridge Construction (2021). The thicker concrete cover of 3.75 in. was also investigated to determine if the splice length could be reduced with increased cover. Per the FDOT Structures Manual (2021), the required concrete cover for concrete placed in an extremely aggressive environment but not in contact with water is 4 in. Considering the tolerance, a value of 3.75 in. was selected for testing. An intermediate cover value of 2.75 in. was also used for the #11 bars because the difference in required splice length was found to be significant for that size bar with 1.75 in. versus 3.75 in. cover. Using the minimum cover conservatively neglects that main reinforcing bars may have higher cover because minimum cover is typically measured to secondary reinforcing. Yuan and Graybeal (2014) and Ronanki et al. (2016) recommend a concrete cover of $3d_b$, which is equal to 3 in. for #8 bars and 4.25 in. for #11 bars. For larger bar sizes, the cover will be less than recommended by those references. For a #11 bar, 1.75 in. of cover is equivalent to $1.24d_b$. That value exceeds the cover used by Dagenais and Massicotte (2015), who found a cover of $1.2d_b$ and a splice of $12d_b$ to be sufficient for #11 bars.

Three different bar spacings were tested: 6 in., 8.5 in., and a contact splice. Non-contact splices were determined to have more capacity than contact splices by Yuan and Graybeal (2014) and therefore would be preferred. However, both contact and non-contact splices have practical merit for construction, as detailed in the Chapter 6. Practical Application section, so they were considered in the test matrix.

Self-Reacting Base Slab

Reinforcing bar splices in UHPC were formed for this project within a strip of UHPC on top of a conventional concrete slab with embedded dowels. The splice was formed in the UHPC between the dowels which protruded from the slab and a test bar. The slab served as a self-reacting base for the hydraulic actuator, which pulled the test bar above the UHPC splice. Two different types of slabs were constructed, to test three bar spacings. Each slab measured 8 ft by 7 ft in plan view and was 3 ft deep. Figure 5 shows elevations of slab types A and C. In total for this project, four slabs were constructed with four rows of the type A bar spacing and two slabs were built with two rows of type A bar spacing and two rows of type C bar spacing. Type A allowed testing a 6 in. center to center bar spacing and a contact bar spacing. The 6 in. bar spacing provides for a test spacing which is within the range found to be acceptable by Yuan and Graybeal (2014) and was used to determine the required bar splice length for a non-contact splice. The contact bar spacing was used to determine the required splice length for a contact splice. Type A allowed for four strips of UHPC splices, with each strip allowing four tests of the 6 in. bar spacing and three tests of the contact bar spacing, although the actual number of tests was less if the failure mode of a test affected adjacent test bars. Type C provided for an 8.5 in. center to center bar spacing for splice tests. The 8.5 in. spacing provides a second check that the splice length determined to be sufficient for the 6 in. spacing is sufficient for a different spacing. #9 and #11 bars were tested with 8.5 in. spacing. The 8.5 in. center to center spacing is within the range recommended by Yuan and Graybeal (2014) for #11 bars and #9 bars with 1.75 in. cover. The 8.5 in. spacing exceeds Yuan and Graybeal’s recommended spacing for #9 bars with 3.75 in. cover because the spacing exceeds the splice length. A center to center spacing of 8.5 in. corresponds to a clear bar spacing of $7.5d_b$ for #9 bars and $5d_b$ for #11 bars.

Since the reinforcing splice was not dependent upon the bond between concrete and UHPC, the top of the base concrete slab had a typical surface treatment, not the exposed aggregate treatment typically required for concrete to UHPC interfaces. The dowel bars used in the slabs were #11 bars, regardless of the size of the test bar. The dowel bars were Grade 60 for tests with #8, #9, and #10 bars. For tests with #11 test bars, the dowel bar grade was 120, to ensure the test bar yielded before the dowel bar. Required embedment of the dowel bar was calculated based on the development length equation from AASHTO LRFD (2014), with a yield strength of 120 ksi.

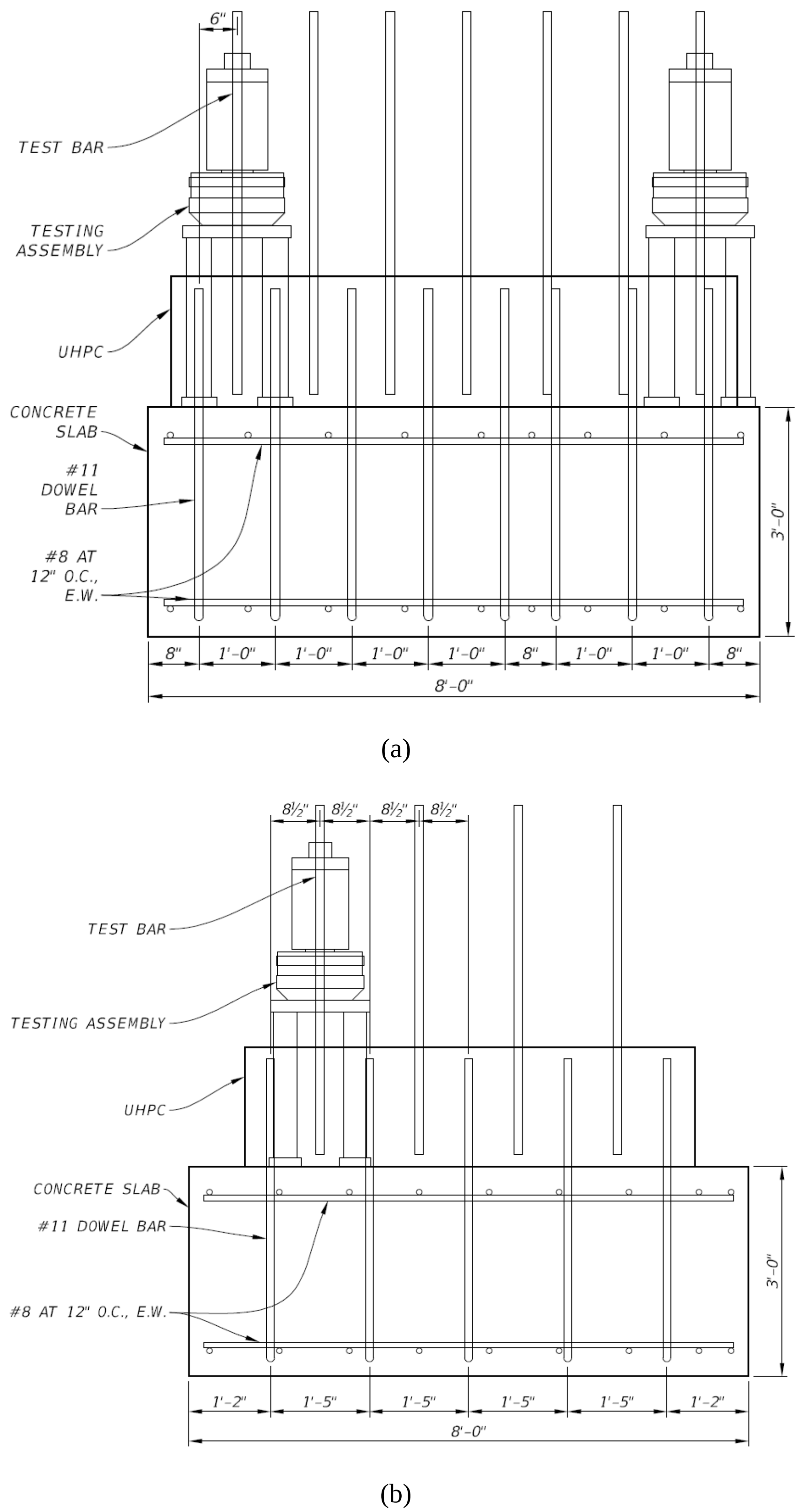

Figure 5: Base slab elevations with (a) 6-in. and contact, and (b) 8.5-in. reinforcement spacing

Testing Equipment

The testing equipment, shown in Figure 7, consisted of a hollow core load cell and hollow core cylinder in sequence. The load cell was a FL300U(C)-2SGKT Strainsert Universal Load Cell, with a load capacity of 300 kips and accuracy of +/- 0.25%. The hydraulic cylinder was an Enerpac Double-Acting, Hollow Plunger Cylinder, model RRH-1508, with a capacity of 300 kips. The load cell and cylinder were attached to each other and to a steel frame which spanned the UHPC strip. A minimum 2 in. diameter hole was provided for the test bar to pass through the test assembly. The test assembly was designed to accommodate testing for lap splices between $6d_b$ and $12d_b$ for #8 to #11 bar sizes. At those splice lengths, a minimum of 6 in. of clearance was provided for instrumentation.

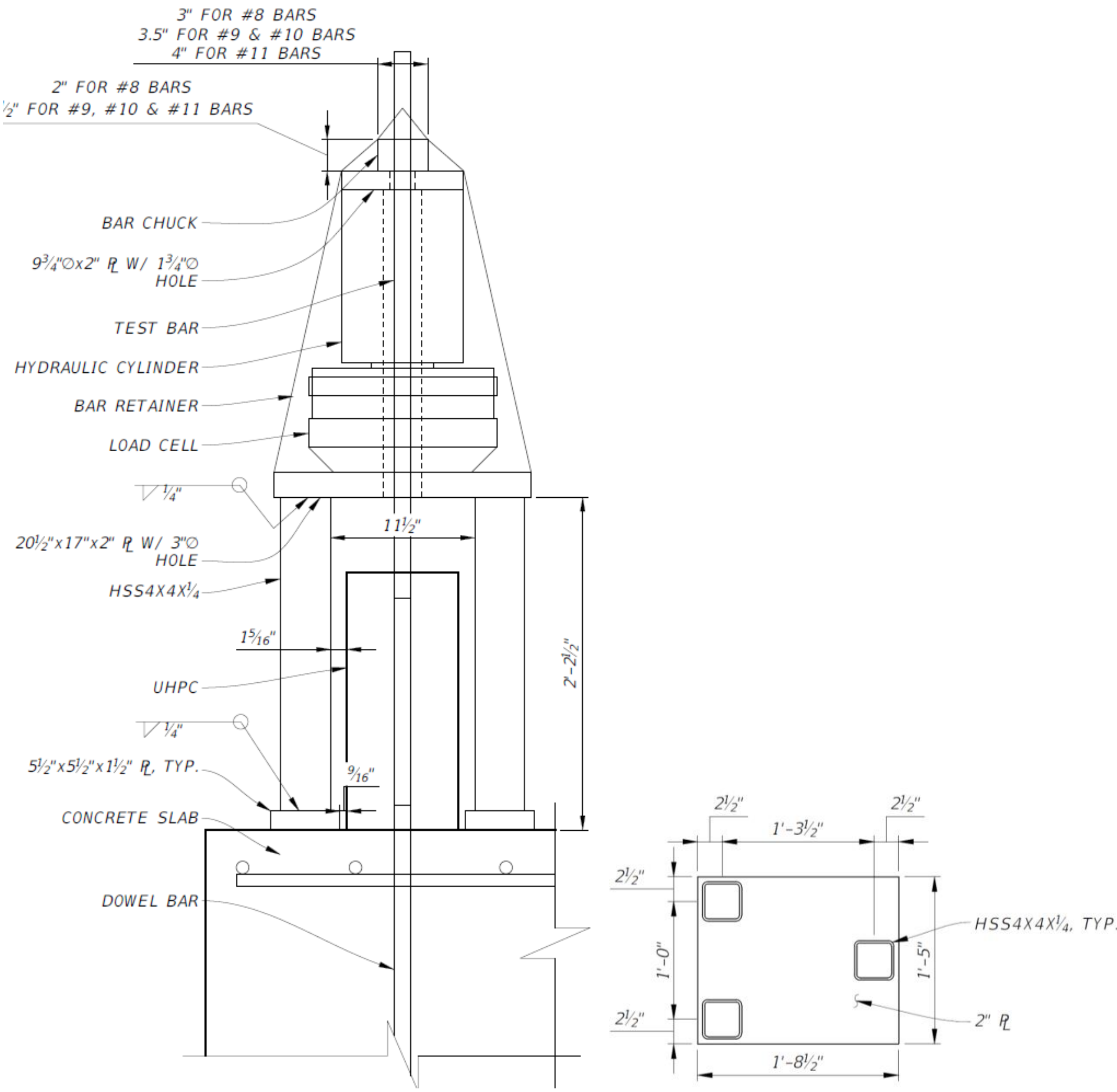

Figure 6: Testing equipment construction drawing with end view of UHPC strip

Figure 7: Testing equipment photograph with side view of UHPC strip

Loading Plan and Data Acquisition

Completed research projects related to splice length in UHPC have not used a consistent test rate. For the work done by Yuan and Graybeal (2014), the test rate was 0.2 in/min for a 36 in. free length of test specimen. That test rate was selected because it corresponded to static loading and at that rate the reinforcing bars and UHPC material would not exhibit increased yield strength or bond strength, respectively, due to high strain rate effects. The rate also allowed a reasonable amount of time during the test to assess behavior and fell within equipment capabilities (Z. Haber, personal communication, Nov. 27, 2017). For a similar test in an MTS machine by Ronanki et al. (2016), with an estimated free length of 36 in., the test rate varied from 0.01 to 0.1 in/min and a recording rate of 1 Hz was used. For another test in a universal testing machine by Lagier et al. (2012) with an estimated 12 in. free length, the test rate was slower, 0.0012 in/min, although the recording rate remained 1 Hz. ASTM A944, the Standard Test Method for Comparing Bond Strength of Steel Reinforcing Bars to Concrete Using Beam-End Specimens, allows between 10% and 33% of the bond strength, which is a much faster rate (ASTM, 2015). Assuming that the bond strength was equal to the rupture strength of the bar, the microstrain was 0.1 at rupture, and the bar free length was 36 in., the test rate would be 0.36 to 1.1 in/min.

The testing assembly planned for this research is closely related to and builds upon the work completed by Yuan and Graybeal (2014). It is less similar to work by Ronanki et al. (2016) or Lagier et al. (2012) because a universal testing machine is not used. Therefore, the test rate for this work matched the test rate used by Yuan and Graybeal, 0.2 in/min. That rate is also within the range used by Ronanki et al. A recording rate of 10 Hz was used, which was sufficient to capture the deflection at failure within 0.0003 in. For a 53 in. free length of test bar, that deflection corresponded to 6 microstrain, approximately 0.006% of the expected strain at failure.

Instrumentation

Instrumentation consisted of a load cell, two strain gauges, eight deflection gauges and four crack gauges. The load cell was in-line with the actuator and included two load outputs. The strain gauges (F1 and F2) were installed on the reinforcement 1 in. above the UHPC splice. One wire deflection gauge (Deflection) was installed between the load cell and hydraulic cylinder, to monitor the test rate. Three pairs of ETI Systems LCP8s-10 deflection gauges were installed around the test bar, attached to each of the testing assembly legs. One of each pair (D1, D2, D3) referenced the test bar at a knife edge clamp attached to the bar above the UHPC closure. The bar length between the top of the UHPC and gauge reference knife edge was 0.75 in. for each test. The other deflection gauge (DU1, DU2, DU3) in the pair referenced a plate attached to the top of the UHPC closure with a separate 0.063 in. aluminum plate used for each of the UHPC deflection gauges. The small plate was attached to the top surface of the UHPC with adhesive (Loctite #410 or Fixit Stick Bonding Putty #31270) to minimize the effects of the uneven UHPC surface. The final deflection gauge (Wedge) was a wire-type Firstmark Controls 60-25-54CI gauge, was placed on the top of the hydraulic cylinder plate and measured the wedge seating for each test. TML PI-5-100 crack opening displacement transducers (C1, C2, C3, C4) were installed around the test bar, with two (C2 and C4) on the top surface of the UHPC and two (C1 and C3) on the face of UHPC. The crack displacement transducers on the face of the UHPC were installed as close to the top of the UHPC as was feasible, considering voids and the irregular top surface. They were attached with Loctite and 15 mm x 15 mm x 10 mm brass blocks and had a gauge length of 4 in.. A diagram of the instrumentation is in Figure 8.

Fourteen tests were additionally instrumented with fiber optic strain gauges. The fiber optic system used a control unit from Sensuron, model number RTS125+ and sensing FBGS fiber, part number AGF-A3A4-000-1546-9-10. The FBGS fiber was grated every 0.25 in. which allowed for strain sensing over a 0.25 in. gauge length. For thirteen of the tests, the sensing fiber was externally adhered to the reinforcing bar and for one test, the sensing fiber was installed in a groove in the bar. For surface adhered fiber, the longitudinal rib of the reinforcing bar was sanded with an 80 grit flapper wheel on an angle grinder, cleaned with alcohol thoroughly, then glued down with M-Bond 200 adhesive and catalyst. For fiber adhered into a groove, the grove was made in a vertical milling machine using a 0.063 in. end mill set at approximately a 0.063 in. depth along the longitudinal rib of the reinforcing bar. The fiber was glued into the groove using the same process as the surface mounted fiber. During data acquisition, the system recorded all points between the start and end of the fiber at 10 Hz.

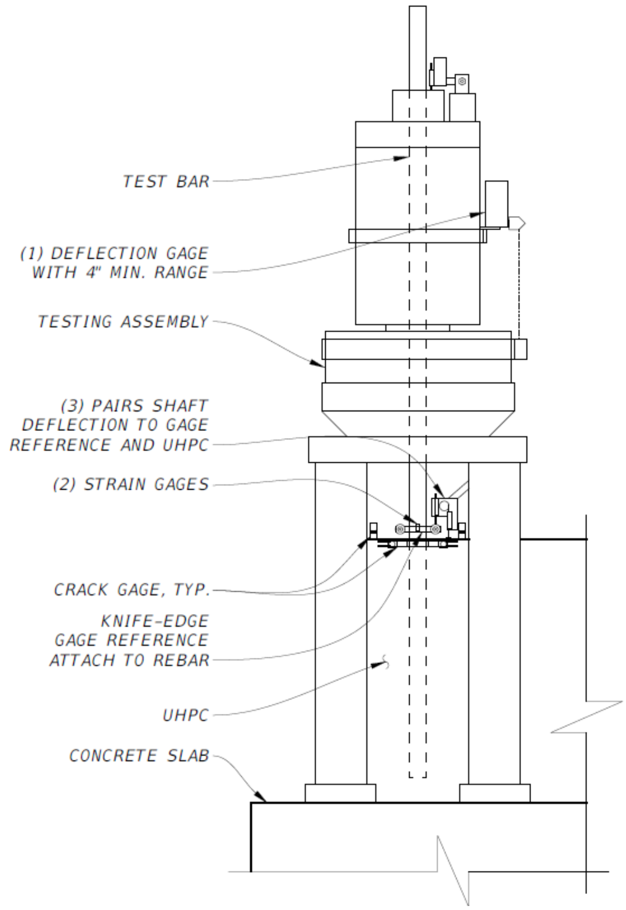

Figure 8: Overall instrumentation plan

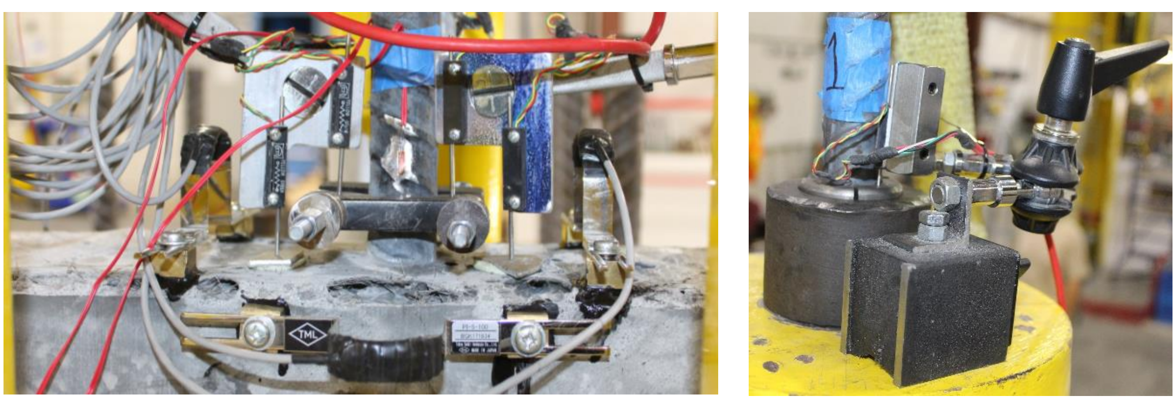

(a) (b)

Figure 9: Instrumentation detail with (a) test bar instrumentation and (b) wedge deflection gauge

Test Matrix

To limit the number of tests conducted, the testing matrix was adaptive instead of parametric. Testing built upon findings of previous tests and followed the flowchart shown in Figure 10.

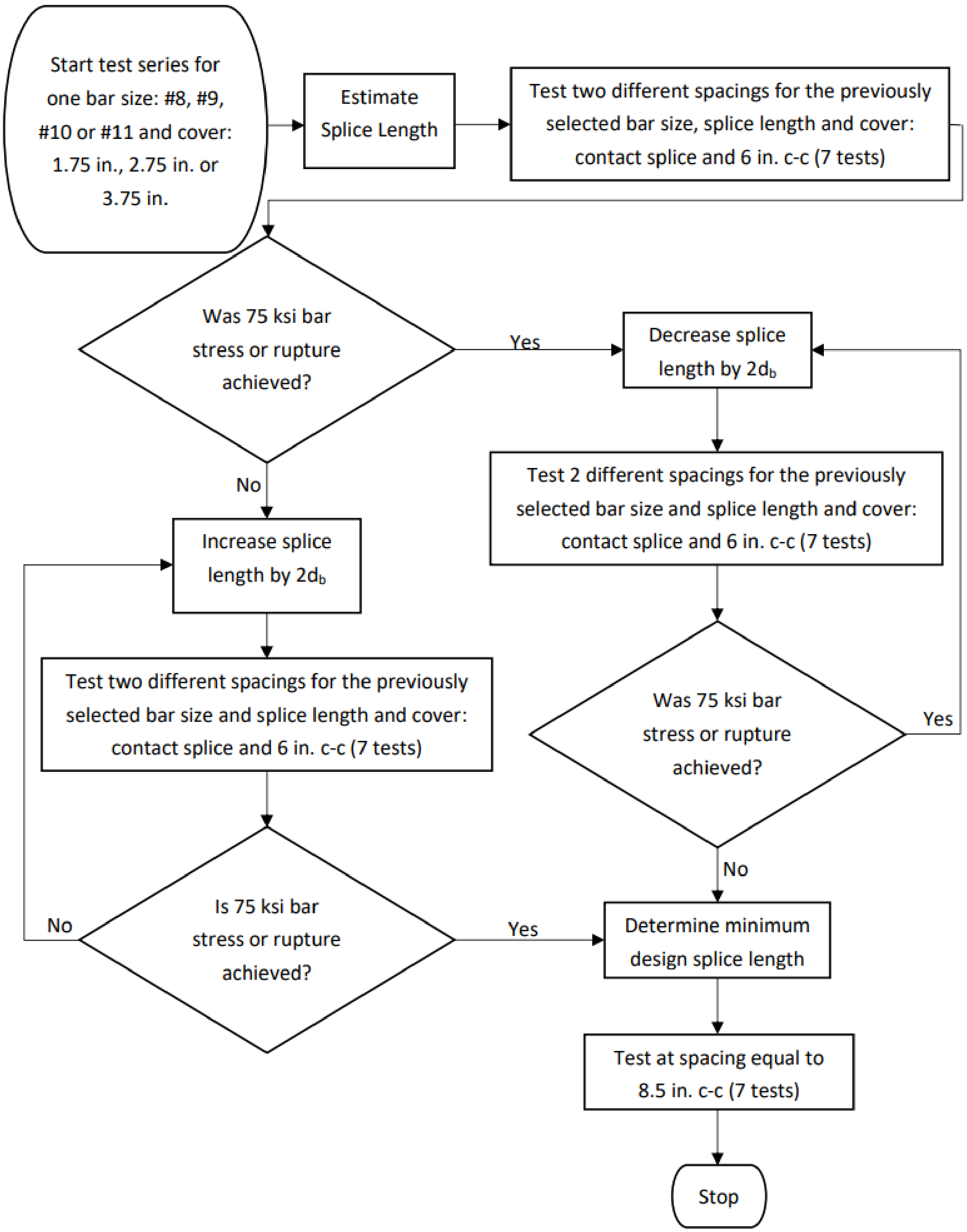

Figure 10: Test matrix flowchart, where c-c is center-to-center bar spacing

Data Processing and Analysis

As-Built Test Specimen Dimensions

The as-built dimensions of the UHPC splice, including bar clear spacing, clear cover provided, embedded bar length, splice length and free length were measured, before or after UHPC placement, as appropriate. The dimensions of the UHPC splice were assigned variables, as seen in Figure 11, where F and G indicate the bar clear spacing, J and K indicate the clear cover, M indicates the test bar embedment and C indicates the splice length. The free length of bar was defined as the length from the top of the UHPC to the middle of the wedge bite markings, calculated as H minus N.

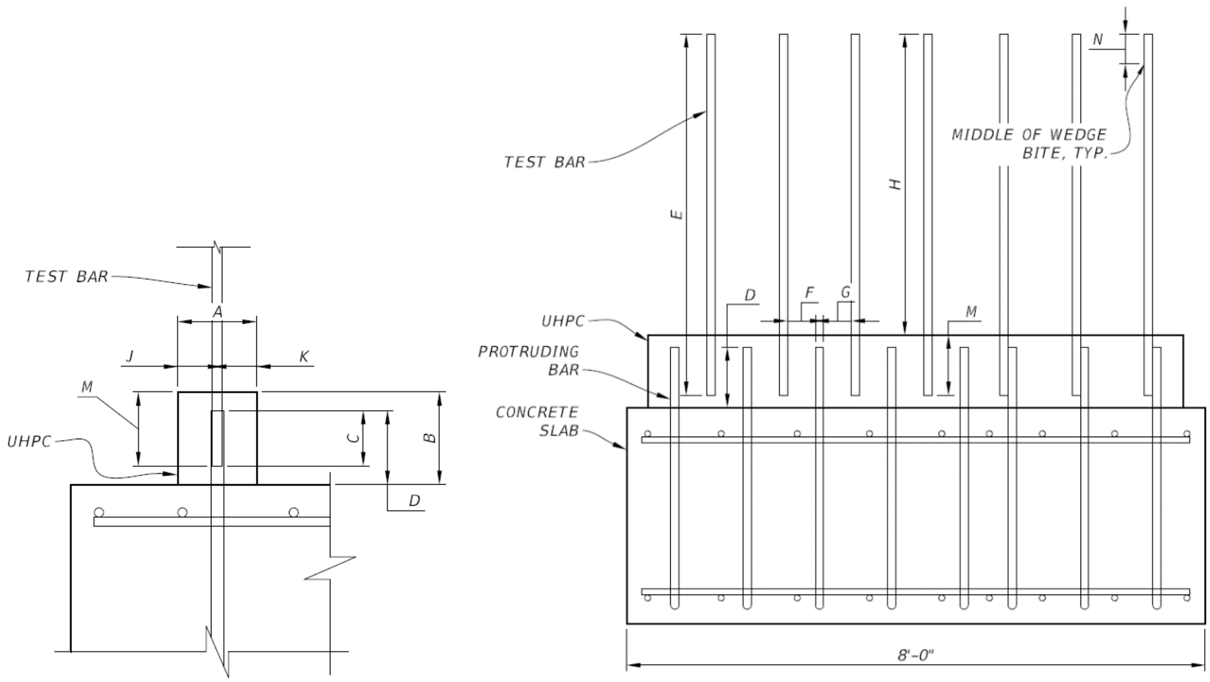

(a) (b)

Figure 11: UHPC splice dimensions with (a) section and (b) elevation

Material Properties

Concrete Strength

Sixteen 3 in. x 6 in. concrete cylinders, for compressive strength testing, were cast every time a row of UHPC splices was poured. Testing of the row typically took two days to complete, so a set of four concrete cylinders were tested at the beginning and end of each test day. A graph of the concrete strength vs. age was plotted using the data obtained from the compressive strength tests. Linear trendlines were introduced for each day as shown in Figure 12. The equations for the trendlines were used to calculate the concrete strength at the specific time each test was performed.

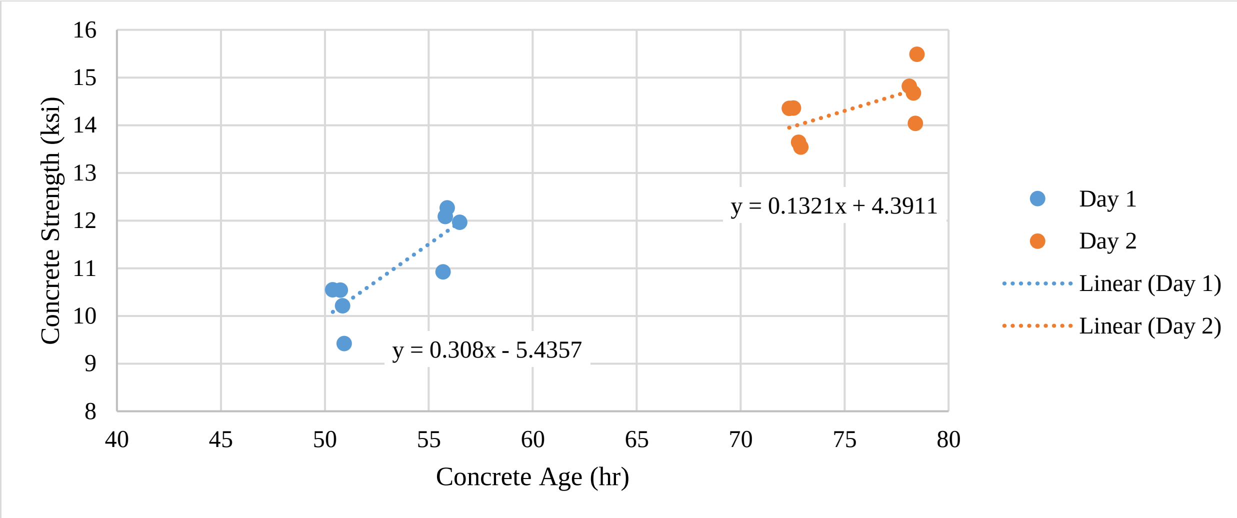

Figure 12: Concrete strength vs. age

Concrete Tensile Properties

Five beams with dimensions of 4 in. x 4 in. x 14 in. were cast with each batch of UHPC. Beam casting was done by placing the UHPC into steel molds from one end, allowing the UHPC to fill the mold by flowing in the long direction. The beams were cured for 2 days while covered with plastic and then the tops of the beams were ground to a level surface and removed from the molds. Testing was conducted by the FDOT State Materials Office according to ASTM C1609 (2019). Material data obtained from the ASTM C1609 testing included modulus of rupture, first peak strength, peak strength, residual strength at L/150 and L/600, toughness, and equivalent flexural strength ratio.

Reinforcing Bar Properties

A certified mill test report was provided for the reinforcing bars used as test bars. Specific properties for the #8-#11 ASTM A615-16 Grade 60 reinforcing test bars are shown in Table 1.

Table 1: Reinforcing Test Bar Material Properties

Material Property	Bar Size			
	#8	#9	#10	#11
Yield Strength (ksi)	68.2	65.8	65.9	67.3
Tensile Strength (ksi)	99.6	96.9	95.9	98.0
Elongation (%)	15	16	16	10
Deformation Average Spacing (in.)	0.676	0.720	0.839	0.919
Deformation Average Height (in.)	0.059	0.069	0.093	0.089
Deformation Maximum Gap (in.)	0.168	0.172	0.184	0.136

Cracking Load

Four crack opening displacement transducers were installed around each test bar, two on the top surface and two on the face. The gauges were labelled C1, C2, C3, and C4 corresponding to their positions. To determine the load at which cracking occurred for each test, the crack displacement was graphed against load. The crack is assumed to have occurred where the slope of the curve first turned to zero and the corresponding load was taken as the cracking load for that gauge. The minimum cracking load from the four gauges was taken as the cracking load for the test.

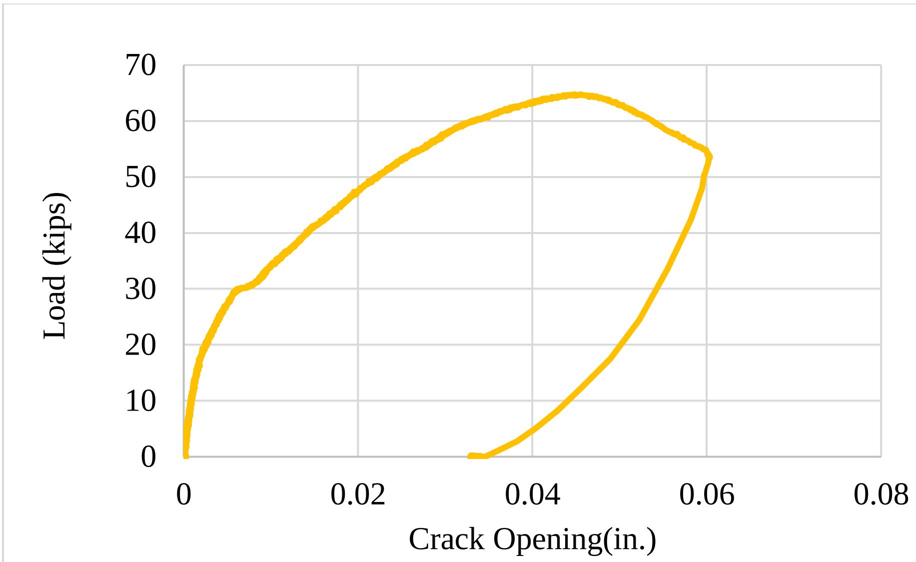

Figure 13: Load vs. crack gauge strain

Bar Slip

Bar slip was calculated using Equation 6, where *Average D* is equal to the average of gauges referencing the knife edge bracket attached to the reinforcing bar (D1, D2, and D3), *Average Du* is equal to the average of gauges referencing the UHPC (DU1, DU2, and DU3), and *Average F* is equal to the average of foil strain gauges (F1 and F2).

Equation 6: Bar Slip

$$Bar\ slip = -(Average\ D) - (-Average\ Du) - Average\ F * 0.75/1000000$$

Only the gauges with good quality response were used to calculate the average.

Chapter 4. Results

Summary of Completed Tests

In total, 127 tests were completed for this research project. The tests included four different bar sizes: #8, #9, #10 and #11. UHPC target covers of 1.75 in. and 3.75 in. were used for #8, #9 and #10 bars. Those same target cover values were used for tests on #11 bars with an additional target cover of 2.75 in. The actual cover tested, averaged for the two faces adjacent to the bar and including the effects of construction imperfections is listed in Table 2. For a target cover of 1.75 in., the mean value constructed and tested was 1.82 in. with a standard deviation of 0.17 in. For a target cover of 2.75 in., the mean was 2.77 in. with a standard deviation of 0.10 in. For a target cover of 3.75 in., the mean was 3.78 in. with a standard deviation of 0.20 in. For #8 bars, the embedment lengths tested ranged from 8 to 8.78d_b and the splice lengths tested ranged from 5.85 to 6.09d_b. For #9 bars, the embedment lengths tested ranged from 6.80 to 11.10d_b and the splice lengths tested ranged from 4.80 to 8.40$d_{b.}$ For #10 bars, the embedment lengths tested ranged from 7.20 to 12.00d_b and the splice lengths tested ranged from 5.80 to 10.30d_b. For #11 bars, the embedment lengths tested ranged from 9.20 to 13.30d_b and the splice lengths tested ranged from 7.20 to 11.20d_b. Table 2 shows the embedment and splice lengths for all tests completed as part of this project.

Table 2: Completed Tests

Bar Size	Target Cover (in.)	Actual Cover (in.)	Bar Spacing (in.)	Target Embedment Length in Bar Diameters	Actual Embedment Length in Bar Diameters	Target Splice Length in Bar Diameters	Actual Splice Length in Bar Diameters	Number of Individual Bar Tests
8	1.75	1.80	6	8	8.73	6	6.07	7
8	1.75	1.82	contact	8	8.78	6	6.09	7
8	3.75	3.80	6	8	7.95	6	5.85	2
8	3.75	3.75	contact	8	8.00	6	6.00	2
9	1.75	1.91	6	8	8.00	6	6.10	3
9	1.75	1.94	6	10	10.25	7.5	7.63	4
9	1.75	1.79	8.5	10	11.00	7.5	8.23	3
9	1.75	1.86	contact	8	8.20	6	6.20	2
9	1.75	1.81	contact	10	10.20	7.5	7.53	3
9	3.75	3.80	6	7	6.90	5	5.00	3
9	3.75	3.77	8.5	8	9.18	6	6.85	4
9	3.75	3.81	contact	7	7.00	5	5.10	3
10	1.75	1.92	6	10	10.07	8.5	8.57	3
10	1.75	1.86	6	12	11.76	10	10.09	8
10	1.75	1.88	contact	10	9.93	8.5	8.43	3
10	1.75	1.86	contact	12	11.73	10	9.84	5
10	3.75	3.84	6	8	8.14	6	6.28	7
10	3.75	3.84	contact	8	8.06	6	6.06	5

11	1.75	1.75	6	11.3	11.23	9.3	9.34	8
11	1.75	1.95	6	12	12.30	10	9.95	2
11	1.75	1.70	6	13	13.23	11	11.03	4
11	1.75	1.81	8.5	13.4	12.90	11.3	11.05	4
11	1.75	1.76	contact	11.3	11.12	9.3	9.25	6
11	1.75	1.80	contact	12	12.00	10	9.90	2
11	1.75	1.65	contact	13	13.17	11	11.07	3
11	2.75	2.75	6	10	9.43	8	7.48	4
11	2.75	2.76	6	11	11.37	9.5	9.73	3
11	2.75	2.84	contact	10	9.35	8	7.50	2
11	2.75	2.76	contact	11	11.27	9.5	9.67	3
11	3.75	3.73	6	10	9.70	8	7.60	2
11	3.75	3.65	6	11	11.30	10	9.97	3
11	3.75	3.75	8.5	10.3	10.83	8.2	8.37	3
11	3.75	3.64	contact	10	9.30	8	7.25	2
11	3.75	3.70	contact	11	10.85	10	9.70	2

Required Splice Length

Continuing upon the work by Yuan and Graybeal (2014), the reinforcing bar was considered to be fully developed in the splice and embedment lengths for a given test if the stress in the bar reached 75 ksi. Also in line with the work by Yuan and Graybeal (2014), a UHPC strength of 14 ksi was targeted for the test. That strength corresponds to what can be achieved with one day of curing time with certain UHPC mixtures. The targeted reinforcing bar stress and UHPC strength can be used to divide a graph of reinforcing bar stress versus concrete strength into four quadrants, as shown in Figure 14. Reinforcing bars can be considered to be fully developed if the test results show a maximum bar stress observed during the test above 75 ksi when the UHPC strength was below 14 ksi. Data from those tests fell within quadrant II of Figure 14. The level of conservatism for those tests ranged from low, near the bottom right corner of that quadrant, where bar stress was close to 75 ksi and concrete strength was close to 14 ksi, to high at the top left corner of the graph, where concrete strength was lower and maximum bar stress was higher. If test results indicated that at least 75 ksi maximum bar stress was achieved, but the concrete strength exceeded 14 ksi, it was unknown if the bar would have been developed within the given embedment and splice lengths at a concrete strength of 14 ksi or lower. Data from those tests would fall in quadrant I of Figure 14. Data close to the concrete strength limit of 14 ksi helped to indicate what test result could be predicted with a concrete strength at or below 14 ksi. Data that fell in quadrant III of Figure 14 was from tests for which the concrete strength at the time of the test was below 14 ksi and the maximum bar stress was also below 75 ksi. The bar was not developed fully given the test dimensions and UHPC material strength. However, if the UHPC strength was much less than 14 ksi, it is possible that the reinforcing bar could have been developed with the same embedment and splice length and a UHPC strength of 14 ksi. So, the level of certainty that a reinforcing bar could not have been developed with the tested splice and embedment length varied from a low level of certainty at the left end of the quadrant to a high level of certainty at the right side of the quadrant. Data which fell in quadrant IV indicates that the reinforcing bar could not be developed with the given splice and embedment lengths at 14 ksi because it was not fully developed at a higher UHPC strength.

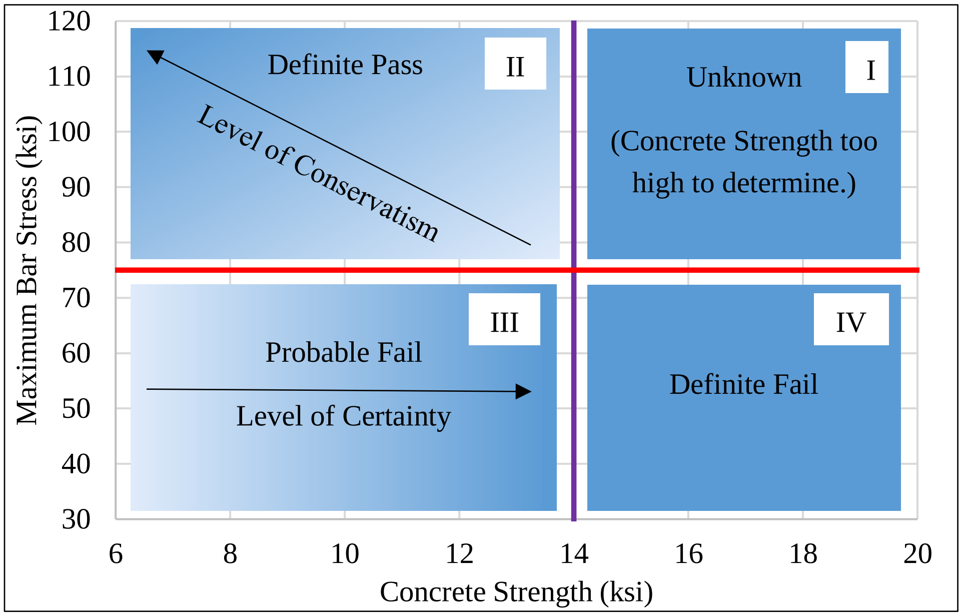

Figure 14: Bar stress vs. concrete strength

The following is documentation of the results of tests completed for this research with a Bar Stress vs. Concrete Strength graph for each combination of bar size and side cover tested. The series names shown in each graph denotes the [Embedment Length in Bar Diameters]-[Splice Length in Bar Diameters]-[Target Center to Center Bar Spacing in in. or "C" for Contact Splice].

First presented are the results for #8 bars with 1.75 in. of side cover, shown in Figure 15. The configurations tested had an embedment length varying from 8.4d_b to 9.1d_b and a splice length varying from 5.8d_b to 6.6d_b. The UHPC strength ranged from 13.19 ksi to 15.62 ksi. Of the 14 tests completed, the maximum bar stress was above 75 ksi for 12 tests. Three of the tests for which at least 75 ksi minimum bar stress was achieved were stopped when 3 in. of deflection in the length of the test bar and UHPC was observed, before failure in the reinforcing bar or UHPC occurred. All other tests were stopped when UHPC failure occurred. For two tests, failure of the UHPC exhibited a cone-shaped tension failure. For two tests, failure occurred when cracks propagated to the side face of the UHPC. Other tests exhibited a combination of failure modes. For two tests, UHPC failure occurred at a bar stress below 75 ksi for the reinforcing bars, which had reached the yield stress, fully yielded and were strain hardening at the time of failure, at bar stresses of 71.4 ksi and 72.4 ksi. The maximum strain measured by the foil strain gauges adhered to the reinforcing bars was 1.5% and 1.7%.

Next presented are the results for #8 bar with 3.75 in. of side cover, shown in Figure 16. For the four tests completed, the embedment length varied from 7.8d_b to 8.1d_b, the splice length varied from 5.7d_b to 6.2d_b and the UHPC strength ranged from 14.66 ksi to 18.32 ksi. For all four tests, the maximum bar stress exceeded 75 ksi and ranged between 91.2 ksi and 100.3 ksi. One test was terminated when the UHPC failed with a combination of longitudinal and side-splitting cracks. All three other tests were terminated when at least 3 in. of deflection was observed in the overall length of test bar and UHPC.

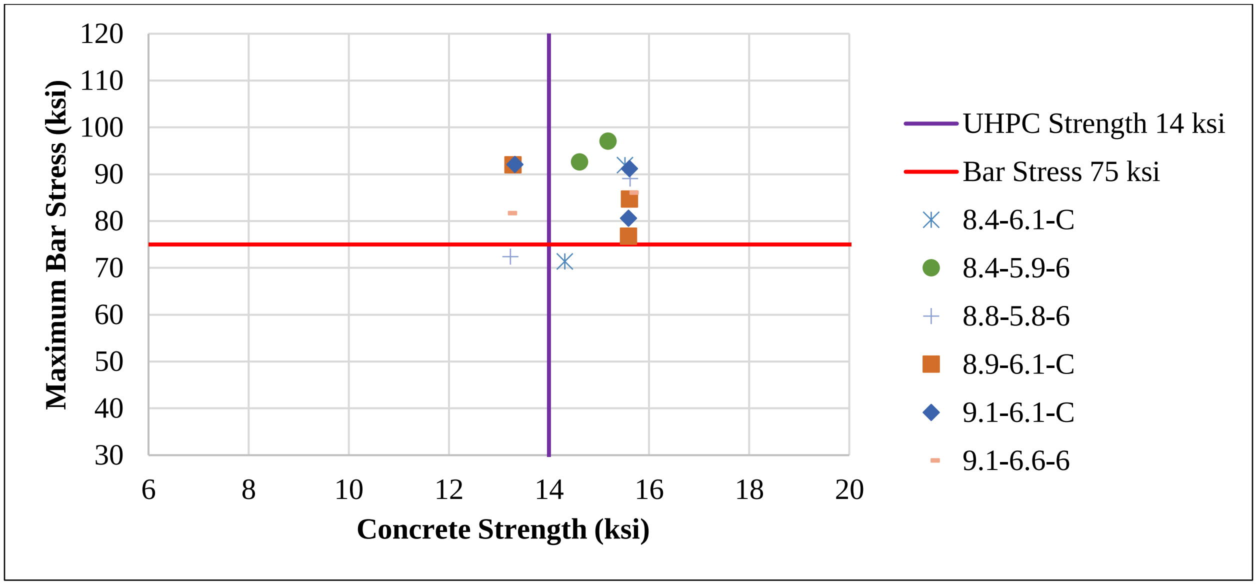

Figure 15: Bar stress vs. concrete strength for #8 bar size, 1.75-in. side cover

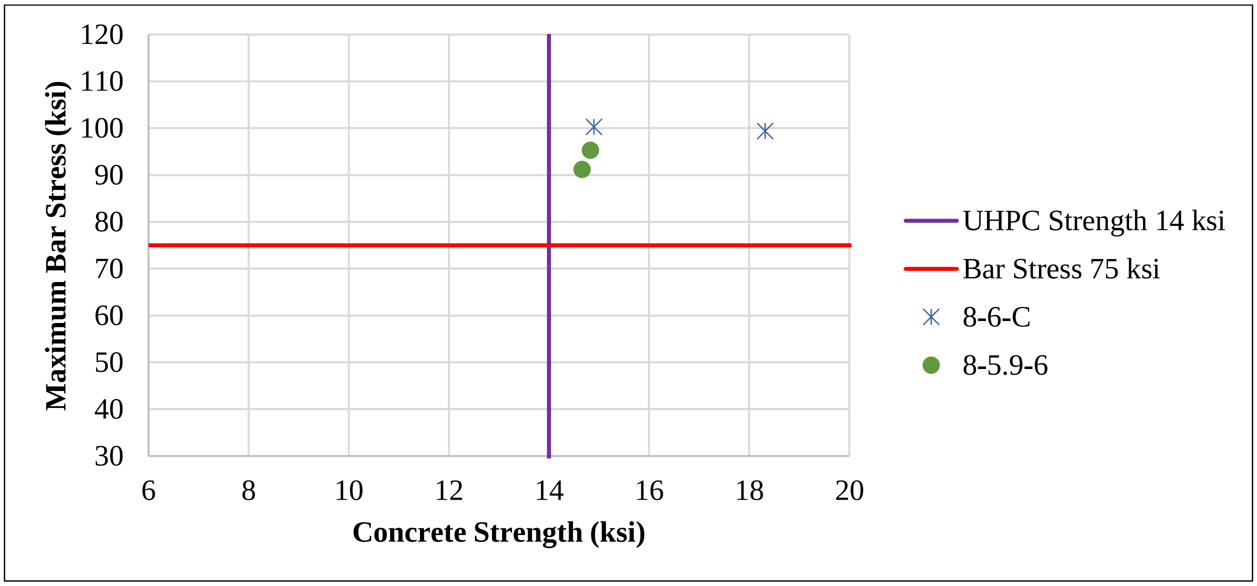

Figure 16: Bar stress vs. concrete strength for #8 bar size, 3.75-in. side cover

The same UHPC cover was used for testing #9 bars. The results of tests with #9 bars and 1.75 in. cover are shown in Figure 17. Two different discrete embedment and splice length ranges were tested. For the first round of tests, the tested embedment length ranged from $7.9d_b$ to $8.4d_b$, the splice length ranged from $6.0d_b$ to $6.2d_b$., and the UHPC strength ranged from 12.6 ksi to 15.4 ksi. For the first round of tests, five tests were completed. For four of the five tests, failure of the UHPC occurred before the bar stress had reached 75 ksi, at values between 37.8 ksi and 64.8 ksi. The tests with failed UHPC exhibited cone-shaped cracking, splitting to the side face or a combination of both failure modes. Based on the results of the first round of tests, it was determined that embedment lengths and splice lengths of approximately 8d_b and 6d_b, respectively, were not sufficient for developing #9 bars in UHPC with 1.75 in. cover. Subsequent tests were conducted with increased embedment and splice lengths. For the second round of tests, the tested embedment length ranged from 10.2d_b to 11.1d_b, the splice length ranged from 7.4d_b to 8.4d_b, and the UHPC strength ranged from 11.6 ksi to 15.1 ksi. For all ten tests conducted, the bar stress exceeded 75 ksi when either the test was stopped or UHPC failure occurred. Six tests were stopped when the reinforcing bar stress reached 83 ksi, or approximately a 10% surplus above the required 75 ksi. UHPC failure with splitting to the side face of the UHPC was observed for three tests and cone-shaped cracking was observed for one test.

The test results for #9 bars with 3.75 in. cover are shown in Figure 18. In total, 10 tests were conducted with embedment lengths ranging from 6.8d_b to 8.2d_b, splice lengths ranging from 4.8d_b to 6.2d_b, and UHPC strength ranging from 12.3 ksi to 16.3 ksi. For all tests conducted, the reinforcing bar stress reached at least 75 ksi before the test was stopped or UHPC failure occurred. One test was stopped when the total test bar and UHPC deflection reached 3 in. and four tests were terminated when the bar stress reached approximately 83 ksi. Three of the tests were terminated when the UHPC failed, exhibiting splitting cracks to the side face of the UHPC. For one of the tests, the UHPC exhibited longitudinal splitting cracks towards the adjacent bar at failure and one test had a combination of longitudinal splitting, side splitting and cone-shaped failure cracks.

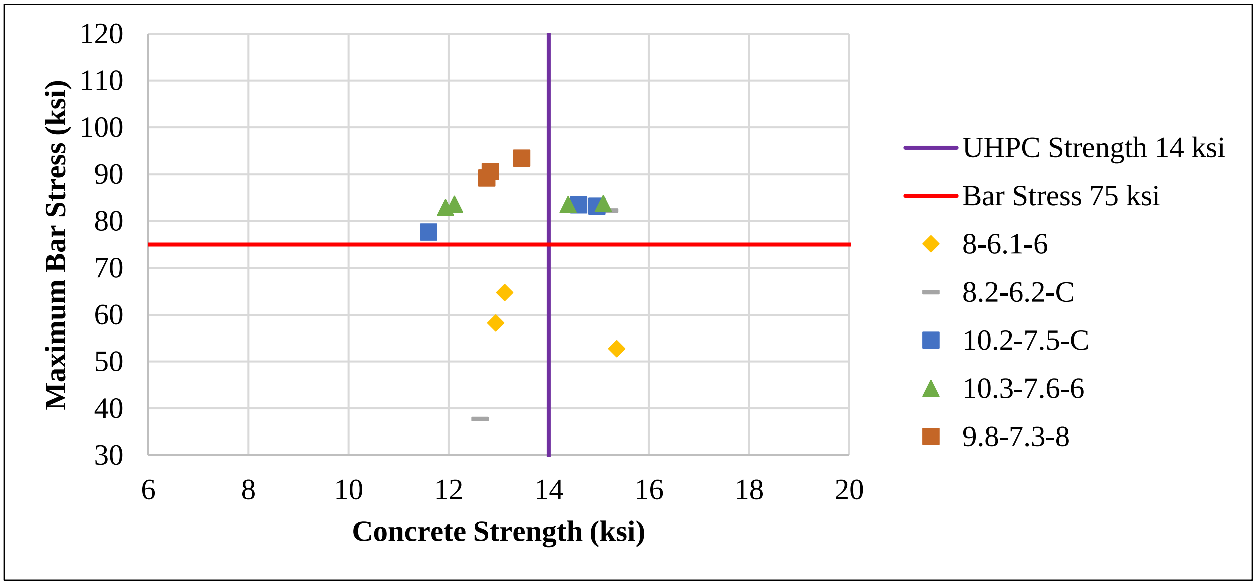

Figure 17: Bar stress vs. concrete strength for #9 bar size, 1.75-in. side cover

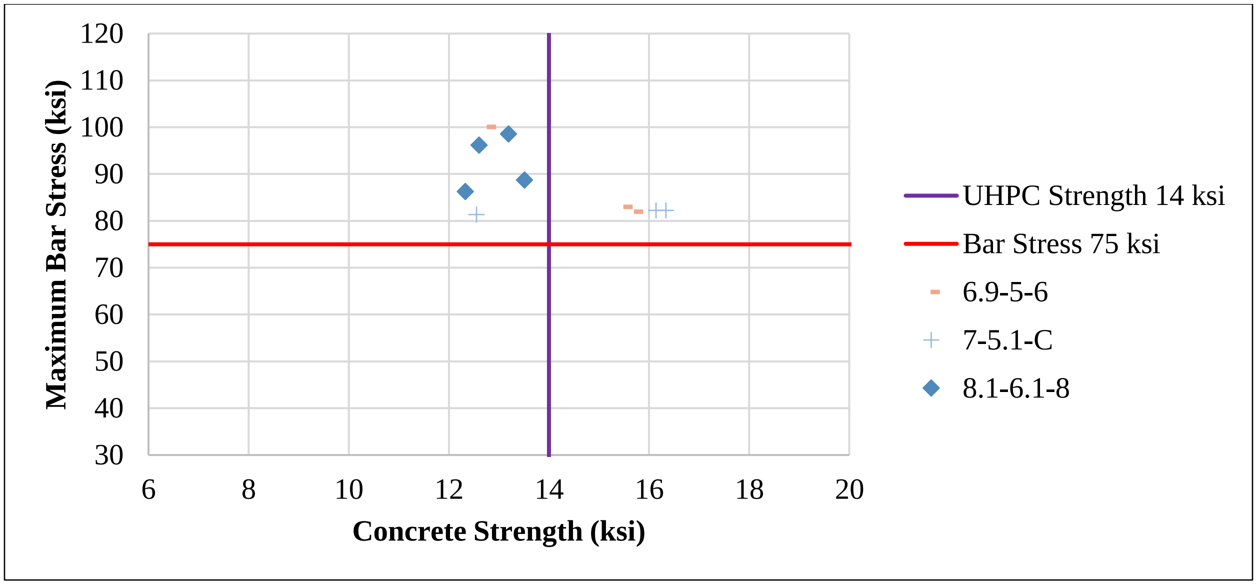

Figure 18: Bar stress vs. concrete strength for #9 bar size, 3.75-in. side cover

The same UHPC cover values were used for testing #10 bars. The results of tests with #10 bars and 1.75-in. cover are shown in Figure 19. Two different discrete embedment and splice length ranges were tested. For the first round of tests, the tested embedment length ranged from $9.7d_b$ to $10.1d_b$, the splice length ranged from $8.3d_b$ to $8.6d_b$., and the UHPC strength ranged from 10.8 ksi to 13.9 ksi. For the first round of tests, six tests were completed. For five of the six tests, failure of the UHPC occurred before the bar stress had reached 75 ksi, at values between 55.1 ksi and 72.3 ksi. The tests with failed UHPC exhibited cone-shaped cracking, splitting to the side face, or a combination of both failure modes. One test was terminated when the bar stress reached 83 ksi. Based on the results of the first round of tests, it was determined that embedment lengths and splice lengths of approximately $10d_b$ and $8.5d_b$ respectively, were not sufficient for developing #10 bars in UHPC with 1.75-in. cover. The embedment and splice lengths were increased for the second round of testing, for which the tested embedment length ranged from $11.6d_b$ to $12.0d_b$, the splice length ranged from $9.5d_b$ to $10.3d_b$., and the UHPC strength ranged from 10.2 ksi to 14.9 ksi. For 11 of the 13 tests completed, the maximum bar stress exceeded 75 ksi when the test was terminated. Two of the 11 tests were terminated when the bar stress reached 83 ksi, and one test was terminated when the bar stress reached the estimated ultimate stress. Eight of the tests were terminated when UHPC failure occurred. Two tests with UHPC failure exhibited splitting cracks on the side face of UHPC. Four tests exhibited a combination of longitudinal and side-splitting cracks. Two tests exhibited a cone-shaped failure in the UHPC.

Of the 13 tests completed, the maximum bar stress was less than 75 ksi for two tests. The maximum stress at UHPC failure for those two tests was 53.2 ksi and 55.8 ksi. The UHPC strength at the time of those tests was 11.3 ksi and 14.3 ksi. Both tests exhibited cracks splitting to the side face of the UHPC upon failure. Both were conducted on row three of slab two. After removing the formwork from that UHPC pour, which had seven spliced test bars, shrinkage cracks were noted in the UHPC side face, which were not generally observed in other UHPC placements. A photograph of the shrinkage cracks observed is shown in Figure 20. The cause of the shrinkage cracking is unknown. The ambient conditions at the time that UHPC row was cast were the hottest ambient conditions recorded for UHPC cast during the project, with an ambient temperature at mixing of 95 degrees and an average ambient temperature over the 4 days after placement of 83.4 degrees. With use of ice, the mix temperature was 78 degrees. The ASTM C1609 test results for the row were consistent with tests on the other UHPC pours, indicating the tensile properties were as expected. The shrinkage cracking may have contributed to the low bar stress reached for two of the tests performed on that row of UHPC. Figure 21 shows a photograph of the UHPC after testing, at a location between test bar 1 and test bar 2. Arrows in Figure 20 and Figure 21 point to approximately the same location in the photographs where crack growth is apparent after the test.

The test results for #10 bars with 3.75 in. cover are shown in Figure 22. Two different discrete embedment and splice length ranges were tested. For the first round of seven tests, the embedment length ranged from $7.2d_b$ to $8.0d_b$, the splice length ranged from $5.8d_b$ to $6.2d_b$., and the UHPC strength ranged from 10.0 ksi to 14.3 ksi. For all but one test conducted, the reinforcing bar stress reached at least 75 ksi before the test was stopped or UHPC failure occurred. Three tests were terminated when the bar stress reached approximately 83 ksi and three tests were terminated when the UHPC failed, exhibiting splitting cracks to the side face of the UHPC. For the test stopped when the UHPC failed before 75 ksi reinforcing bar stress had been reached, the UHPC exhibited splitting cracks to the side face. The maximum bar stress reached was 70.9 ksi. At a UHPC strength of 10.0 ksi, that test had the lowest concrete strength of the group of tests.

Five tests were completed with longer embedment and splice lengths, $8.2d_b$ to $8.6d_b$ and $6.0d_b$ to $6.7d_b$ respectively. The UHPC strength ranged from 11.3 ksi to 14.6 ksi. Four tests were terminated when the bar stress reached approximately the ultimate stress for the bar and one test was terminated when the UHPC failed, exhibiting a combination of longitudinal and side-splitting cracks. The bar stress when the UHPC failed was 88.8 ksi.

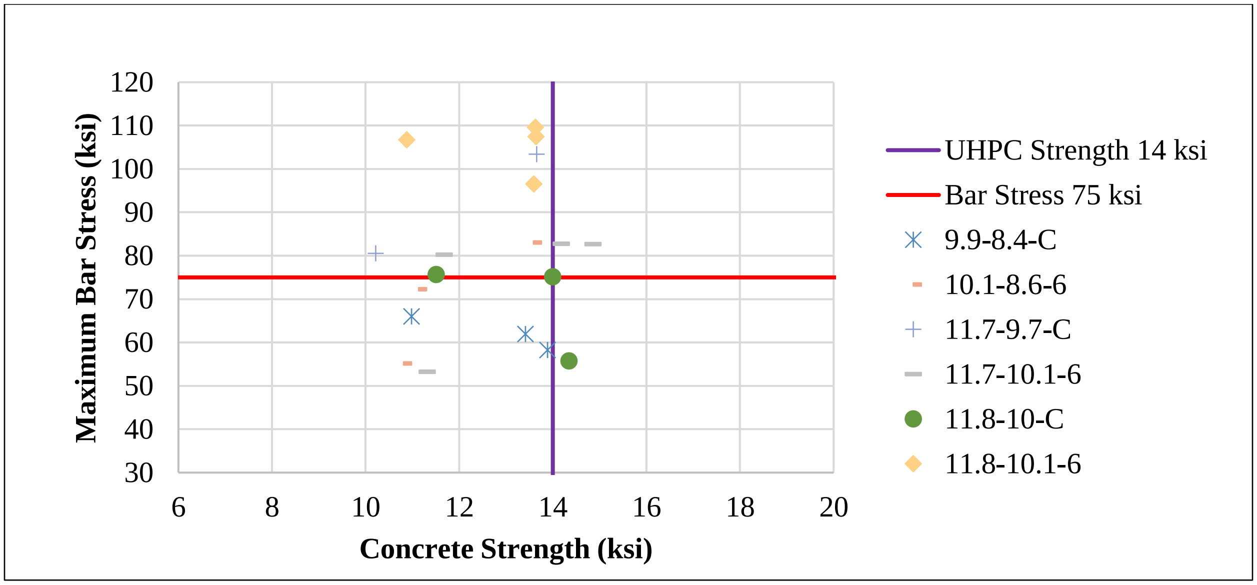

Figure 19: Bar stress vs. concrete strength for #10 bar size, 1.75-in. side cover

Figure 20; Shrinkage cracking in Slab 2, Row 3 before testing

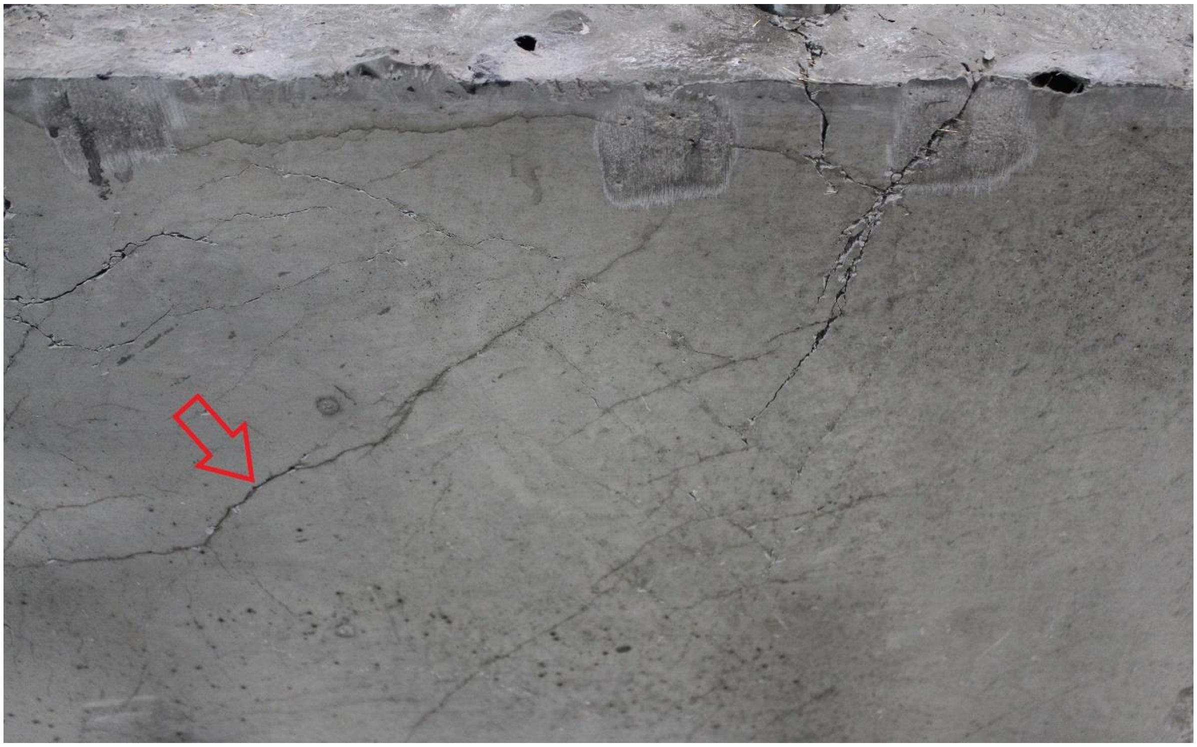

Figure 21: Cracking in Slab 2, Row 3 after testing

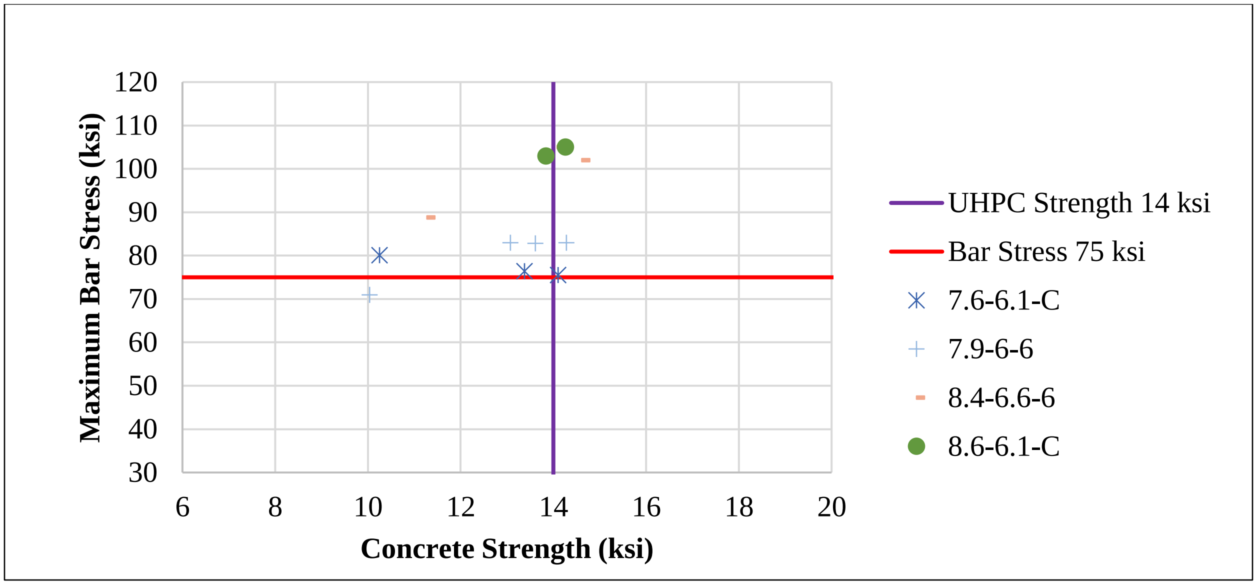

Figure 22: Bar stress vs. concrete strength for #10 bar size, 3.75-in. side cover

The test results for #11 bars with 1.75 in. cover are shown in Figure 23. In total, 29 tests were conducted with embedment lengths ranging from 10.5d_b to 13.3d_b, splice lengths ranging from 8.9d_b to 11.2d_b, and UHPC strength ranging from 8.5 ksi to 16.0 ksi. For all but two tests conducted, the reinforcing bar stress reached at least 75 ksi before the test was stopped or UHPC failure occurred. Six tests were terminated when the bar stress reached approximately 83 ksi and nine other tests were terminated when the bar stress reached approximately the ultimate stress for the bar. Twelve tests were terminated when the UHPC failed, with eight exhibiting splitting cracks to the side face of the UHPC, two exhibiting a combination of longitudinal and side-splitting cracks and two exhibiting a combination of cone-shaped and side-splitting cracks. For the two tests stopped when the UHPC failed before 75 ksi reinforcing bar stress had been reached, the UHPC exhibited splitting cracks to the side face. For one of those tests, the maximum bar stress reached with an embedment length of 12.3d_b and a splice length of 10.0d_b was 55.7 ksi, which was below the yield stress of the reinforcing bar. For an increased embedment length of 13.2d_b and splice length of 11.1d_b there was only one instance observed for which UHPC failure occurred before the bar stress reached 75 ksi. For that test, the bar had reached the yield stress, fully yielded and was strain hardening at the time of failure, at a bar stress of 74.5 ksi and strain of 2.5%.

The test results for #11 bars with 2.75 in. cover are shown in Figure 24. In total, 12 tests were conducted with two different discrete embedment and splice lengths. For the first set of tests with embedment lengths ranging from 11.1d_b to 11.5d_b, splice lengths ranging from 9.5d_b to 9.8d_b, and UHPC strength ranging from 9.5 ksi to 13.7 ksi, the reinforcing bar stress was at least 75 ksi before the test was stopped or UHPC failure occurred. Three tests were terminated when the bar stress reached approximately the ultimate stress for the bar and three tests were terminated when UHPC failure occurred with splitting cracks to the side face of the UHPC. For the second round of tests with reduced embedment and splice lengths, the embedment lengths ranged from 9.3d_b to 9.5d_b, splice lengths ranged from 7.4d_b to 7.5d_b, and UHPC strength ranged from 10.9 ksi to 12.4 ksi. In four tests conducted, the reinforcing bar stress reached at least 75 ksi before the test was stopped or UHPC failure occurred. Two were terminated when the bar stress reached approximately the ultimate stress for the bar and two tests were terminated when UHPC failure occurred with a combination of splitting cracks to the side face of the UHPC and splitting cracks to the adjacent bar. For two tests conducted, the UHPC failed before a bar stress of 75 ksi was reached and before the bar a yielding plateau. One test exhibited splitting cracks to the side face of the UHPC and the other test exhibited a combination of splitting cracks to the UHPC side face and the adjacent bar.

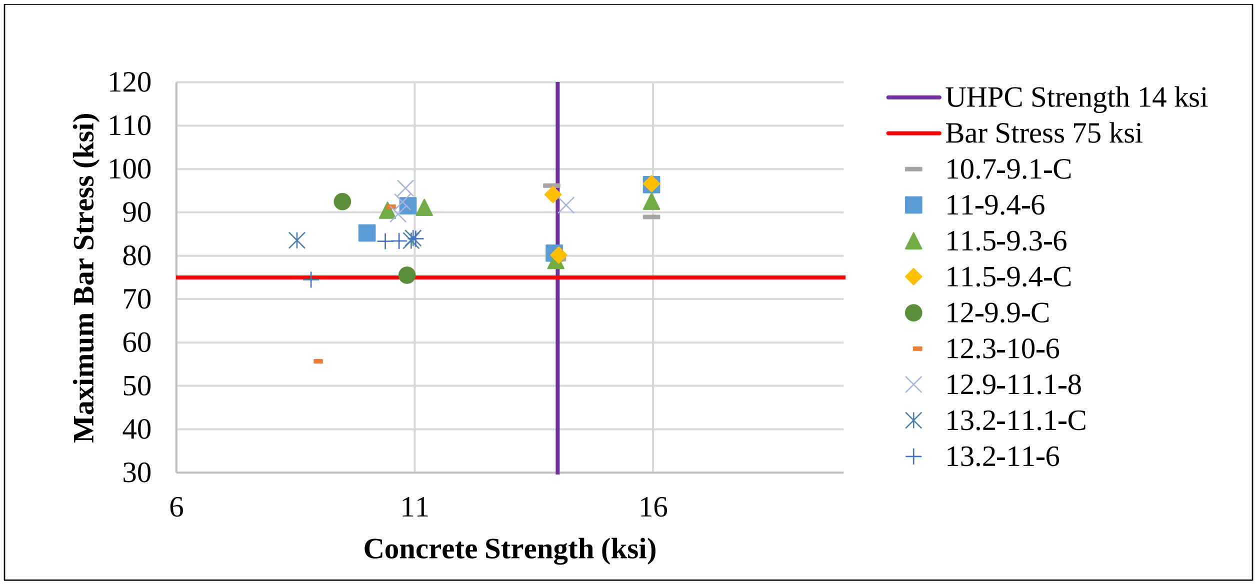

Figure 23: Bar stress vs. concrete strength for #11 bar size, 1.75-in. side cover

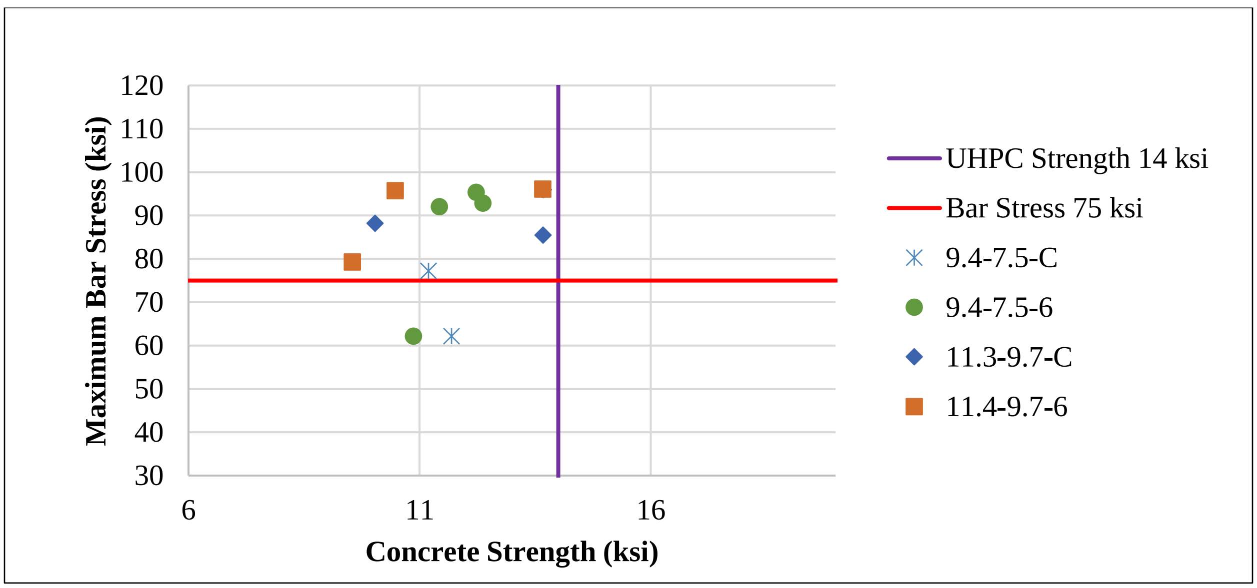

Figure 24: Bar stress vs. concrete strength for #11 bar size, 2.75-in. side cover

The final results presented are for #11 bar with 3.75 in. of side cover, shown in Figure 25. For the 12 tests completed, the embedment length varied from $9.2d_b$ to $11.5d_b$, the splice length varied from $7.2d_b$ to $10.1d_b$ and the UHPC strength ranged from 8.2 ksi to 14.8 ksi. For all tests completed, the maximum bar stress exceeded 75 ksi and was between 75.8 ksi and 96.0 ksi. Eight tests were terminated when at least 75 ksi or

83 ksi was achieved in the test bar and two tests were terminated when the bar stress reached approximately the ultimate stress for the bar. One test was terminated when UHPC failed, exhibiting splitting cracks to the side of the UHPC and one test was terminated when the UHPC failed, exhibiting a combination of side-splitting and cone-shaped failure cracks.

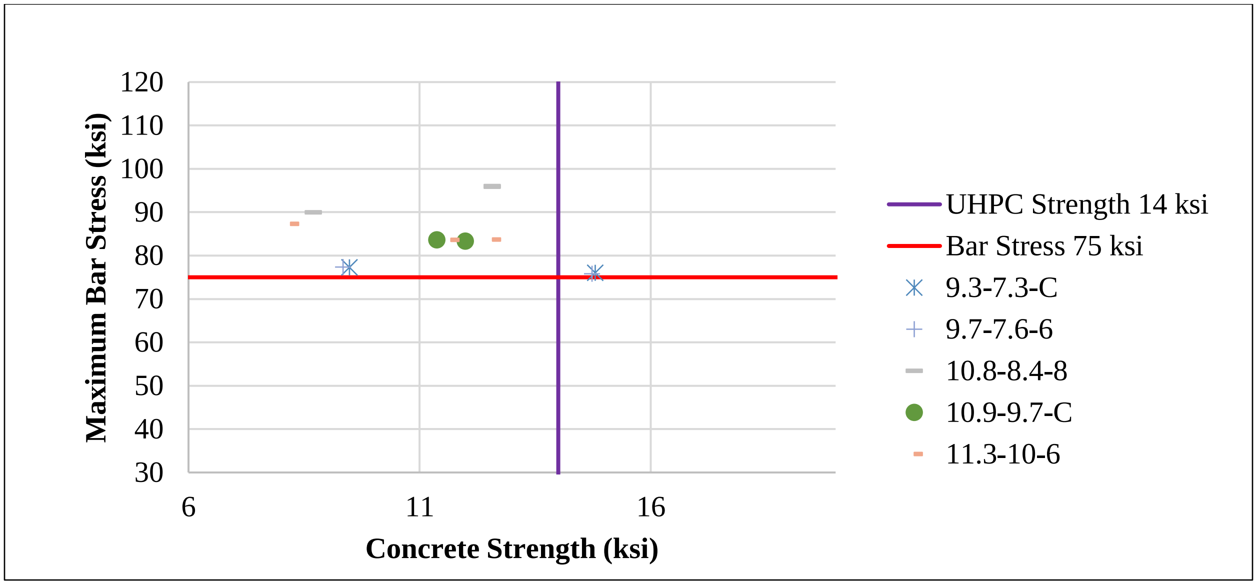

Figure 25: Bar stress vs. concrete strength for #11 bar size, 3.75-in. side cover

Effect of Steel Fiber Orientation

Two comparative series of tests were completed to evaluate the effect of fiber orientation: one with #8 bars and the other with #11 bars. For each bar size, two sets of UHPC splices were cast with identical test parameters, i.e., bar size, UHPC dimensions, embedment length and splice length. In total, four test rows were cast, two for each bar size. The two rows for each bar size were cast using the same UHPC batch to ensure identical concrete properties, but the concrete placement differed. For one of each pair of rows, the UHPC was placed from one end of the row and allowed to flow along the length of the row. UHPC fibers were expected to align in the direction of flow, which was parallel to a line connecting each pair of spliced bars. For the second of the pair of rows, UHPC was placed at several distinct locations along the row to produce a random flow pattern. The first comparative set of tests was for #8 bars with 1.75 in. side cover and average embedment and splice lengths of 9.0d_b and 6.1d_b, respectively. The second comparative set of tests was for #11 bars with 1.75 in. side cover and average embedment and splice lengths of 11.2d_b and 9.3d_b, respectively. The results of all tests are shown in Figure 26. In total, 24 tests were completed, 10 with #8 bars and 14 with #11 bars. Only one test resulted in failure of the UHPC before the bar reached 75 ksi stress. For that test, a maximum bar stress of 72.4 ksi was reached, beyond the yield stress, with 8.8d_b embedment length and 5.7d_b splice length provided for the #8 bar in 13.2 ksi UHPC. Six other bar tests were terminated when the bar stress reached approximately the maximum bar stress. All other tests were terminated when UHPC failure occurred. For the tests with random UHPC placement, 10 tests resulted in UHPC failure. Four tests showed a failure mode of splitting to the side face of the UHPC, three exhibited a combination of longitudinal and side splitting, two exhibited a combination of side splitting and cone failure and one exhibited all three failure modes. For the tests in which UHPC was placed with the intention to align fibers in the flow direction, eight tests resulted in UHPC failure. Five tests resulted in UHPC failure with splitting to the side face of the UHPC, one exhibited a combination of longitudinal and side splitting, one exhibited a UHPC cone failure, and one exhibited a combination of side splitting and cone failure.

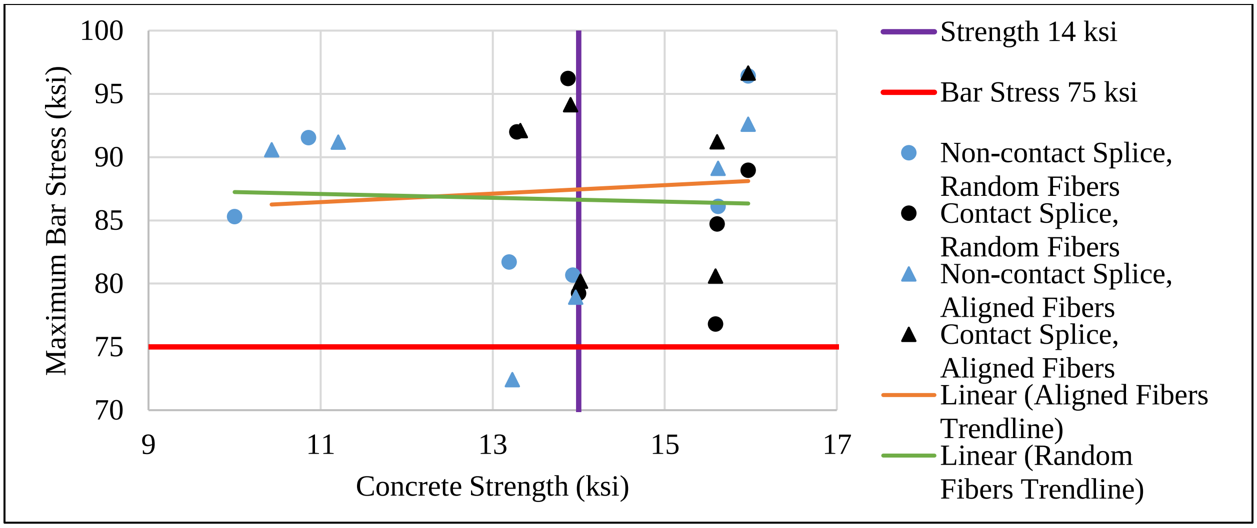

Figure 26: Bar stress vs. concrete strength for random and aligned fibers

There is no apparent difference in splice capacity between the two different casting methods for UHPC. It is possible that both placements resulted in a random fiber alignment in the UHPC, due to the large diameter bars disturbing the UHPC flow sufficiently that random fiber orientation was present for all tests. To evaluate that possibility, two cores were removed from the UHPC with random placement and two cores were removed from the UHPC with supposedly aligned fiber orientation. Each core was 2 in. diameter and at least 4 in. long. The fiber alignment in the cores was measured by the University of Florida by x-ray computed tomography scanning, with images prepared using the Phoenix Datos-X software and information extracted using VGS max software. The alignment in the long direction of the UHPC row (the direction of flow for the rows with supposedly aligned fibers) was compared and is shown in Figure 27. The data shown in Figure 27 is the count of fibers normalized by the total count of fibers, versus the deviation angle from the direction evaluated. The SINE curve shows the expected pattern of the plot if fibers were evenly distributed in every direction. There is no apparent difference in the fiber alignment between the UHPC placement methods.

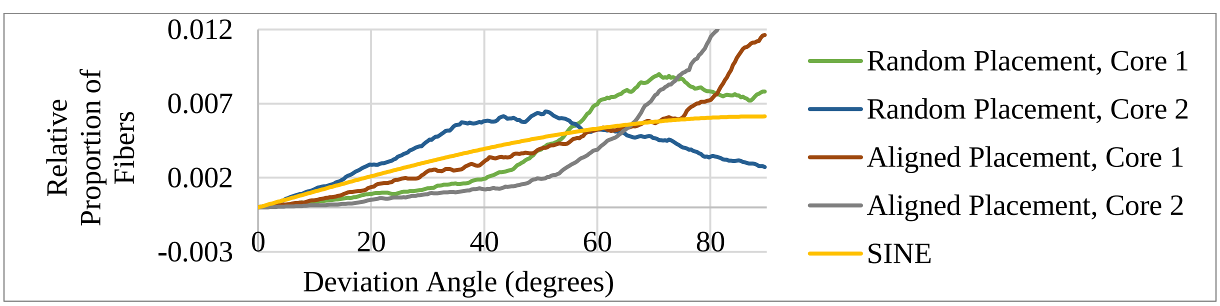

Figure 27: Proportion of fibers in longitudinal direction of UHPC row

Reinforcing Bar Engagement

Fiber optic strain gauges were adhered to the vertical ribs of the reinforcing bars for 14 tests. For 12 of those tests, fiber optic gauges were installed on both longitudinal ribs of the bar. The bars had deformations which alternately reversed direction on each side of the axis of the bar. For all tests with fiber optic strain gauges adhered, undulations in microstrain along the bar were apparent that approximately coincide with the spacing of deformations. The undulations indicate local stress concentrations along the length of the bar and are apparent because the fiber was adhered to the surface of the bar and not centered in the bar. Figure 28 and Figure 29 show the results from two tests for which fiber optics were installed on only one longitudinal rib of the bar. Both tests were for #11 reinforcing bars embedded approximately 16 in., with 2.75 in. clear cover. The recorded microstrain at low strain levels (less than 2300 microstrain) is shown in the figures. The gray region in each figure indicates the length of bar which was exposed, while the blue region indicates the length of bar which was embedded in UHPC. Each data series is a discrete time during the test for which the applied load was equal to the series name. Locations of bar ribs are shown as vertical gray lines. As shown in Figure 28, when the fiber optic was adhered to the longitudinal rib at which the deformations formed a "V" with the bar held vertically, the stress concentrations occurred at each bar deformation. As shown in Figure 29, when the fiber optic was adhered to the longitudinal rib at which the deformations formed an upside-down "V" with the bar held vertically, the stress concentrations occurred between each bar deformation.

As shown in Figure 28 and Figure 29, the strain along the bar appears to be bilinear, which was the typical behavior for all of the tests when the test load was below the reinforcing bar yield strain. Disregarding the undulations, the first segment of the bilinear curve consists of constant strain in the free length of the bar and some portion of embedment in the top of the UHPC. In the second segment of the bilinear curve, the strain decreases towards zero as embedment increases. The apparent intersection point for the two bilinear segments did not occur at the same embedment length for all test configurations. Additionally, the apparent intersection point for the two bilinear segments did not remain at a constant embedment location as load level varied during individual tests. Both tests shown in Figure 28 and Figure 29 were on a #11 reinforcing bar with 2.75 in. concrete cover and 16 in. bar embedment. Both tested splices were constructed with the same batch of UHPC although, due to the time difference between tests, the concrete strength for the test shown in Figure 28 was 9.5 ksi and the concrete strength for the test shown in Figure 29 was 10.0 ksi. For the test shown in Figure 28, the bar spacing was 6 in. and a cracking load of 56 kips was observed. For the test shown in Figure 29, a contact bar spacing was used and a cracking load of 87 kips was observed.

For the test shown in Figure 28 and Figure 30, the fiber optic gauge was installed so that gauges 262 through 274 were above the top of the UHPC and the gauge numbers continued to increase along the bar embedded in UHPC, i.e., the gauge number increased as the level of bar embedment increased. During the test, the fiber optic gauge typically failed at approximately 14,500 microstrain with different sensing locations along the gauge reaching that strain level at differing times during the test. Sensing locations along the bar were spaced at 0.25 in., but Figure 30 presents the microstain measured at sensing locations at 1 in. spacing with no averaging. The series name includes the gauge number and embedment length at the gauge (in.), for which a negative number indicates the gauge is along the exposed length of bar. The microstrain is graphed versus the external load applied to the bar. As can be seen in Figure 30, as the embedment increased along the length of the bar, the load required to reach 14,500 microstrain in the fiber optic gauge at that location increased. Yielding of the bar occurred when the microstrain measured by the foil strain gauge during the test was approximately 2,600 and the ultimate microstrain recorded by the foil strain gauge during the test was 32,804. Yielding is apparent in Figure 30 with a slope change at approximately 2,600 microstrain. The exposed portion of the reinforcing bar yielded before the portion of the bar embedded in UHPC. Less load was required to yield the exposed length of bar compared to the embedded portion. Yielding progressed down the bar length towards increasing embedment. The sensing locations along the exposed portion of the bar display similar behavior on the left side of Figure 30, along with several sensing locations slightly embedded in UHPC (278 and 282). Location 278 was embedded 0.75 in. in UHPC and location 282 was embedded 1.75 in. in UHPC. Location 310 was embedded 8.75 in. in UHPC and the bar itself was embedded 15.94 in. in UHPC.

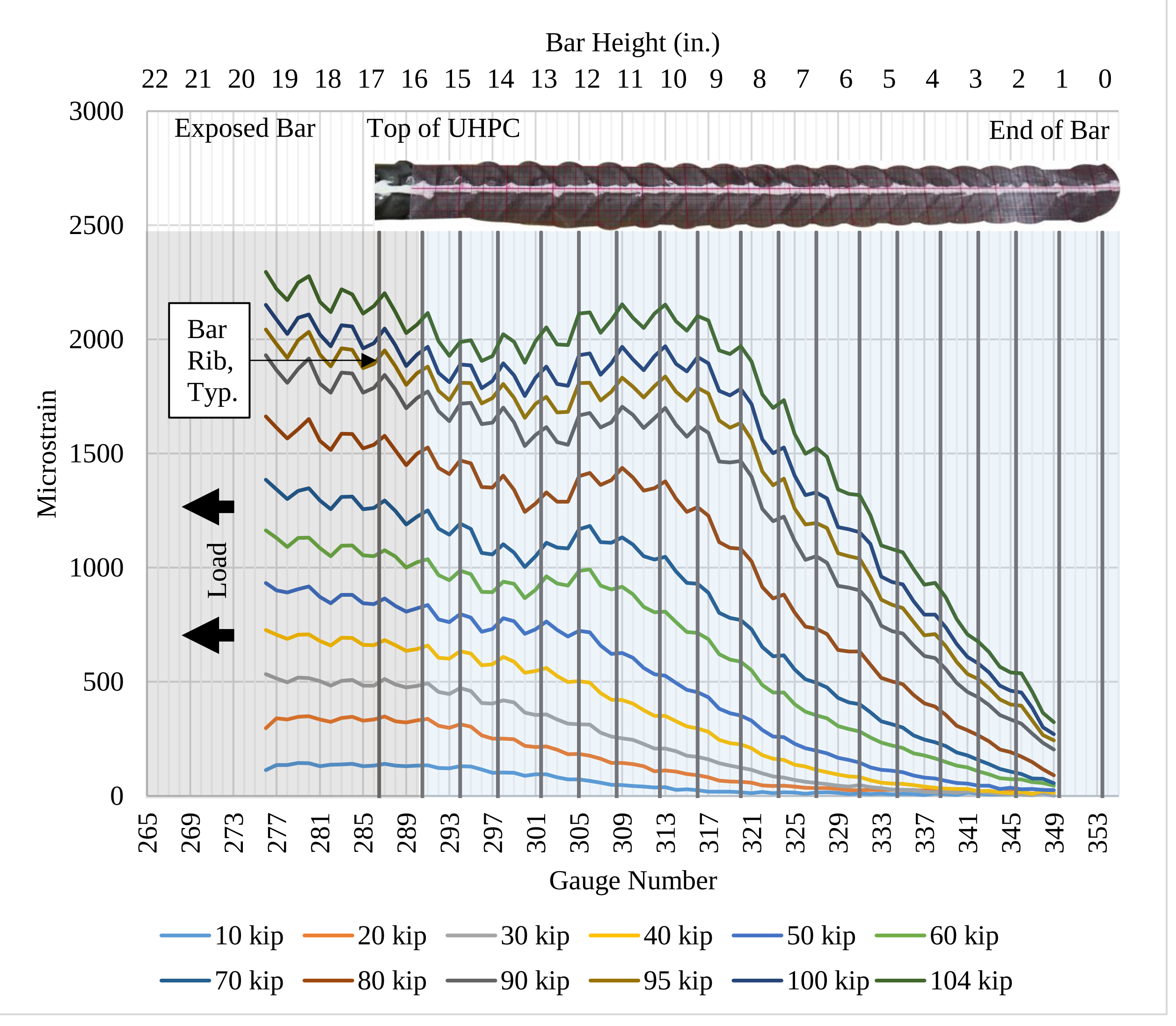

Figure 28: Microstrain along #11 bar length (Test A)

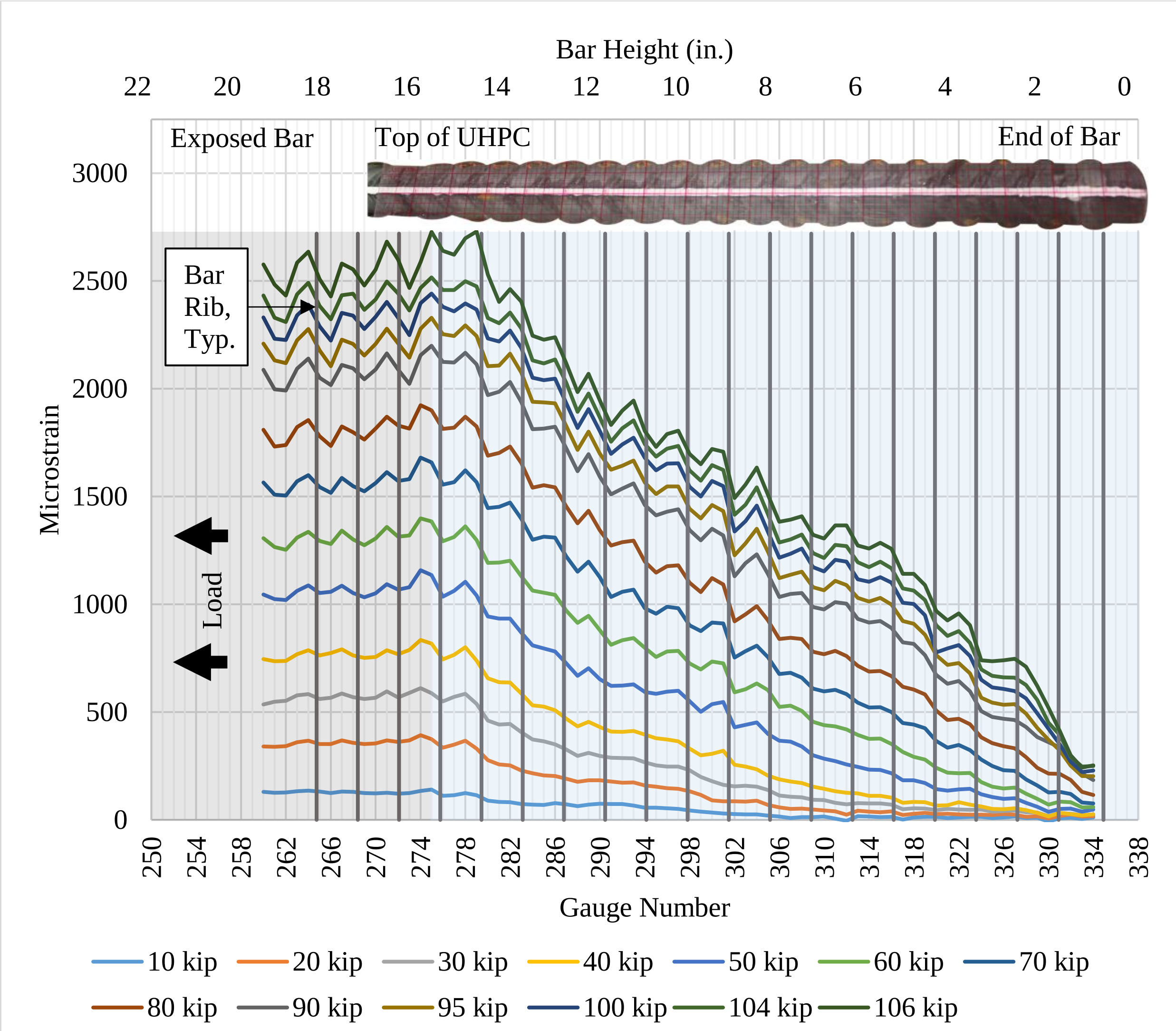

Figure 29: Microstrain along #11 bar length (Test B)

Figure 31 also presents the external load compared to microstrain at sensing locations at 1 in. spacing. For the test presented in Figure 31, the fiber optic strain gauge was installed so that sensing locations 335 through 330 were above the top of the UHPC and the numbering continued to decrease along the bar embedded in UHPC, i.e., the location number decreased as the level of bar embedment increased. All sensing locations along the length of the bar show the same behavior, despite being at different strain values. For the sensing locations adhered to the exposed portion of the bar (331 and 335), the load vs. strain chart is a typical stress-strain diagram for a reinforcing bar, with a clear yield plateau and transition to strain hardening. As embedment in the UHPC increased, the strain increases along the yield plateau decreased, as can be seen in the data recorded at locations 319, 323 and 327. The bar was embedded 0.56 in. into UHPC at location 327, 1.56 in. at location 323 and 2.56 in. at gauge location 319. For gauge locations where the bar is embedded 3.56 in. and more (283-315), there is no plateau apparent, as shown in Figure 31. At higher bar embedment levels, the UHPC prevented the embedded bar from yielding. At higher embedment of 7.56 in. and more, corresponding to locations 299 – 283, the maximum microstrain achieved at the location was reduced as well. The maximum microstrain observed at 7.56 in. embedment at gauge location 299 was 7,464. At increased embedment lengths, the maximum microstrain decreased to 2626 at 9.56 in. embedment (location 291) and 925 at 11.56 in. embedment (location 283). At 6.56 in. and less embedment length (locations 303-335), the maximum microstrain observed exceeded 14,000. Thus, for this particular test, at an embedment length of 7.56 in. and more, the UHPC reduced the maximum strain which could be achieved in the bar at that location. For the test presented in Figure 31, the crack gauge indicated that a crack occurred at approximately 100 kips. At that load, the fiber optic strain sensors seem to exhibit a slip and engauge behavior, circled in red in the figure.

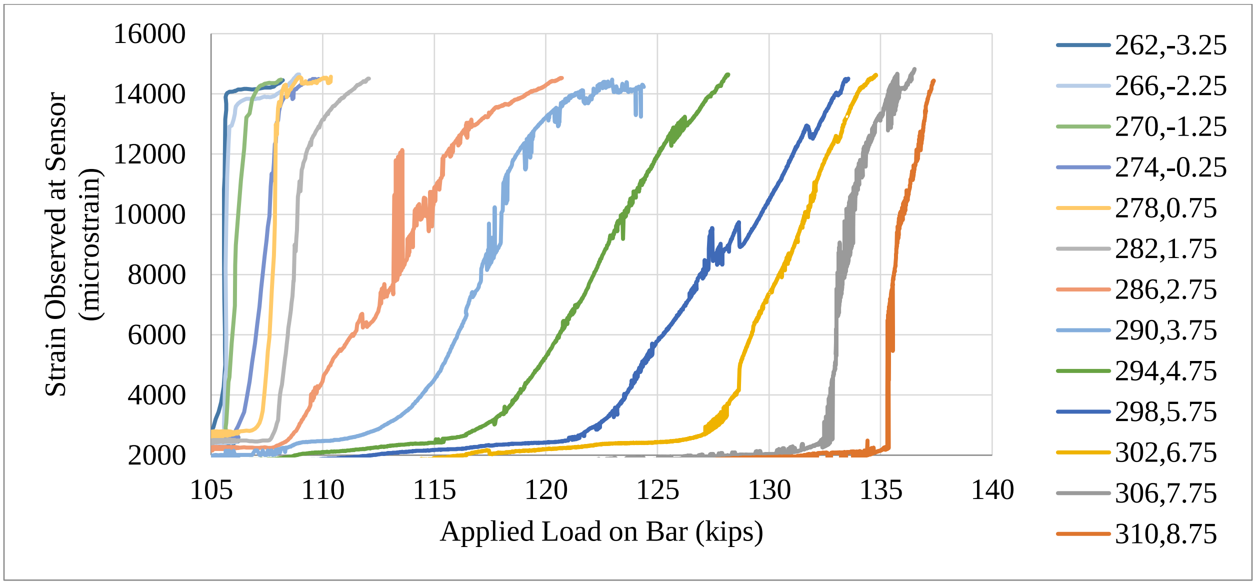

Figure 30: Microstrain vs. load for #11 bar (Test B)

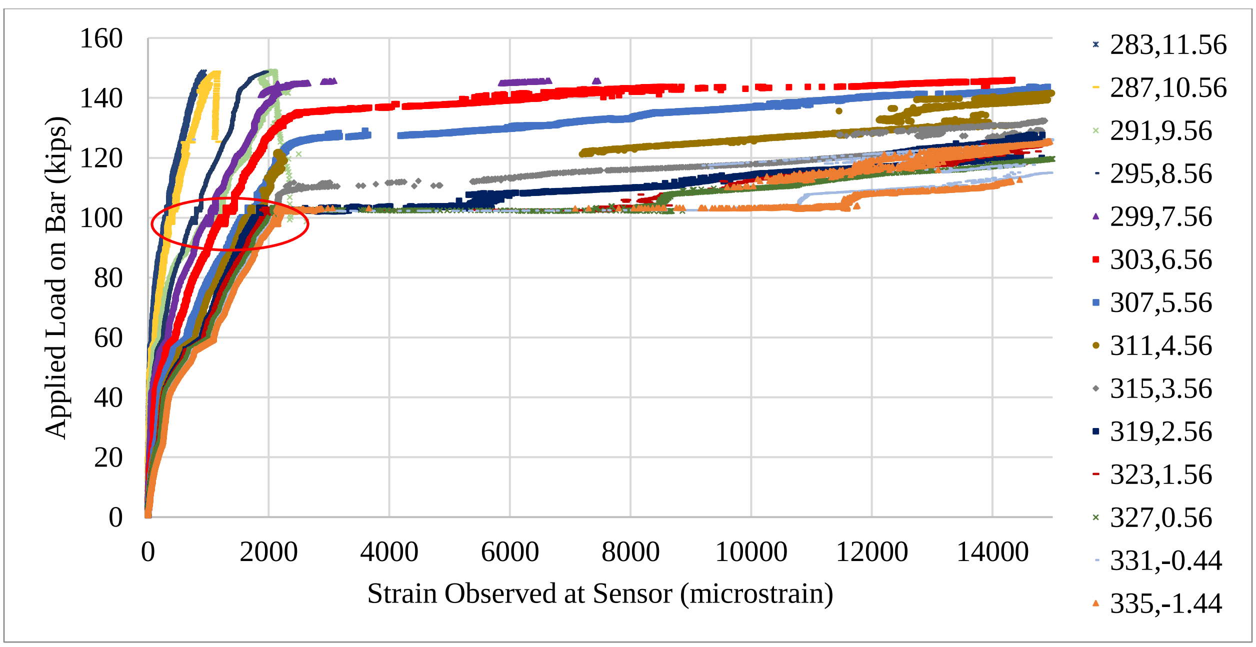

Figure 31: Load vs. microstrain along #11 bar (Test C)

Chapter 5. Discussion

The required embedment for various bar sizes and cover in UHPC was determined from the information presented in the previous Required Splice Length section. The reinforcing bar was considered to be fully developed if at least 75-ksi reinforcing bar stress was achieved when the UHPC compressive strength was 14 ksi or lower. Based on the testing completed during this project, the minimum required reinforcing bar embedment and splice lengths vary based on the bar size and UHPC cover and are presented in Table 3. The requirements for #8 bars are the same as given in FHWA (2014). For the #8 bars with 1.75-in. cover, two of the 14 tests exhibited UHPC failure before 75 ksi was reached in the reinforcing bar. However, the reinforcing bars had completely yielded and were exhibiting strain hardening behavior at failure, reaching a bar stress of 71.4 ksi and 72.4 ksi. So, the provided embedment and splice lengths were deemed acceptable. For the #10 reinforcing bars with 1.75-in. cover, two of the 13 tests exhibited UHPC failure before 75 ksi stress was achieved in the reinforcing bar. The reason for UHPC failure before the reinforcing bar stress reached 75 ksi was attributed to shrinkage cracks noted in the UHPC; so the provided embedment and splice lengths were deemed acceptable.

Table 3: Required Embedment and Splice Lengths

		Required Embedment Length in Bar Diameters				Required Splice Length in Bar Diameters			
		Bar Size				Bar Size			
		#8	#9	#10	#11	#8	#9	#10	#11
Cover	1.75 in.	8	9.8	11.7	12.9	6	7.3	9.7	11.1
	2.75 in.	-	-	-	11.3	-	-	-	9.7
	3.75 in.	8	6.9	8.4	9.3	6	5	6.6	7.3

To describe the influence of confinement on bond characteristics, the normalized bond strength was plotted versus the normalized cover and is shown in Figure 32. The normalized bond strength is equal to the bond strength, calculated as development length divided by the square root of the concrete strength. The normalized cover is equal to the concrete cover divided by the reinforcing bar diameter. The experimental results are presented as two data series, with the filled markers showing the experimental results for which the test was stopped due to failure in the UHPC. For instance, when a splitting crack formed to the side face of the UHPC or a cone-shaped tensile failure occurred. The experimental results from this work were compared to the curve suggested by Marchand et al. (2016), which would produce an unconservative estimate of bond strength. In 53% of the experimental tests, the bond strength was below what would have been predicted by the Marchand et al. curve. The difference may be due to fiber volume or reinforcing bar size. Marchand et al. tested #3-#5 reinforcing bars in a UHPC with 2.5% steel fiber by volume and additional polypropylene fibers, while this research tested #8-#11 reinforcing bars in UHPC with 2% steel fiber by volume. The curve which would produce a 95% confidence interval is shown in Figure 32 and represented by Equation 7, where τ_{max} is the bond strength (maximum average bond stress), f_c' is the concrete strength, c is the concrete cover, $\emptyset$ is the reinforcing bar diameter, $f_{s.max}$ is the maximum bar stress, d_b is the bar diameter, and l_E is the embedment length. Marchand et al. noted a plateau at a normalized cover equal to four. For this research, the predicted bond strength with a normalized concrete cover above four is unknown because the maximum normalized cover tested for this research was less than four. However, a plateau is evident in the experimental results below the normalized cover of 4. For a 95% confidence interval, the plateau is at a normalized bond strength equal to 0.70, as indicated in Equation 7.

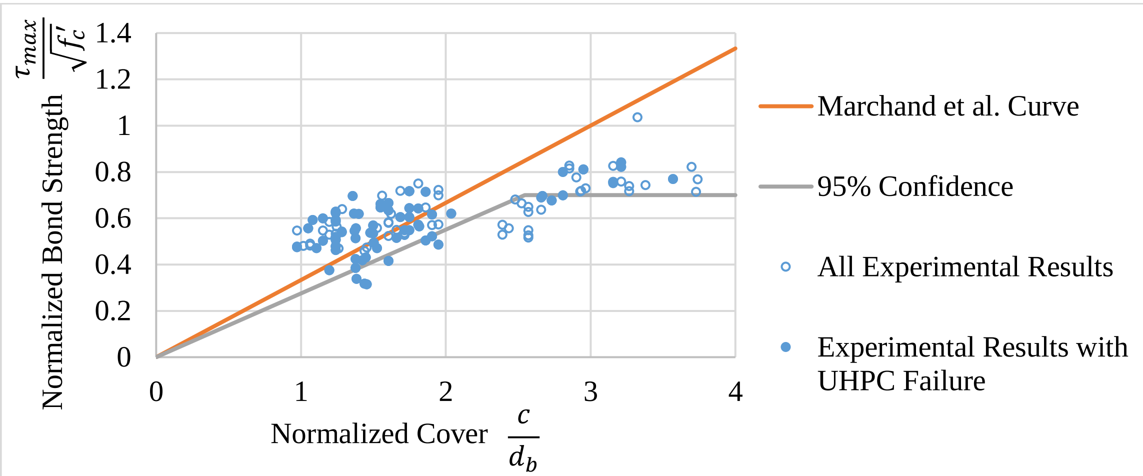

Figure 32: Normalized bond strength vs. normalized cover

Equation 7: Confinement and Bond Stress 95% Confidence Curve

$$\frac{\tau_{max}}{\sqrt{f'_c}} = 0.275\frac{c}{\emptyset} < 0.70$$

Equation 8: Bond Strength

$$\tau_{max} = \frac{f_{s.max} \times d_b}{4 \times l_E}$$

As embedment in UHPC along the reinforcing bar increased, the form of the load-strain diagram for the reinforcing bar transitioned from a typical load-strain (or stress-strain) diagram for a reinforcing bar, to a form with a shorter length of flat yield plateau, then to a diagram with no zero slope yield plateau, and then to a shape without significant yielding. Pictorially, this transition is shown in Figure 33, with Figure 33 (a) being the diagram at a shallow embedment of reinforcing bar and (b), (c) and (d) showing the form of the load-strain diagram at discrete locations along the bar as embedment increased. The solid line is the axial strain in the reinforcing bar at the embedment of interest. In Figure 33 (b), (c) and (d), the dashed line is the axial strain in the reinforcing bar at shallow embedment - a duplicate of Figure 33 (a). In each of these diagrams, the axial load is the external load applied to the splice, consisting of both UHPC and reinforcing bar. Other than at shallow embedment, the load is shared by the reinforcing bar and UHPC. The contribution of load resistance from the UHPC, individually, is equal to the distance between the solid and dashed lines in Figure 33 (b), (c) and (d).

As the embedment of the reinforcing bar increased, the initial slope of the load-strain diagram (from zero stress to 60 ksi) at discrete locations along the bar increased as well, as shown in Figure 31. The slope of the initial portion of the stress-strain diagram versus the embedment along the length of the bar is graphed in Figure 34 for #9 bars and in Figure 35 for #11 bars. The series names shown in each graph denotes the [Bar Size]-[Embedment Length in Bar Diameters]-[Splice Length in Bar Diameters]-[Target Center to Center Bar Spacing in in. or "C" for Contact Splice]-[Test Number]. If two fiber optic gauges were adhered to a single reinforcing test bar, the test number includes an "A" or "B" indicating the gauge shown. The relationship between bar embedment and initial stress-strain slope follows a power trend. A trendline and equation which is based on all tests completed for the #9 bar size is presented in Figure 34. For the #11 bar size, the trend in the data is different for the two different embedment/splice lengths tested. To fit a curve to the data, it was separated into two sets. The first set included tests with 11.3 or 11.4d_b embedment length and 9.7d_b splice length. The second set included tests with 9.4d_b embedment length and 7.5d_b splice length. A different coefficient was required in the power equation for the trendline fit to each set of data, as shown in Figure 35.

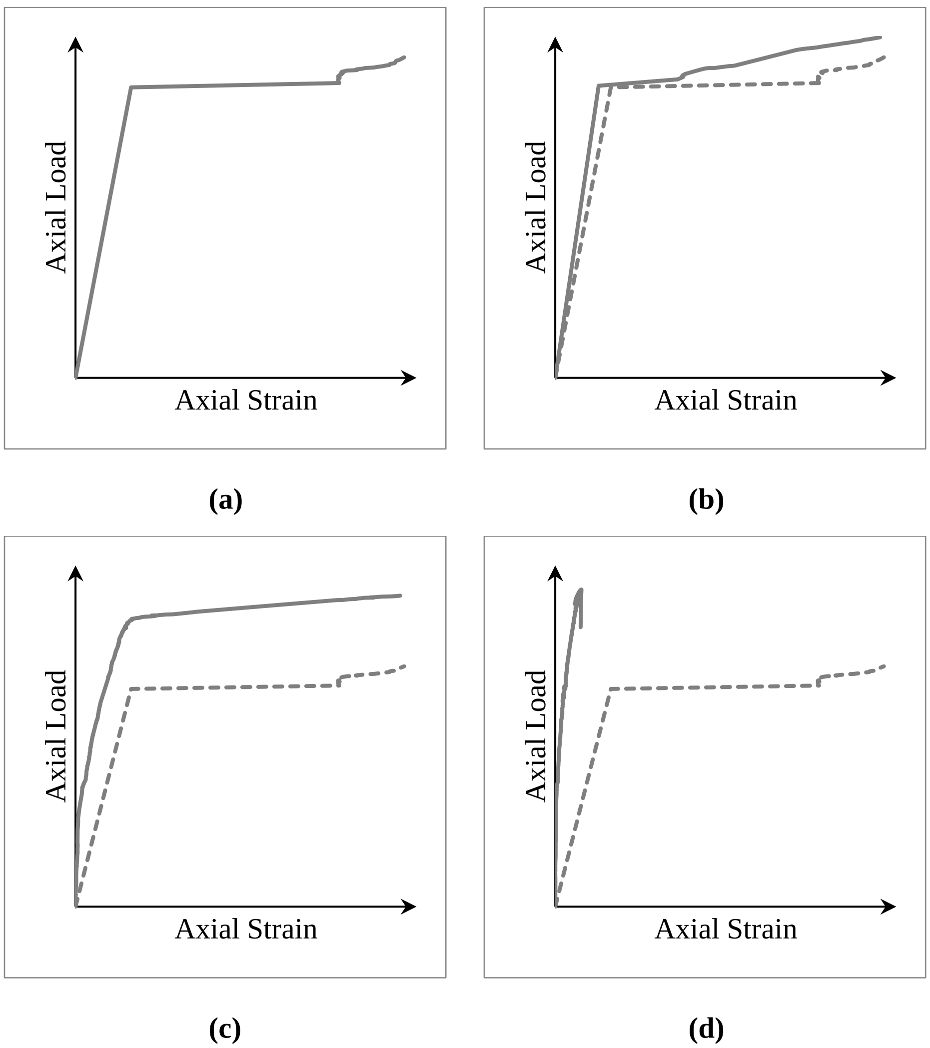

Figure 33: Load vs. strain for reinforcing bar at multiple embedment depths

The strain along the embedded portion of the reinforcing test bar could typically be described as uniformly linear along the bar length before the bar began to yield. After yielding, the strain became bilinear, with higher strain at shallower embedment, as shown in Figure 36. The measured strain in #9 bars is shown in Figure 37 (a) before yielding (at 60 ksi reinforcing bar stress) and Figure 37 (b) after yielding (at 75 ksi reinforcing bar stress). Similar data is presented in Figure 38 for #11 bars.

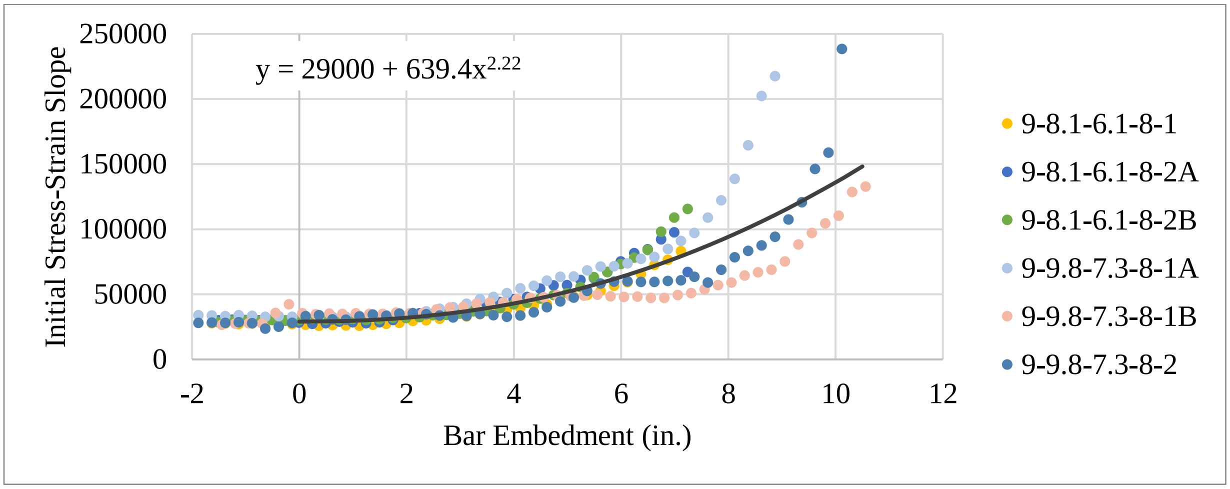

Figure 34: Initial load-microstrain slope vs. bar embedment for #9 bars

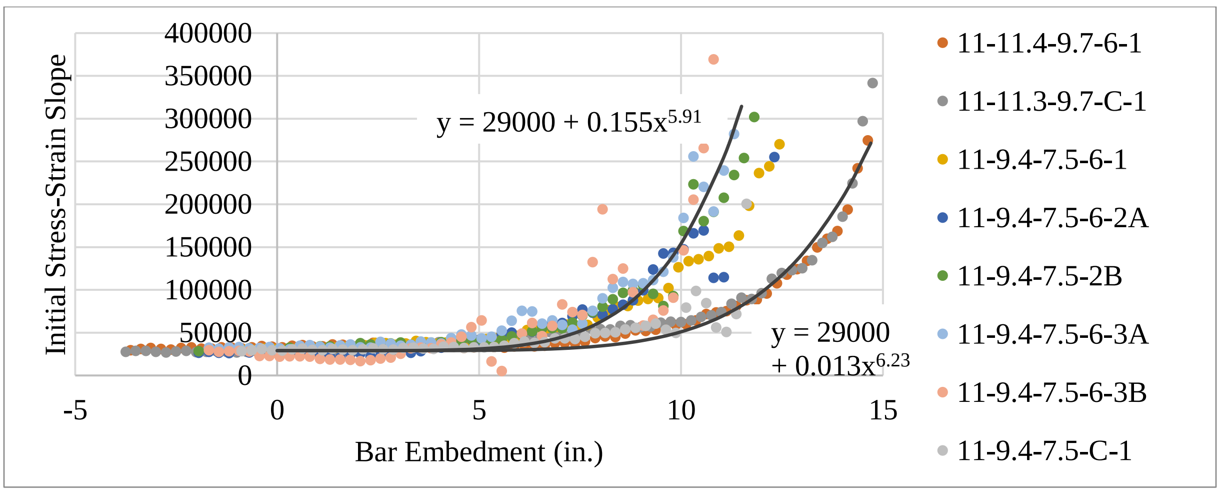

Figure 35: Initial load-microstrain slope vs. bar embedment for #11 bars

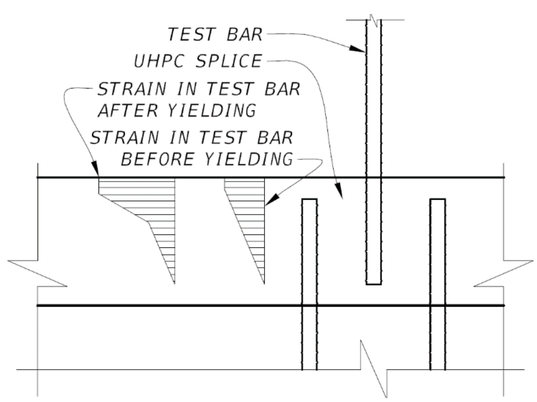

Figure 36: Strain diagram for reinforcing test bar

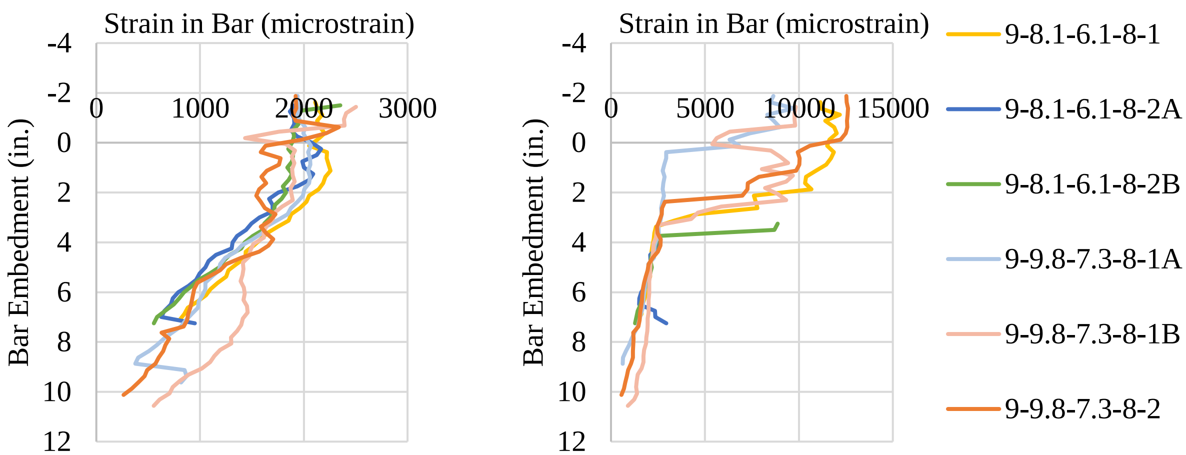

(a) (b)

Figure 37: Bar embedment vs. microstrain for #9 bars (a) at 60 ksi in the free end of the bar (before yielding), and (b) at 75 ksi in the free end of the bar (after yielding)

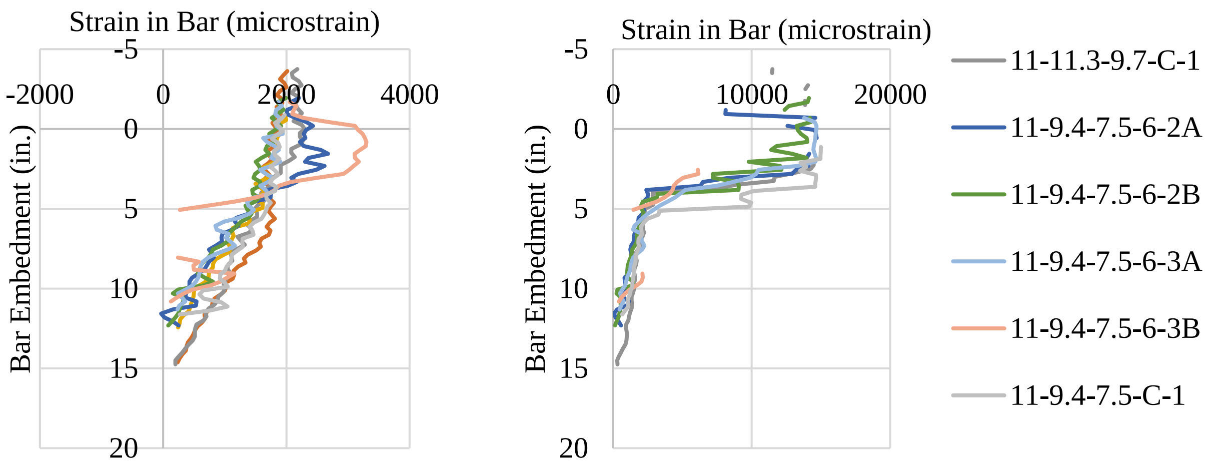

(a) (b)

Figure 38: Bar embedment vs. microstrain for #11 bars (a) at 60 ksi in the free end of the bar (before yielding), and (b) at 75 ksi in the free end of the bar (after yielding)

A hypothesis describing the internal behavior of UHPC in a spliced reinforcing bar connection is suggested herein based on the information collected in this research. The splice of the reinforcing bars can be idealized as having struts and ties of UHPC between the test bar and adjacent bars, as shown in Figure 39. At shallow embedment, adhesion and friction resists pull-out of the reinforcing bar, causing tensile forces in the UHPC in the shallow embedment region. At the strain when the reinforcing bar begins to yield, the UHPC has passed the first cracking stage, as defined in the material characterization shown in Figure 40. Direct tension test results for the material used in this research is shown in Figure 41 for three representative samples. The direct tension tests were conducted with 17 in. long and 2 in. square prismatic sections using the test method described in Graybeal and Baby (2013). As shown in Figure 41, beyond first cracking, the UHPC used for this project exhibits a plateau in the multi-cracking stage and as strain increases, stress resistance decreases during the crack straining and localized phases. At shallow embedment, pull-out of the bar is resisted primarily by friction, which causes tensile stresses in the UHPC. Beyond first cracking, increasing strain does not result in increased load resistance in the UHPC used for this project. Thus, the UHPC does not affect the load-strain diagram for the reinforcing bar, at shallow embedment. At shallow embedment and exposed portions of the reinforcing bar the load-strain diagram is similar and can be represented by Figure 33 (a).

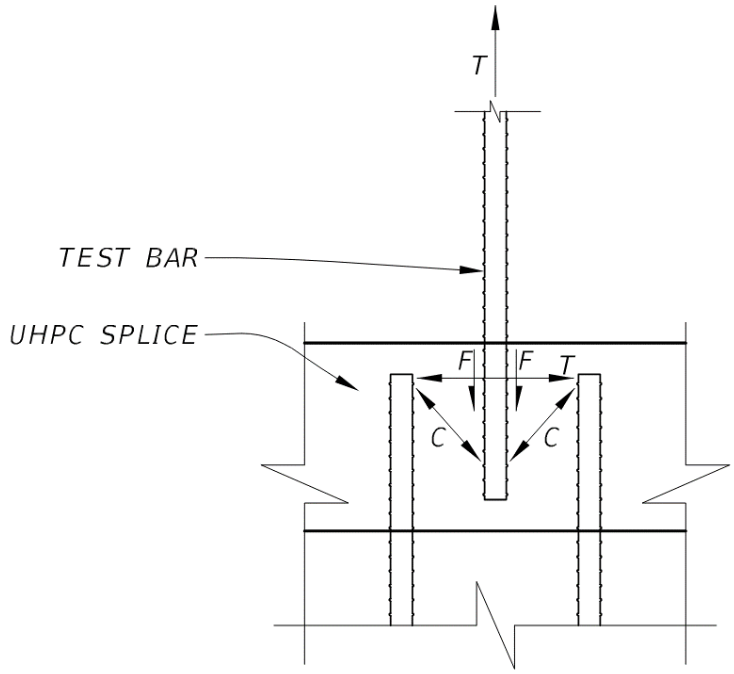

Figure 39: Free-body diagram of UHPC splice

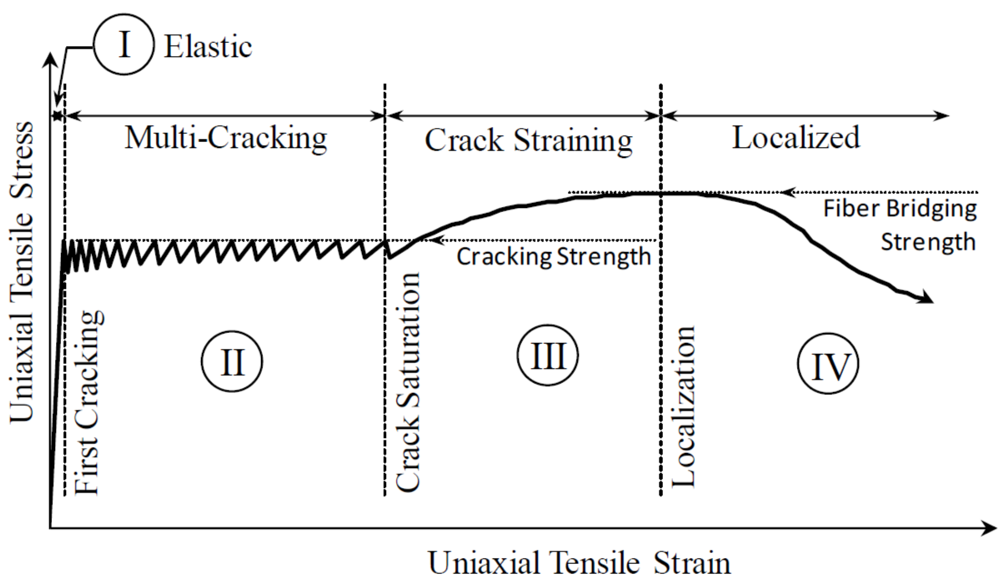

Figure 40: Idealized uniaxial tensile mechanical response of a UHPC per Graybeal & Baby (2013)

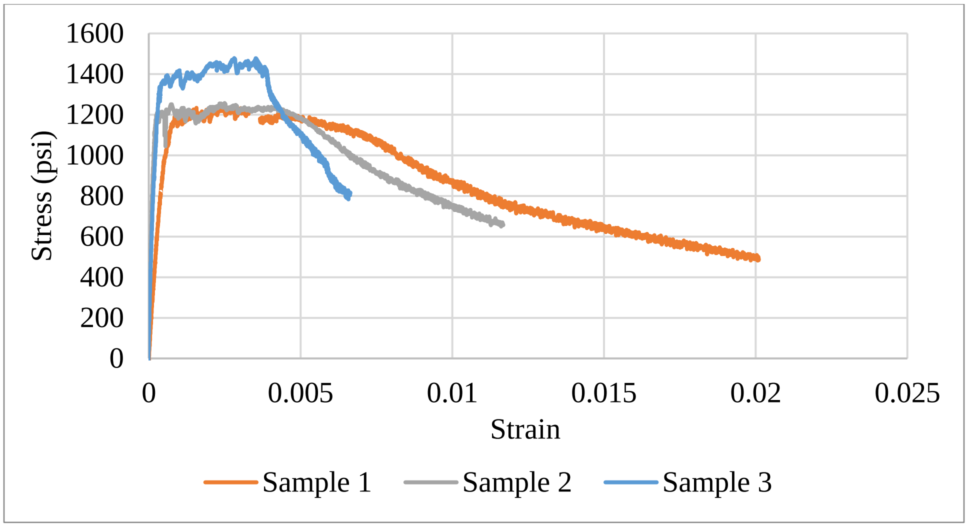

Figure 41: Stress vs. strain for direct tension test of 3 samples

As embedment increases along the reinforcing bar, resistance to pull-out of the reinforcing bar is from compression struts in UHPC, between the test bar and adjacent reinforcing bars, as shown in Figure 38. Unlike the tensile stress-strain curve, the stress-strain curve for UHPC in compression exhibits a curve with increasing stress associated with increasing strain until failure, as shown in Figure 42. Load cannot be increased without added strain, so the yield plateau at deeper embedment along the reinforcing bar is lost, as shown in Figure 33 (c) and (d). Because strain in the compressive UHPC strut will not increase without application of additional load, yielding of the reinforcing bar is prevented at increased levels of embedment, where the UHPC compressive strut is effective.

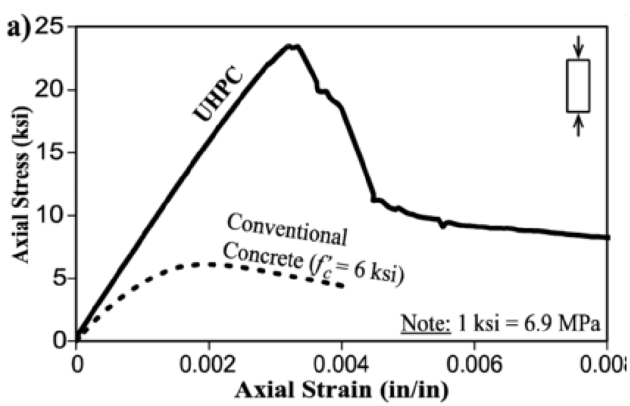

Figure 42: UHPC in compression, per El Helou & Graybeal **(2019)**

To counteract the force in compression struts, tension ties must be idealized transverse to the test bar. Evidence of those tension ties is apparent in the vertical cracks on the face of the UHPC which occurred during 45 of the 127 tests completed. An example of the vertical side crack is shown in Figure 43 (a). An example of a crack typical for a cone-shaped failure mode is shown in Figure 43 (b). Those types of cracks were observed in 18 of the 127 tests completed. Ten tests exhibited both types of cracks. The type of crack shown in Figure 43 (b) was parallel to the assumed compression struts in the UHPC.

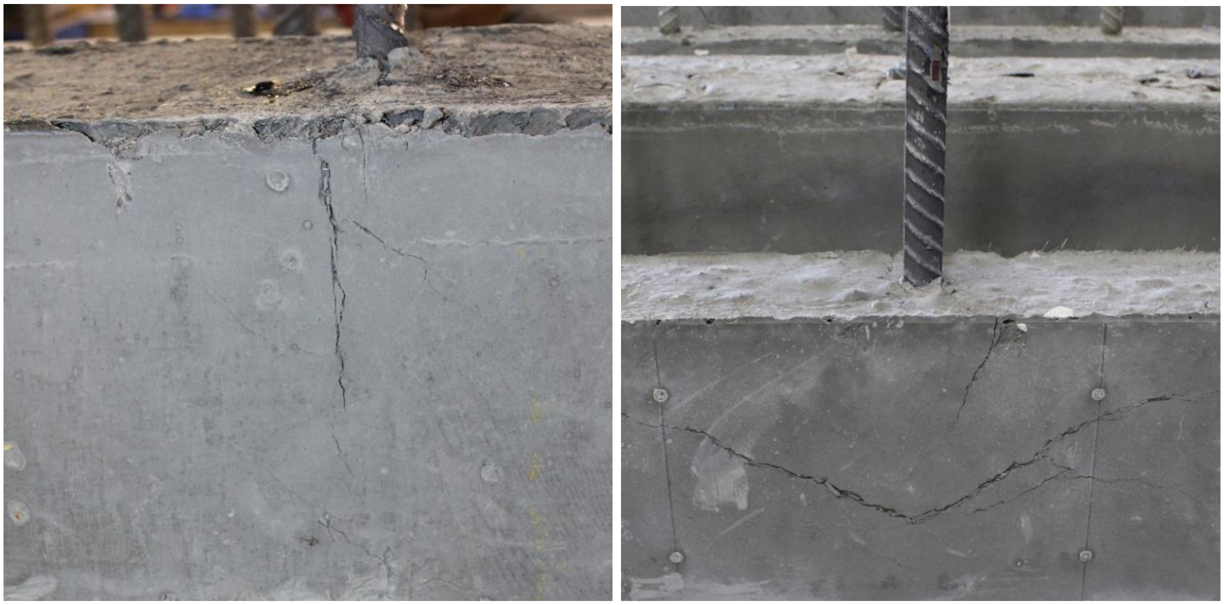

(a) (b)

Figure 43: UHPC failure modes

Slip was previously described in Equation 6 as the difference between the displacement gauges which referenced the UHPC and the displacement gauges which referenced the reinforcing bar, corrected for strain in the short length of bar between the top of the UHPC and the location where the displacement gauge attached to the bar. The measured slip was used along with the fiber optic strain to determine the relative displacement between the UHPC and reinforcing bar, at fiber optic sensing locations along the length of reinforcing bar embedded in UHPC. The relationship is shown in Equation 9, where δ is the relative displacement, $\varepsilon(x)$ is the strain along the bar, and l_g is the gauge length, 0.25 in. To adjust for undulations in the fiber optic strain measurements due to the reinforcing bar deformations, the measured fiber optic strain, $\varepsilon(x)$, was smoothed using a moving 3rd order polynomial interpolation over an interval at each sensing location of +/- 0.75 in. The fiber optic strain measurement was additionally used to determine the stress in the reinforcing bar at each discrete location, based on the reinforcing bar material characteristics measured in the free length of the reinforcing bar during the test or the steel modulus of elasticity. The calculation of reinforcing bar stress is shown in Equation 10, where σ is the stress in the reinforcing bar and E is the modulus of elasticity. Below the yield stress of the reinforcing bar, the stress is equal to strain times the steel modulus of elasticity, assumed to be 29,000 ksi. Above the yield stress of the reinforcing bar, the stress is determined by a curve fit to the stress-strain measurements collected during the reinforcing bar test. The local bond stress is calculated per Equation 11 from Marchand et al. (2016).

Equation 9: Relative Displacement between Reinforcing Bar and UHPC along Embedment

$$\delta(x) = Bar\ slip - \sum_{0}^{x} \varepsilon(x) \times l_g$$

Equation 10: Reinforcing Bar Stress along Embedment

$$\sigma(x) = \begin{cases} \dfrac{\varepsilon(x)}{10^6} \times E, & \sigma(0) < f_y \\ f(\sigma, \varepsilon), & \sigma(0) \geq f_y \end{cases}$$

Equation 11: Local Bond Stress

$$\tau(x) = \frac{d_b}{4} \frac{d\sigma}{dx}(x)$$

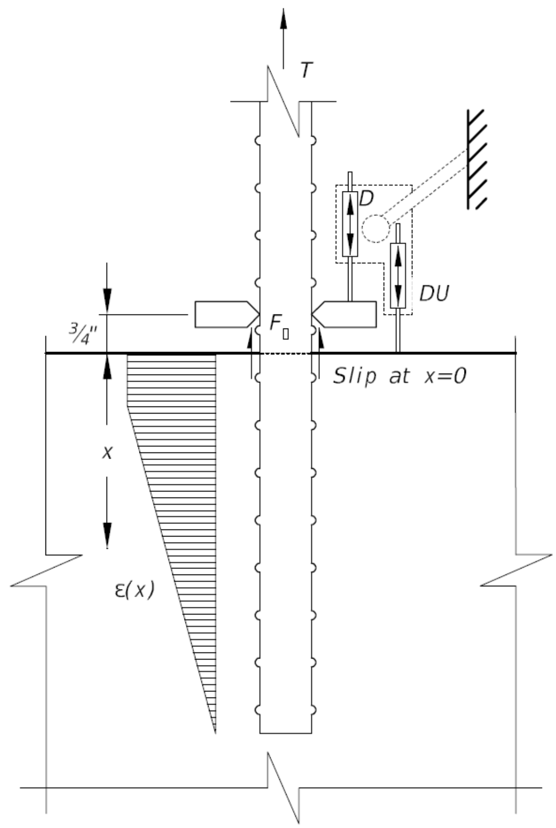

Figure 44: Method to obtain local reinforcing bar stress and relative displacement

The relationship between relative displacement and local bond stress is shown in Figure 45 for a select reinforcing bar test for five different stress levels in the free length of the reinforcing bar. The test shown was on a #9 reinforcing bar with an embedment and splice length equal to 8.2 and 6.2 times the bar diameter, respectively. The average clear side cover was equal to 3.781 in. and the average clear bar spacing was 7.438 in. At time of testing, the UHPC compressive strength was 13.51 ksi. The local bond-slip relationship proposed by Marchand et al. (2016) is additionally shown in Figure 45 for comparison purposes. Differences in the observed behavior and proposed bond-slip relationship could be due to fiber volume or reinforcing bar size. Marchand et al. tested #3-#5 reinforcing bars in a UHPC with 2.5% steel fiber by volume and additional polypropylene fibers, while the data presented is for a #9 reinforcing bar in UHPC with 2% steel fiber by volume. While bond stress versus relative displacement data was collected for 12 different reinforcing bond tests, most of the data had significant scatter which made fitting a curve to all collected data difficult.

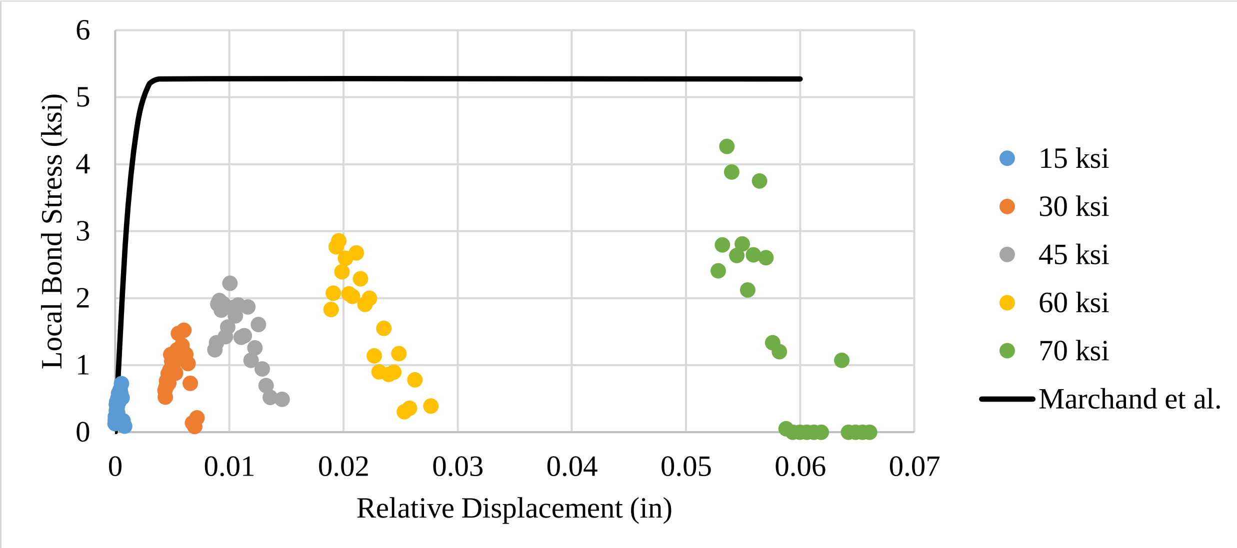

Figure 45: Local bond stress vs. relative displacement for #9 bar

The local bond stress calculated using Equation 11 indicates that there are peaks in the bond stress along the embedded portion of the bar, as shown in Figure 45. The bond stress is not constant along the reinforcing bar length embedded in UHPC. At low stress levels in the free length of the reinforcing bar (15-30 ksi), the peaks occur at shallower embedments than at higher stress levels (45-70 ksi). When the global bond stress is calculated using Equation 2, it will be a lower value than the local bond stress calculated using Equation 11. The global bond stress versus slip for the same reinforcing bar test is shown in Figure 47. The maximum global bond stress is less than 3 ksi, while a local bond stress over 4 ksi was observed, when the stress in the free length of the reinforcing bar was equal to 70 ksi.

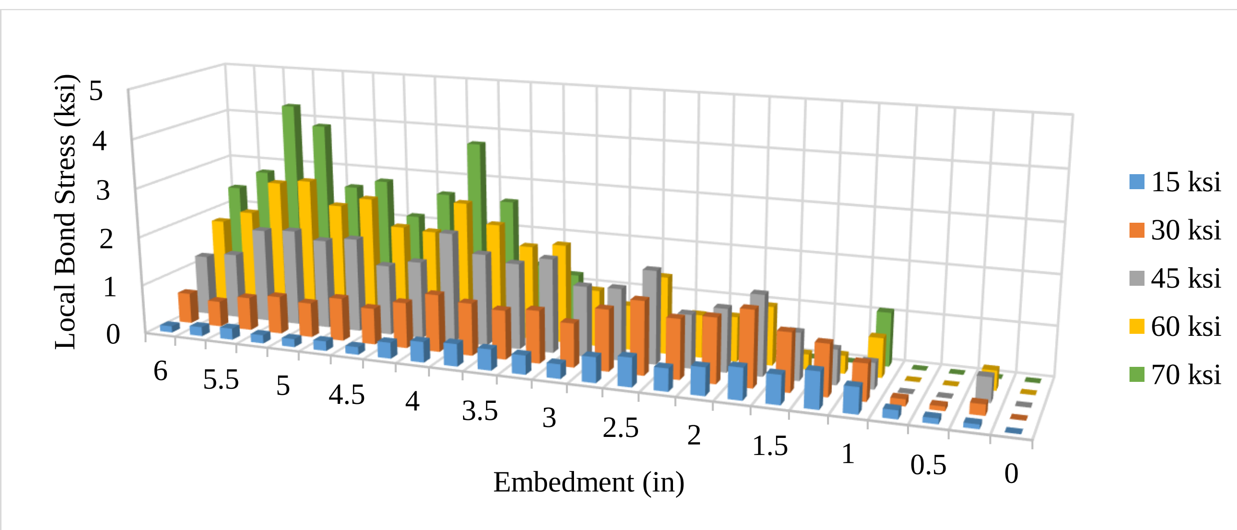

Figure 46: Local bond stress vs. embedment for #9 bar

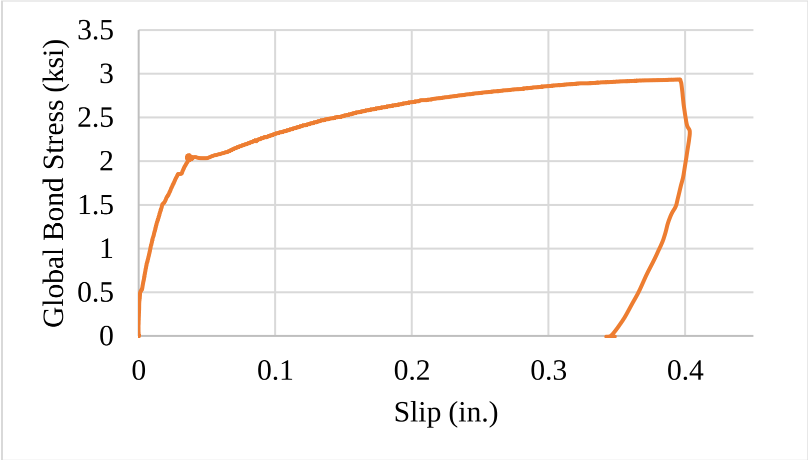

Figure 47: Global bond stress vs. slip for #9 bar

Chapter 6. Practical Application

Introduction

This section considers the feasibility of using UHPC for four different details selected from recent projects which used prefabricated bridge elements. The details chosen address connections between various types of bridge components, including drilled shafts, piles, bent caps, footings, piers, and beams. Each connection is presented first unmodified, exactly as presented in the actual construction drawings. For each connection, one or two modified concept detail(s) are presented, which use UHPC as a connecting medium. Advantages, disadvantages, and relative merits are recognized for the original and modified detail(s). This evaluation considers allowable tolerances, UHPC volume, inspectability, and whether design requirements are met.

Both vertical and horizontal tolerances for details with UHPC closures are compared to the original details. In general, tolerances are improved with the use of non-contact lap splices. Contact splices typically require extreme control over tolerances, similar to the tight tolerances when using grouted couplers. For most cases, larger tolerances are allowed by non-contact splices. However, the Footing-to-Column Connection presented herein provides an example where a contact splice results in a larger tolerance than a non-contact splice.

Easy inspectability is preferred for UHPC details. A detail is considered non-inspectable if the UHPC is cast in a blind pocket. It is inspectable if forms can be removed and the vertical surface of the UHPC and edge of the interface between the UHPC and prefabricated component can be viewed. Constructability is generally discussed but is not particularly important in this evaluation because the compared details have similar characteristics in regard to the size of prefabricated elements, shims, and bracing. The primary constructability aspect is the tolerances, as discussed above.

Drilled Shaft to Bent Cap Connection

The first detail presented is a drilled shaft to bent cap connection recently used for a bridge construction project. The bent caps were prefabricated with 4-in. diameter steel ducts. Dowel bars were cast in the drilled shaft and extended into ducts in the bent cap. The ducts were filled with precision grout to join the drilled shaft and bent cap. The connection detail allows for limited construction tolerance between the dowel bar and metal duct, which proved to be a problem during construction. For that project, the work schedule was not significantly affected because the bent caps were cast after the dowel bars were placed, so the duct placement was modified to match the as-built location of the bars. But, for accelerated bridge construction, it would be preferable for the bent cap to be constructed before drilled shafts, so that construction can continue uninterrupted once the drilled shafts are completed.

For connecting a drilled shaft or column and bent cap, a UHPC connection may facilitate accelerated bridge construction by allowing for larger tolerances between field work and prefabricated components. Research has been completed by Tazarv and Saiidi (2014) to modify the original detail to use UHPC instead of precision grout for filling corrugated ducts. The UHPC provides for less development length than required for grout and less damage during cyclic loading. However, the tolerances are not improved. Option 1, shown in Figure 49, allows for a much larger tolerance than the original detail (see Table 4) and requires less filler material than option 2. Option 2, shown in Figure 50, allows a slightly lower tolerance than option 1, but the closure material is more easily inspected. A third option for which the UHPC closure is moved to the drilled shaft is shown in Figure 51. Option 3 requires a larger volume of UHPC but provides the largest tolerance and is easily inspectable. For all three options with UHPC closure connections, the design requirements are met. The required development length within the precast bent cap is 32 in. for the #9 dowel bars extending from the bent cap into the closure pour. As currently shown, at least 36 in. of development length is provided, with at least $6d_b$ splice length and $8d_b$ embedment length provided in the UHPC closure. Although options 1 and 2 limit the volume of UHPC required in the connection, option 3 is the detail recommended for further research purposes. The option 3 detail allows for greater tolerance than the other options 2 and requires simpler forming processes.

Table 4: Drilled Shaft or Column to Bent Cap Connection Comparison

	Original Detail	Option 1	Option 2	Option 3
Vertical Tolerance	1.5 in.	2 in.	2 in.	2 in.
Horizontal Tolerance	1.4 in.	4.4 in.	2 in.	4.9 in.
Filler Material Volume (UHPC, Grout or Concrete)	4 cubic ft	6 cubic ft	7.8 cubic ft	12.9 cubic ft
Inspectable?	No	No	Yes	Yes
Design Requirements Met?	Yes	Yes	No	Yes

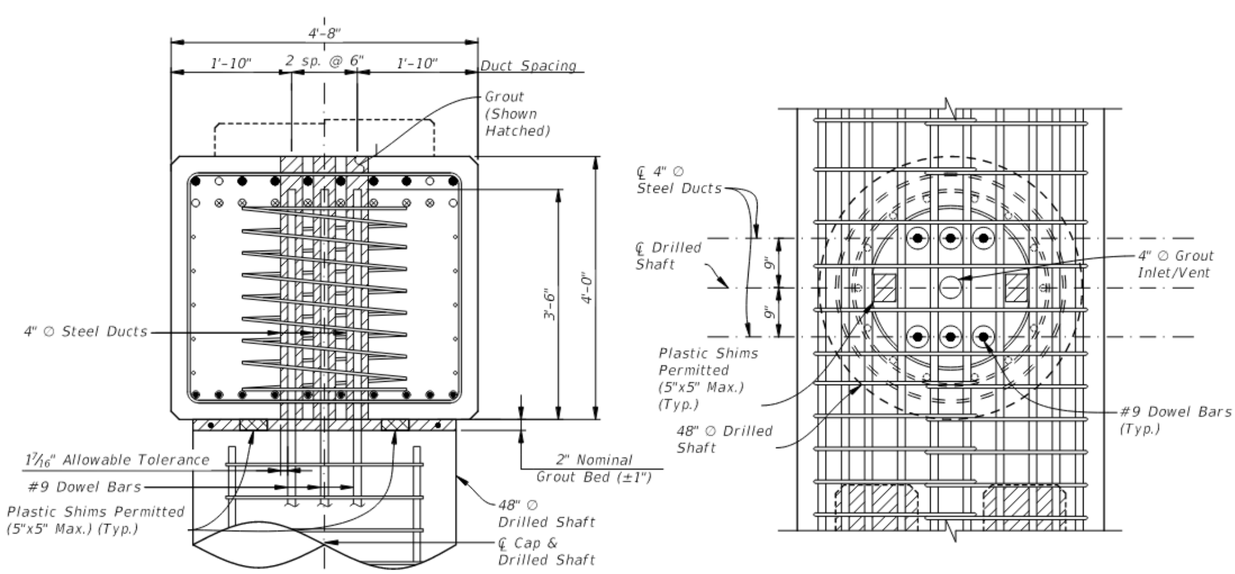

Figure 48: Drilled shaft or column to bent cap connection

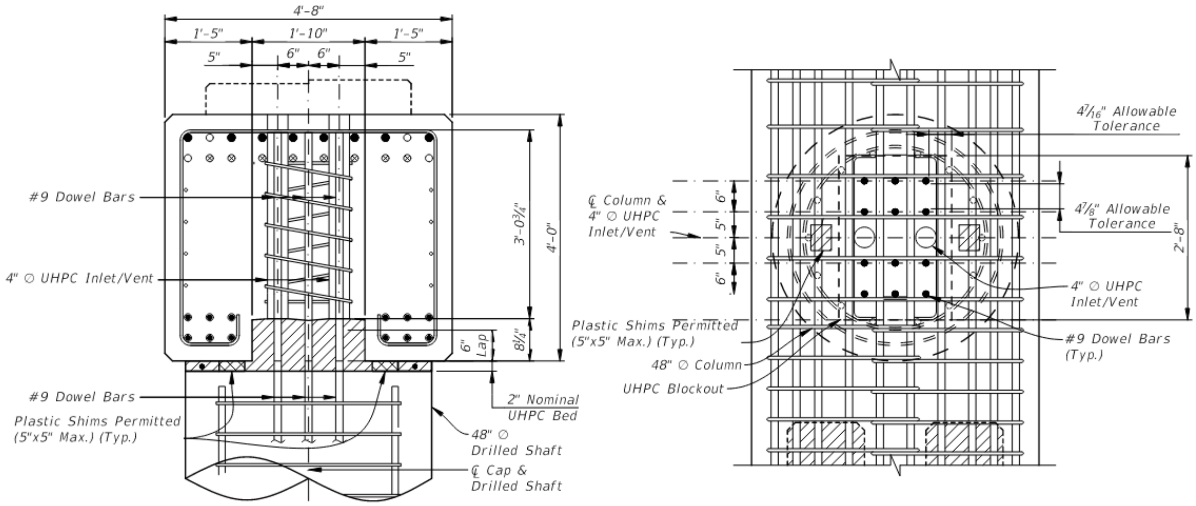

Figure 49: Modified for UHPC drilled shaft or column to bent cap connection, option 1

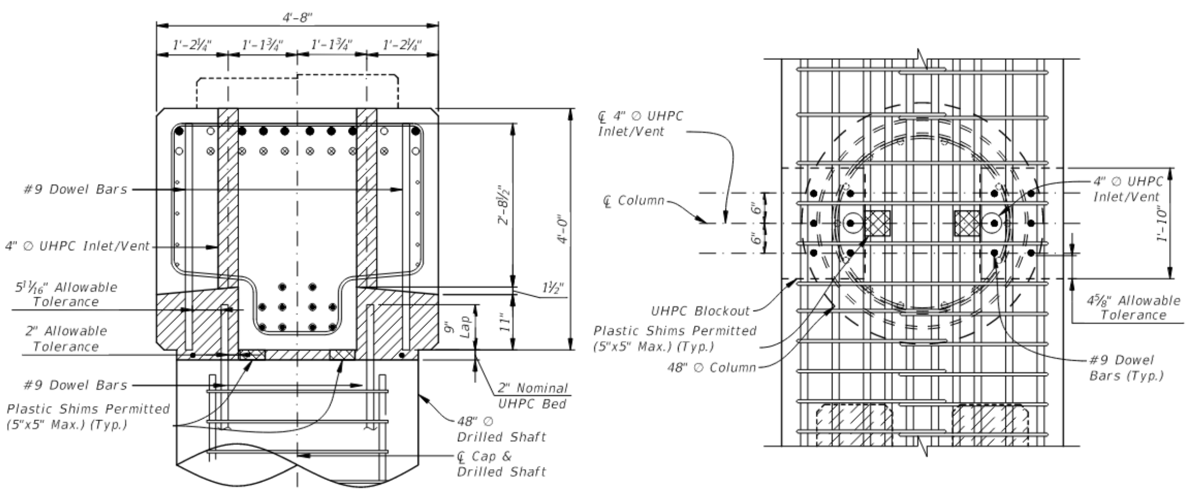

Figure 50: Modified for UHPC drilled shaft or column to bent cap connection, option 2

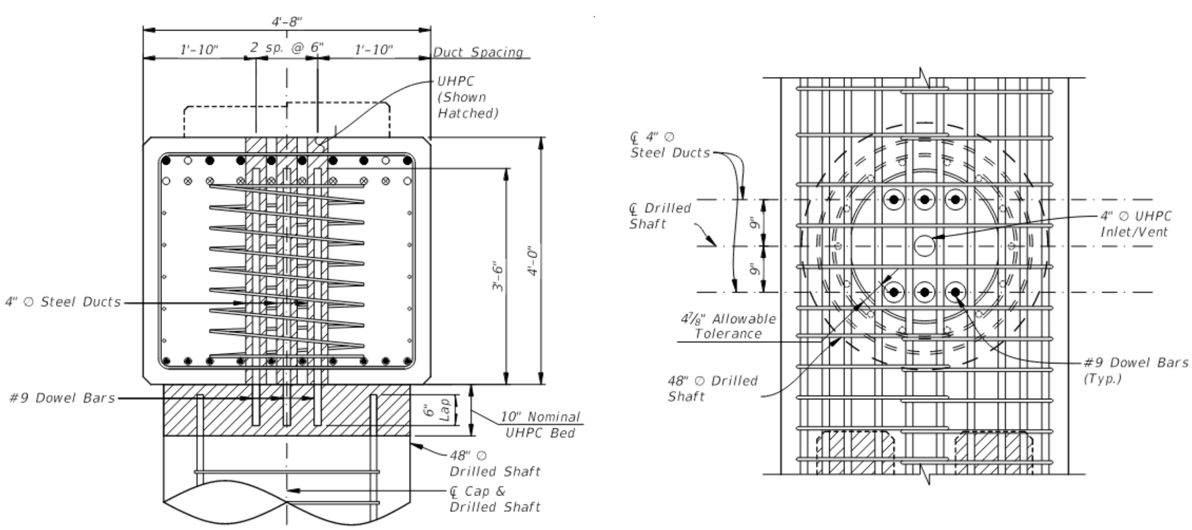

Figure 51: Modified for UHPC drilled shaft or column to bent cap connection, option 3

Pile-to-Footing Connection

The second detail considered for a UHPC connection alternative is a recently proposed pile to footing connection, shown in Figure 52. The original detail shows bars protruding from the pile into a void cast in the precast footing. Load is transferred by corrugations in the side of the void. A large void around the pile is provided to allow for sufficient pile tolerance of 4.25 in. Figure 53 shows an alternative connection, using UHPC as a joining material between bars protruding from the footing and pile. The proposed UHPC detail provides for less tolerance than the original detail. In addition, only 11.5 in. of development length is provided for the splice bars in the footing. A development length of at least 22 in. is required. In the UHPC closure, 11 in. splice length is provided, and 13 in. embedment length is provided. For the #11 bars used, with 1.75 in. cover, 15.75 in. splice length and 18.25 in. embedment length would be required. The detail shown does not meet design requirements. For those requirements to be met, the footing would have to be deepened by at almost 16 in. For that reason, the original detail is preferred over the modified UHPC detail. The use of UHPC is not needed in a pile to cap connection and greater success can be achieved with the original detail and grout as a connecting material. Other connection locations can benefit more from the use of UHPC.

Table 5: Pile-to-Footing Connection Comparison

	Original Detail	Option 1
Vertical Tolerance	3 in.	3 in.
Horizontal Tolerance	4.25 in.	2.5 in.
Filler Material Volume (UHPC, Grout or Concrete)	38.5 cubic ft	31.7 cubic ft
Inspectable?	No	No
Design Requirements Met?	Yes	No

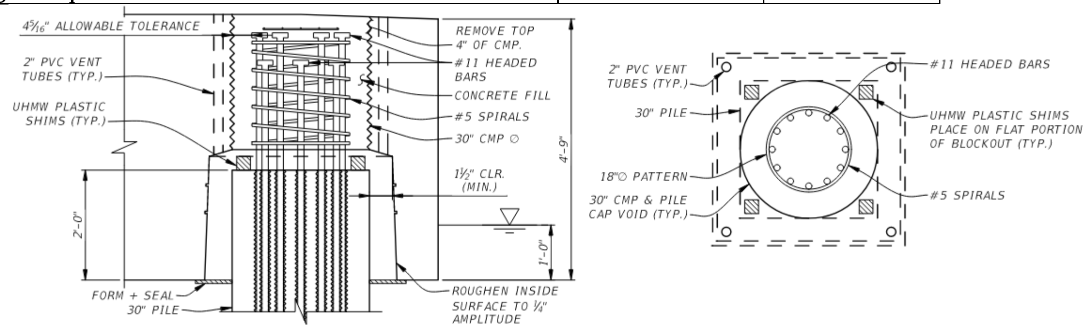

Figure 52: Pile-to-footing connection

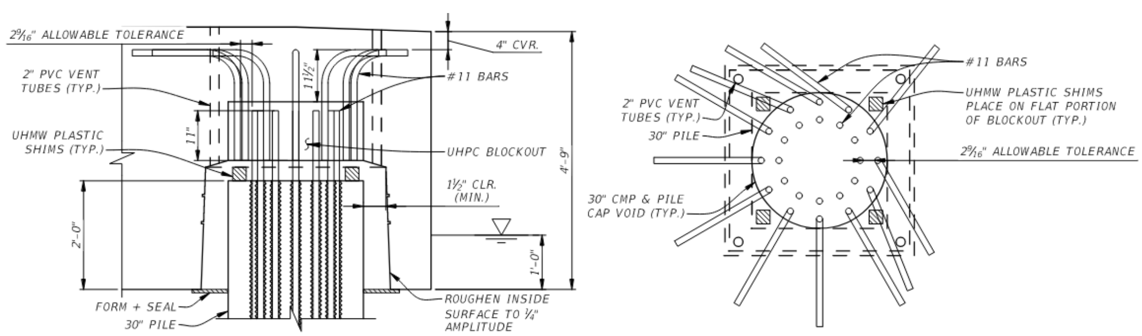

Figure 53: Modified for UHPC pile-to-footing connection

Footing-to-Column Connection

The third detail considered is from the same plans as the pile to footing detail and is shown in Figure 54. The detail is for a connection between a prefabricated footing and prefabricated pier assembly. Intermediate connections between prefabricated column segments would be similar to the connection shown at the base. The original detail allows for only 1.625 in. tolerance between bars protruding from the column and footing. For the original detail, the cast-in-place field splice is 8.5 ft tall. Much of that height is required for a lap splice between the #11 bars. Due to the large splice, shims cannot be used. Erection falsework is required until the field splice is completed.

Two alternative details are presented which use UHPC as the joining material instead of conventional concrete. Option 1, shown in Figure 55, details a non-contact splice between the column and footing bars. The connection is similar to the original detail, except that the field splice is much shorter. Allowable tolerances between bars (in the horizontal direction) are the same as the original detail. For option 2, shown in Figure 56, the field splice is taller. The bars protruding from the footing and column do not overlap. Instead, a short reinforcing bar is added to splice between the footing and column bars. The short splice bar used in option 2 creates a contact splice between one or both protruding bars. Unlike conventional concrete, non-contact splices are common in UHPC. For that reason, the splice bar need only be spliced to a bar protruding from the column or footing – not both. If the bars protruding from the footing and column do not align, the splice can still be made. This research has found that a longer splice and embedment length is not required for contact splices than for non-contact splices, so the splice length provided in options 1 and 2 are the same.

Both UHPC options require significantly less cast-in-place material for the closure pour between the column and footing, when compared to the original detail. Because the closure pour is much shorter, shims could be used to set the pier assembly to the correct elevation, eliminating the erection falsework required for the original detail. Stability bracing may be required but is simpler to install than falsework.

The option 1 detail provides the same horizontal tolerance as the original detail, while option 2 provides almost double the tolerance. As drawn, the UHPC options provide less vertical tolerance than the original detail. The original detail has 8.5 in. of vertical tolerance. It is unclear why such a large vertical tolerance is shown in the original detail and may not be necessary. If it is necessary, the UHPC details could have increased vertical tolerance with a corresponding increase in the field splice height and filler material volume.

Table 6: Footing-to-Column Connection Comparison

	Original Detail	Option 1	Option 2
Vertical Tolerance	8.5 in.	2 in.	2 in.
Horizontal Tolerance	1.6 in.	1.6 in.	3 in.
Filler Material Volume (UHPC, Grout or Concrete)	239 cubic ft	27.1 cubic ft	39.3 cubic ft
Inspectable?	Yes	Yes	Yes
Design Requirements Met?	Yes	Yes	Yes

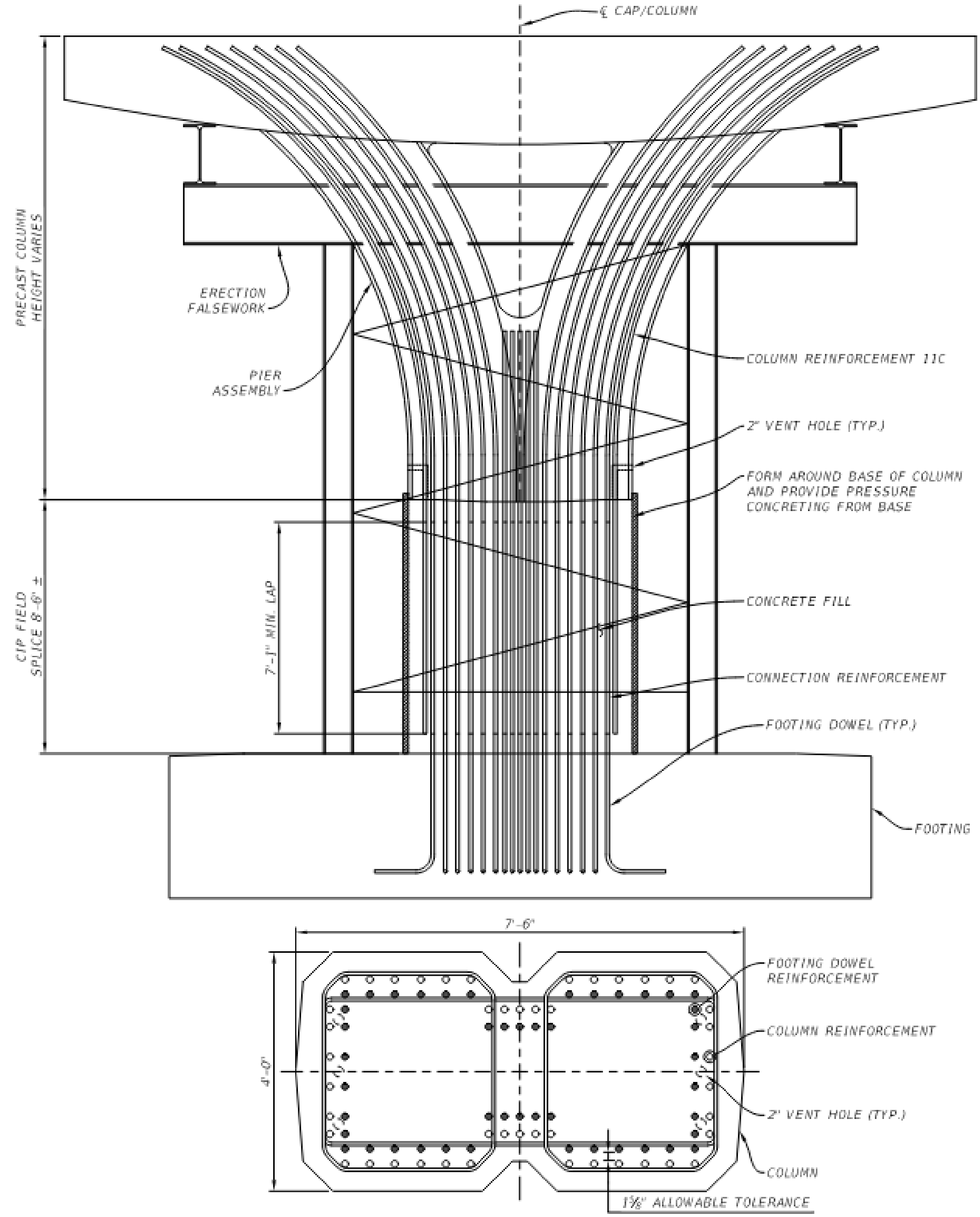

Figure 54: Column-to-footing connection

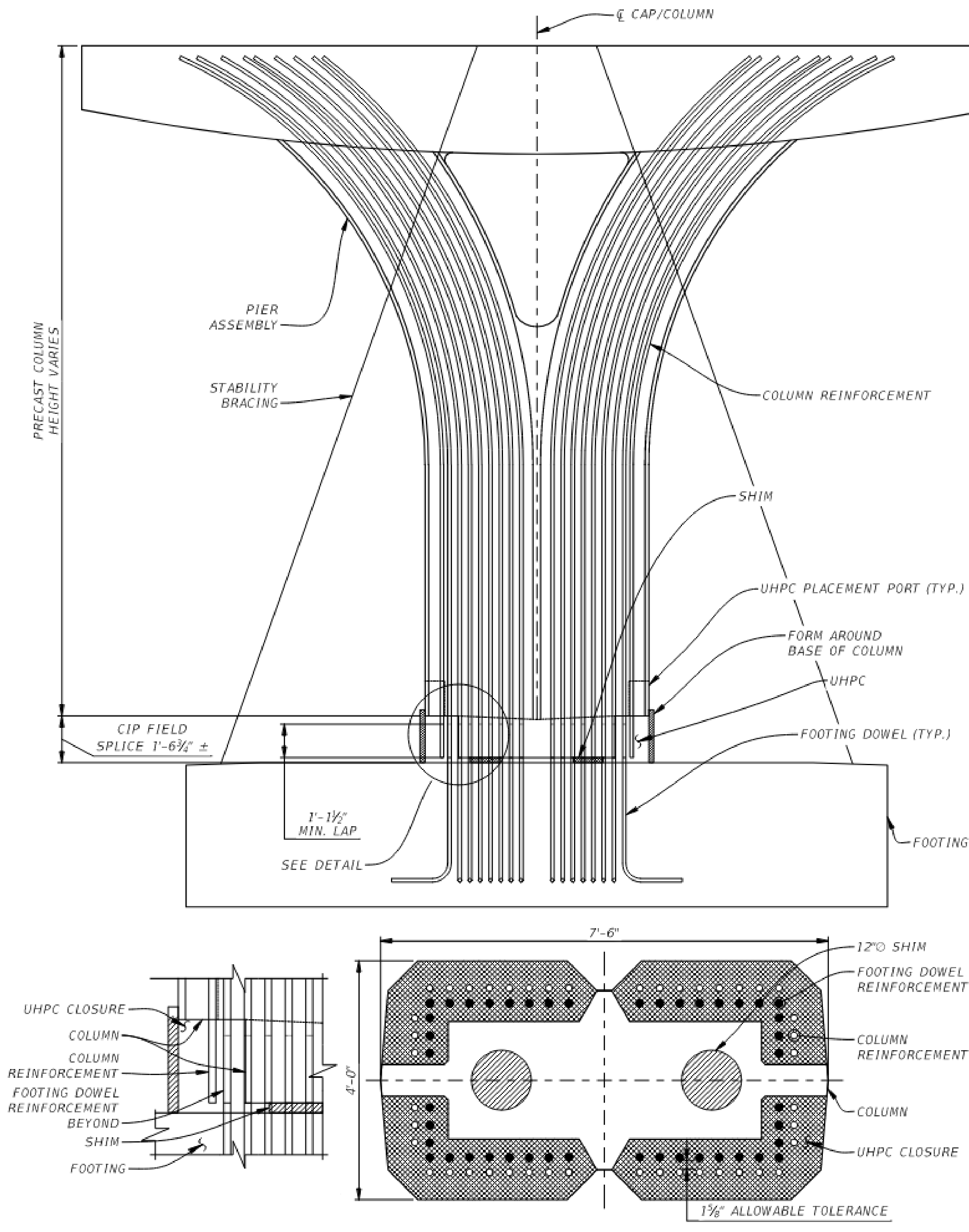

Figure 55: Modified for UHPC column-to-footing connection, option 1

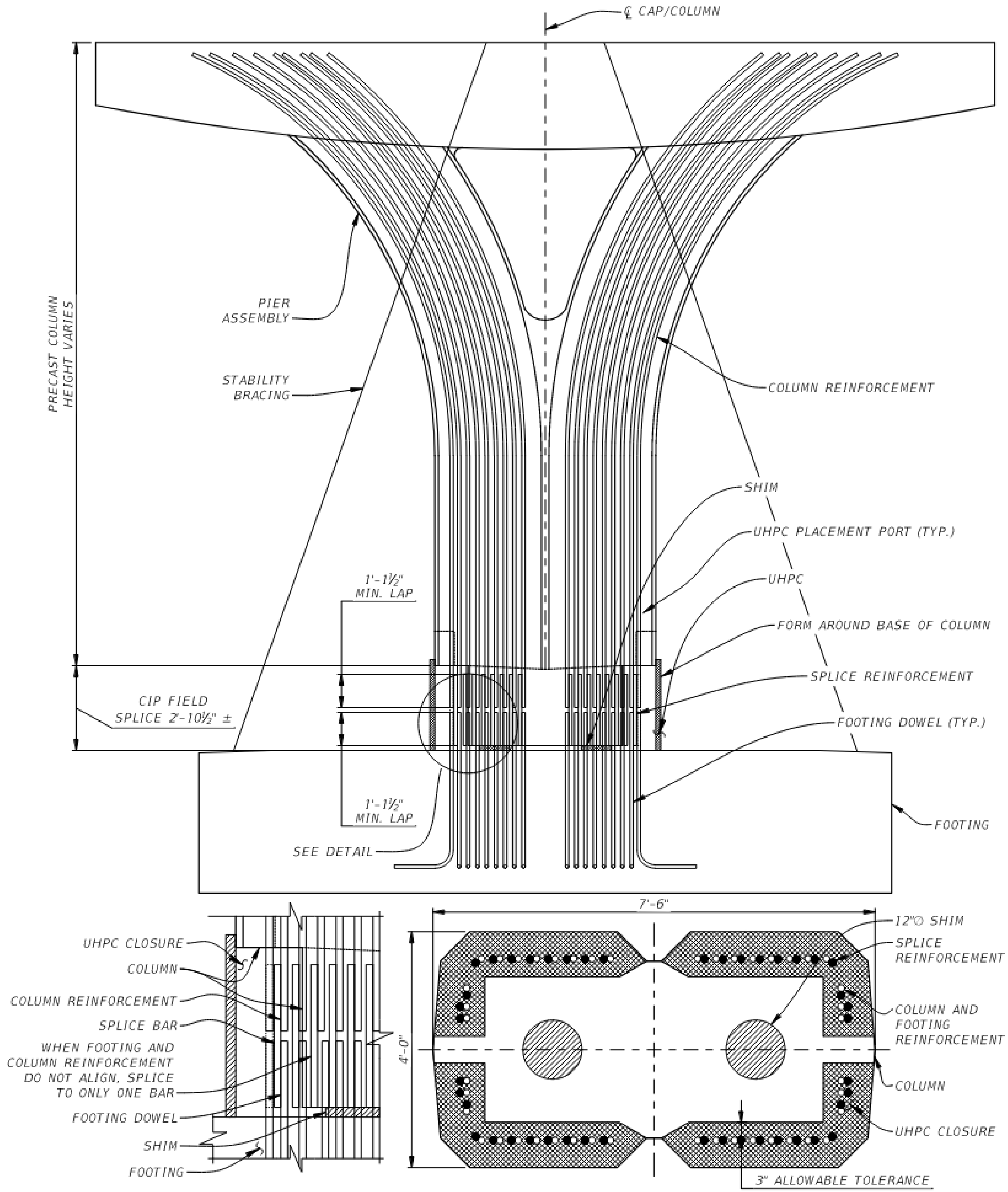

Figure 56: Modified for UHPC column-to-footing connection, option 2

Beam-to-Beam Connection

The final prefabricated bridge component connection considered is an arch rib closure from recently proposed plans, as shown in Figure 57. Although not a substructure connection, #11 bars are developed in the closure pour and so the findings from this research on required large bar development and splice lengths apply. The original detail for the closure pours between arch segments requires hooked #11 bars and headed #8 bars. When modified for UHPC materials, the detail remains similar, but the closure pour size is decreased. In addition, the hooked and headed bars are eliminated and tolerances are increased. As shown in Figure 58, the UHPC closure provides for 9.6d_b splice length between the #11 bars. Both the original and UHPC details have similar inspectability.

Table 7: Arch Rib Connection Comparison

	Original Detail	Option 1
Vertical Tolerance	N/A	N/A
Horizontal Tolerance	2.1 in.	2.6 in.
Filler Material Volume (UHPC, Grout or Concrete)	33.8 cubic ft	20.8 cubic ft
Inspectable?	Yes	Yes
Design Requirements Met?	Yes	Yes

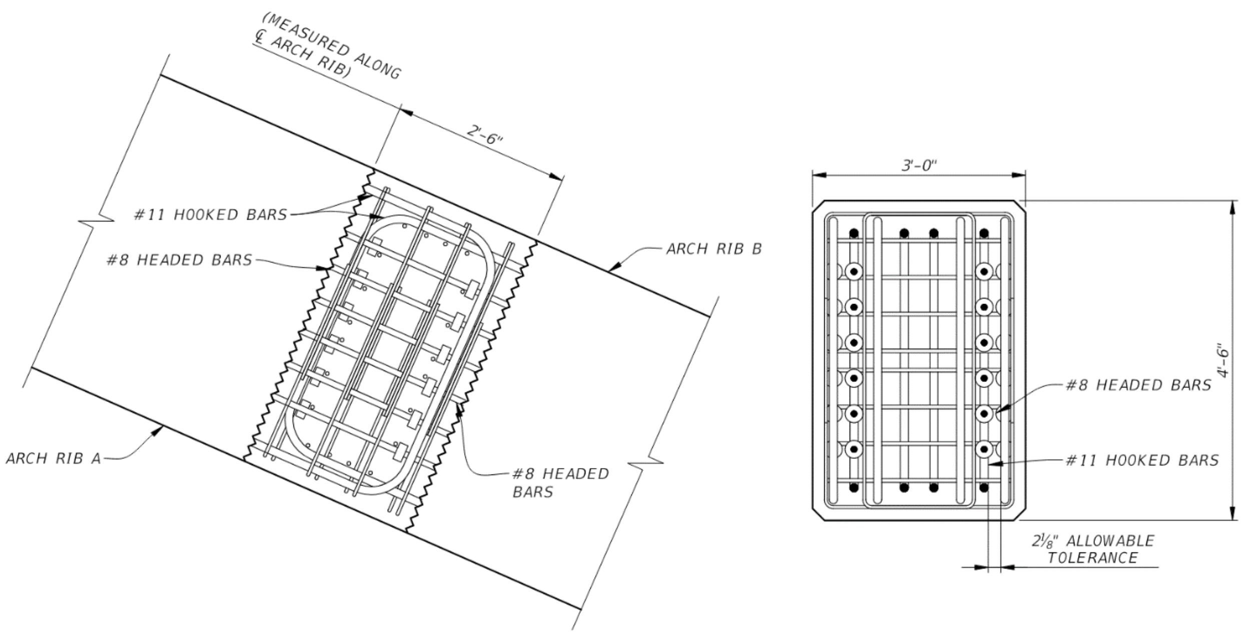

Figure 57: Arch rib connection

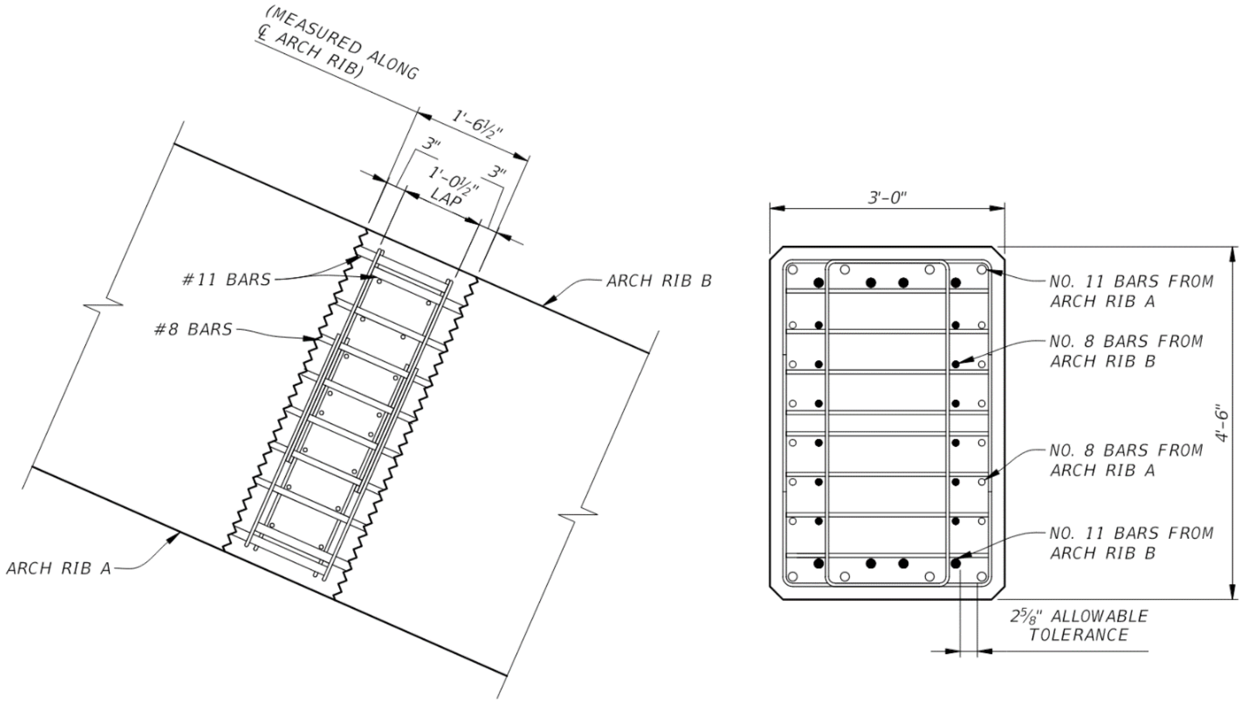

Figure 58: Modified for UHPC arch rib connection

Four details recently proposed or constructed for bridges with prefabricated concrete components were presented. The four details show connections between a drilled shaft and bent cap, pile and footing, footing and column, and two beams. The connections between components have been conceptually modified to allow for the use of UHPC and those concepts are presented pictorially. Differences between the original and UHPC detail are discussed and summarized. Three of the four details are improved with the use of UHPC; these include connections between a drilled shaft and bent cap, footing and column, and beam to beam. In general, closure pour volumes are decreased and tolerances remain the same or increase. The connection presented between a pile and footing was not improved using UHPC.

Chapter 7. Conclusions

This research determined the required splice lengths for steel deformed reinforcing bars embedded in UHPC. Two primary variables were included in the testing matrix: bar size (#8, #9, #10 and #11 bars) and concrete cover (1.75 in, 2.75 in., and 3.75 in.). The tested splice length was varied to determine the appropriate splice length and associated embedment length for future designs. In this research, the reinforcing bar was fully developed if 75 ksi bar stress could be achieved when the UHPC strength was 14 ksi or lower. Conclusions of the research are presented in Table 8, which can be used as design guidelines for projects using UHPC to join prefabricated members. The guidelines are in keeping with the minimum values presented in Table 3, but have been rounded to even 0.25 in. increments. In addition, the difference between the embedment and splice lengths is set to a consistent 2.5 in. for the #10 and #11 bars, and for the #9 bars with 1.75 in. cover. The requirements for #8 bars and #9 bars with 3.75 in. cover are the same as given in FHWA (2014).

Table 8: Required Embedment and Splice Lengths

		Required Embedment Length in Inches				Required Splice Length in Inches			
		Bar Size				Bar Size			
		#8	#9	#10	#11	#8	#9	#10	#11
Cover	1.75 in.	8	11	15	18.25	6	8.5	12.5	15.75
	2.75 in.	-	-	-	16	-	-	-	13.5
	3.75 in.	8	9	11	13	6	6.75	8.5	10.5

Additional findings from this research are summarized as follows:

- There was no apparent difference in spliced bond strength when UHPC was placed at one end of a connection and allowed to flow along the connection and when UHPC was placed at multiple locations along the connection. The large diameter bars and small cover (1.75 in.) created random fiber orientation for both placement methods.
- For one set of the tests, shrinkage cracking was apparent in the UHPC prior to testing and the results of those tests showed lower than expected bond strength. However, the results of tensile specimens did not indicate reduced capacity. It will be important that shrinkage cracking is minimized during construction to ensure UHPC connections have adequate capacity. Tensile sample testing will not be satisfactory to evaluate UHPC with shrinkage cracks.
- Fiber optic strain gauges adhered to the reinforcing bars indicated that the top of the reinforcing bar, extending above the UHPC, reached yielding strains first, and then yielding progressed down the length of the bar towards increasing embedment.
- At locations of high embedment, the UHPC prevents the steel reinforcing bar from yielding at that embedment location.

- Before yielding, the microstrain along the bar decreases linearly from the free end of the bar towards increasing embedment. After yielding, the strain diagram along the bar becomes bilinear.
- A hypothesis was presented herein that struts are formed within the UHPC to resist bar pull-out in splice connections. At shallow embedment, adhesion and friction resist pull-out of the reinforcing bar while, at deeper embedment, resistance is provided primarily by UHPC struts. In a cone-shaped failure mode, cracks form parallel to the compression struts. In a side-splitting failure mode, the tension tie connecting the compression struts near the top of the UHPC has failed.
- UHPC is a suitable material for joining prefabricated substructure elements. Specific connections which can benefit from the use of prefabricated elements joined with UHPC are connections between a drilled shaft to bent cap, footing to column, and beam to beam. A connection between a pile and footing is not ideal for the use of UHPC based on the assumed detailing practices adopted from a recent bridge project which used prefabricated elements.

Research on bond between UHPC and conventional concrete for the blind casting inherent to a substructure connection is lacking. Previous research on bond between the two materials considered UHPC cast against a vertical concrete face and UHPC cast on top of conventional concrete (Graybeal & Haber, 2016). Substructure connections would require UHPC cast between two concrete surfaces. For top formed UHPC, voids and air bubbles commonly form on the top surface of the finished product. Future research work can be done to evaluate the bond between the two materials and determine the extent of slope on the bottom surface of a precast concrete component that is required to minimize voids. Future work can also be completed to determine constructability requirements for these details, including the minimum UHPC depth between two precast components and the required head pressure for successful casting.

This research scope included static physical testing of single bar splices. It may be appropriate to conduct full-scale connection testing before implementation of the connection detail. Future research work could focus on performance as well as constructability of the full-scale detail, and ultimate and fatigue connection strength testing.

References

AASHTO. (2014). *LRFD Bridge Design Specifications, Seventh Edition (with 2015 and 2016 Interims).* Washington, DC: AASHTO.

ACI. (2003). *Bond and Development of Straight Reinforcing Bars in Tension.* Farmington Hills, MI: American Concrete Institute.

ASTM. (2015). *Standard Test Method for Comparing Bond Strength of Steel Reinforcing Bars to Concrete Using Beam-End Specimens.* West Conshohocken, PA: ASTM International.

ASTM. (2019). *Standard Test Method for Flexural Performance of Fiber-Reinforced Concrete (Using Beam With Third-Point Loading).* West Conshohocken, PA: ASTM International.

Azizinamini, A., Pavel, R., Hatfield, E., & Ghosh, S. K. (1999, September-October). Behavior of Lap-Spliced Reinforcing Bars Embedded in High-Strength Concrete. *ACI Structural Journal, 96*(5), 826-835.

Azizinamini, A., Stark, M., Roller, J. J., & Ghosh, S. K. (1993, September-October). Bond Performance of Reinforcing Bars Embedded in High Strength Concrete. *ACI Structural Journal, 90*(5), 554-561.

Dagenais, M.-A., & Massicotte, B. (2015, July). Tension Lap Splices Strengthened with Ultra High Performance Fiber Reinforced Concrete. *ASCE Journal of Materials in Civil Engineering, 27*(7), 10 pages.

Dagenais, M.-A., Massicotte, B., & Boucher-Proulx, G. (2018). Seismic Retrofitting of Rectangular Bridge Piers with Deficient Lap Splices Using Ultrahigh-Performance Fiber-Reinforced Concrete. *Journal of Bridge Engineering, 23*(2), 1-13.

El Helou, R., & Graybeal, B. A. (2019). The Ultra Girder: A Design Concept for a 300-foor Single Span Prestressed UHPC Bridge Girder. *2nd International Interactive Symposium on Ultra-High Performance Concrete.* Albany, NY: International Interactive Symposium on Ultra-High Performance Concrete (UHPC).

FHWA. (2014). *Bond Behavior of Reinforcing Steel in Ultra-High Performance Concrete.* McLean, VA: Federal Highway Administration.

FHWA. (2014). *Design and Construction of Field-Cast UHPC Connections.* McLean, VA: Federal Highway Administration.

FHWA. (2014). *TechNote Design and Construction of Field-Cast UHPC Connections.* McLean, VA: Federal Highway Administration.

fib. (2013). *fib Model Code for Concrete Structures.* Berlin, Germany: Ernst & Sohn.

Florida Department of Transportation (FDOT). (2016). *FDOT Structures Manual.* Tallahassee, FL: Florida Department of Transportation (FDOT).

Florida Department of Transportation (FDOT). (2021). *FDOT Structures Manual.* Tallahassee, FL: Florida Department of Transportation (FDOT).

Florida Department of Transportation (FDOT). (2021, January). *Standard Specifications eBook.* Retrieved September 26, 2017, from Standard Specifications Library: https://fdotwww.blob.core.windows.net/sitefinity/docs/default-source/programmanagement/implemented/specbooks/january2021/1-21ebook.pdf?sfvrsn=1c62cb58_2

Goto, Y. (1971). Cracks Formed in Concrete Around Deformed Tension Bars. *ACI Journal, Proceedings, 68*(4, Apr.), 244-251.

Graybeal, B. A., & Baby, F. (2013). Development of Direct Tension Test Method for Ultra-High-Performance Fiber-Reinforced Concrete. *ACI Materials Journal*, 177-186.

Graybeal, B. A., & Haber, Z. (2016). Performance of Multiple UHPC-Class Materials in Prefabricated Bridge Deck Connections. *Conference Paper - First International Interactive Symposium on UHPC.* Des Moines.

Haber, Z. B., & Graybeal, B. A. (2018). Lap-Spliced Rebar Connections with UHPC Closures. *Journal of Bridge Engineering*, 1-12.

Kim, S., Lee, J., Joh, C., & Kwahk, I. (2016). Flexural Bond Behavior of Rebar in Ultra-High Performance Concrete Beams Considering Lap-Splice Length and Cover Depth. *Engineering, 8*, 116-129.

Lagier, F., Massicotte, B., & Charron, J.-P. (2012). Bond splitting strength of lap splice embedded in ultra high performance. *Bond in Concrete 2012.* Brescia.

Lagier, F., Massicotte, B., & Charron, J.-P. (2015). Bond strength of tension lap splice specimens in UHPFRC. *Elsevier Construction and Building Materials*.

Marchand, P., Baby, F., Khadour, A., Battesti, T., Rivillon, P., Quiertant, M., . . . Toutlemonde, F. (2016). Bond behavior of reinforcing bars in UHPFRC. *Materials and Structures*, 1979-1995.

Marchand, P., Baby, F., Khadour, A., Rivillon, P., Renaud, J.-C., Baron, L., . . . Toutlemonde, F. (2019). Response of UHPFRC Columns Submitted to Combined Axial and Alternate Flexural Loads. *Journal of Structural Engineering*, 1-13.

McMullen, K. F., & Haber, Z. B. (2019). Effect of Steel Reinforcement Type and Diameter on the Strength of Non-Contact Lap Splice Connections using UHPC. *Second International Interactive Symposium on Ultra-High Performance Concrete* (pp. 1-9). Albany: Iowa State University Digital Press.

Precast/Prestressed Concrete Institute. (2004). *PCI Design Handbook.* PCI.

Rolland, A., Quiertant, M., Khadour, A., Chataigner, S., Benzarti, K., & Argoul, P. (2018). Experimental investigations on the bond behavior between concrete and FRP reinforcing bars. *Construction and Building Materials*, 136-148.

Ronanki, V. S., Aaleti, S., & Valentim, D. B. (2018). Experimental investigation of bond behavior of mild steel reinforcement in UHPC. *Engineering Structures*, 707-718.

Ronanki, V. S., Valentim, D. B., & Aaleti, S. (2016). Development length of reinforcing bars in UHPC: An experimental and analytical investigation. *First International Interactive Symposium on UHPC - 2016.* Des Moines.

Tazarv, M., & Saiidi, M. S. (2014). *Next Generation of Bridge Columns for Accelerated Bridge Construction.* Reno: University of Nevada.

Yuan, J., & Graybeal, B. A. (2014). *Bond Behavior of Reinforcing Steel in Ultra-High Performance Concrete.* McLean: FHWA.

Appendix A: Table of Test Results

Test Records

Slab Number	Row Number	Order for Graphs	UHPC Batch Number	Test Bar Number	Bar Size	Bar Diameter (in)	Bar Area (in^2)	Target Clear Spacing (in)	Target Cover (in)	As-Built Dimensions (in.)															Failure Mode	Concrete Strength (ksi)	Maximum Load (kip)	Cracking Load (kip)	Maximum Bar MicroStrain	Load at Max. Bar MicroStrain	Maximum Bar Stress (ksi)	Bond Stress based on (Developmet Length) (ksi)
										Embedment M	Embedment M in bar diameters	Splice Length C	Splice Length C in bar diameters	Splice length C	Bar Clear Spacing					Side Cover												
															F	G	Maximum	Minimum	Average	J	K	Maximum	Minimum	Average								
1	4	4	1	1	8	1.00	0.79	6.00	3.75	7.75	7.80	5.69	5.70	0.7M	5.04	4.91	5.04	4.91	4.97	3.57	4.12	4.12	3.57	3.85	c	14.66	72.05	NA	49965.67	71.66	91.203	2.94
1	4	5	1	3	8	1.00	0.79	6	3.75	8.06	8.10	6.03	6.00	0.7M	4.96	4.79	4.96	4.79	4.87	3.74	3.76	3.76	3.74	3.75	e	14.83	75.27	NA	60902.55	73.91	95.278	2.96
1	4	6	1	5	8	1.00	0.79	0.00	3.75	7.91	7.90	5.84	5.80	0.7M	0.38	NA	0.38	0.38	0.38	3.77	3.70	3.77	3.70	3.73	e	14.90	79.24	NA	61531.4813	78.27	100.3	3.17
1	4	7	1	6	8	1.00	0.79	0.00	3.75	8.13	8.10	6.19	6.20	0.8M	0.43	NA	0.43	0.43	0.43	3.73	3.79	3.79	3.73	3.76	e	18.32	78.55	NA	61157.8633	74.94	99.43	3.06
1	3	8	2	1	8	1.00	0.79	0.00	1.75	8.25	8.30	6.19	6.20	0.8M	9.56	0.00	9.56	0.00	4.78	2.06	1.81	2.06	1.81	1.94	d	14.32	56.40	54.2	14842.45	56.01	71.392	2.16
1	3	9	2	3	8	1.00	0.79	6	1.75	8.44	8.40	5.91	5.90	0.7M	4.50	5.00	5.00	4.50	4.75	2.00	1.69	2.00	1.69	1.84	e	14.61	73.19	49.5	21993.42	64.54	92.646	2.75
1	3	10	2	4	8	1.00	0.79	6	1.75	8.31	8.30	5.81	5.80	0.7M	4.75	4.88	4.88	4.75	4.81	2.06	1.81	2.06	1.81	1.94	e	15.18	76.71	53.46	16498.37	57.28	97.101	2.92
1	3	11	2	5	8	1.00	0.79	0.00	1.75	8.38	8.40	6.00	6.00	0.7M	0.25	5.50	5.50	0.25	2.88	2.13	1.56	2.13	1.56	1.84	e	15.52	72.65	NA	60521.54	71.15	91.962	2.75
1	2	12	3	1	9	1.128	1.00	0.00	3.75	7.88	7.00	6.00	5.30	0.8M	9.50	0.00	9.50	0.00	4.75	3.63	4.00	4.00	3.63	3.81	b	12.55	81.33	67.4	22137.12	81.3	81.33	2.91
1	2	13	3	2	9	1.128	1.00	6	3.75	7.63	6.80	5.47	4.80	0.7M	4.25	5.19	5.19	4.25	4.72	3.88	3.75	3.88	3.75	3.81	e	12.77	100.09	67.82	61440.1412	96.77	100.09	3.70
1	2	14	3	3	9	1.128	1.00	6	3.75	8.00	7.10	5.91	5.20	0.7M	4.38	5.25	5.25	4.38	4.81	3.81	3.81	3.81	3.81	3.81	e	15.50	83.01	68.66	20192.46	82.34	83.01	2.93
1	2	15	3	4	9	1.128	1.00	6	3.75	7.69	6.80	5.69	5.00	0.7M	4.56	5.06	5.06	4.56	4.81	3.94	3.63	3.94	3.63	3.78	e	15.71	81.96	68.3	24001.45	81.31	81.96	3.01
1	2	16	3	5	9	1.128	1.00	0.00	3.75	7.81	6.90	5.69	5.00	0.7M	0.00	5.38	5.38	0.00	2.69	3.94	3.69	3.94	3.69	3.81	e	16.14	82.23	67.78	28386.6	81.61	82.23	2.97
1	2	17	3	6	9	1.128	1.00	0.00	3.75	8.00	7.10	5.75	5.10	0.7M	0.00	9.50	9.50	0.00	4.75	3.94	3.69	3.94	3.69	3.81	e	16.34	82.23	65.01	35750.18	81.63	82.23	2.90
1	1	18	4	1	9	1.128	1.00	0.00	1.75	9.44	8.40	7.00	6.20	0.7M	9.56	0.00	9.56	0.00	4.78	1.63	2.00	2.00	1.63	1.81	b,d	12.63	37.8	37.5	1454.94	37.61	37.8	1.13
1	1	19	4	2	9	1.128	1.00	6	1.75	8.88	7.90	6.75	6.00	0.8M	4.63	4.88	4.88	4.63	4.75	1.88	1.88	1.88	1.88	1.88	d	12.94	58.25	26.55	2446.21	57.95	58.25	1.85
1	1	20	4	4	9	1.128	1.00	6	1.75	9.19	8.10	7.00	6.20	0.8M	4.88	4.81	4.88	4.81	4.84	1.94	1.94	1.94	1.94	1.94	d	13.12	64.75	30.27	2278.1	64.71	64.75	1.99
1	1	21	4	6	9	1.128	1.00	0.00	1.75	8.94	7.90	6.88	6.10	0.8M	0.00	9.31	9.31	0.00	4.66	2.00	1.81	2.00	1.81	1.91	b	15.22	82.23	64.5	35750.18	81.63	82.23	2.59
1	1	22	4	7	9	1.128	1.00	6.00	1.75	9.13	8.10	6.94	6.20	0.8M	2.75	6.81	6.81	2.75	4.78	2.00	1.81	2.00	1.81	1.91	b,d	15.36	52.74	36.51	1860.7	52.55	52.74	1.63
2	1	23	5	1	9	1.128	1.00	0.00	1.75	11.56	10.20	8.31	7.40	0.7M	9.50	0.00	9.50	0	4.75	1.85	1.19	1.85	1.19	1.5188	b	11.6	77.67	67.8	17469.89	76.88	77.67	1.89
2	1	24	5	2	9	1.128	1.00	6	1.75	11.63	10.30	8.56	7.60	0.7M	4.81	4.81	4.81	4.8125	4.8125	1.81	2.13	2.13	1.81	1.9688	e	11.94	82.95	67.5	25253.65	82.3	82.95	2.01
2	1	25	5	3	9	1.128	1.00	6	1.75	11.69	10.40	8.75	7.80	0.7M	4.81	5.00	5.00	4.8125	4.9063	1.81	2.13	2.13	1.81	1.9688	e	12.12	83.64	67.7	27220.65	82.92	83.64	2.02
2	1	26	5	4	9	1.128	1.00	6	1.75	11.31	10.00	8.47	7.50	0.7M	4.88	4.75	4.88	4.75	4.8125	1.88	2.06	2.06	1.88	1.9688	e	14.39	83.57	66.64	25147.44	83.09	83.57	2.08
2	1	27	5	5	9	1.128	1.00	0.00	1.75	11.50	10.20	8.81	7.80	0.8M	0.00	5.50	5.50	0	2.75	2.00	1.94	2.00	1.94	1.9688	e	14.6	83.5	67.19	29172.67	83.06	83.5	2.05
2	1	28	5	6	9	1.128	1.00	0.00	1.75	11.50	10.20	8.31	7.40	0.7M	0.00	9.63	9.63	0	4.8125	1.94	1.94	1.94	1.94	1.9375	e	14.96	83.19	68.3	26301.08	82.61	83.19	2.04
2	1	29	5	7	9	1.128	1.00	6.00	1.75	11.63	10.30	8.53	7.60	0.7M	2.75	6.81	6.81	2.75	4.7813	1.88	1.81	1.88	1.81	1.8438	e	15.09	83.75	67.93	20924.57	83.02	83.75	2.03
2	2	30	6	1	10	1.270	1.27	6	1.75	12.75	10.00	10.84	8.50	0.9M	5.00	4.38	5.00	4.38	4.69	2.00	1.81	2.00	1.81	1.91	b,d	10.812	70	36.48	2084.9	69.99	55.118	1.37
2	2	31	6	2	10	1.270	1.27	6	1.75	12.81	10.10	10.97	8.60	0.9M	4.94	4.56	4.94	4.56	4.75	1.94	1.88	1.94	1.88	1.91	d	11.13	91.8	53.61	4159.7	91.05	72.283	1.79
2	2	32	6	3	10	1.270	1.27	6	1.75	12.81	10.10	10.88	8.60	0.8M	4.69	4.75	4.75	4.69	4.72	1.94	1.94	1.94	1.94	1.94	e	13.589	105.41	94.81	20069.72	104.74	83	2.06
2	2	33	6	5	10	1.270	1.27	0.00	1.75	12.31	9.70	10.56	8.30	0.9M	0.00	5.31	5.31	0.00	2.66	2.00	1.75	2.00	1.75	1.88	b,d	10.981	83.8	83.8	2161.63	83.69	65.984	1.70
2	2	34	6	6	10	1.270	1.27	0.00	1.75	12.69	10.00	10.63	8.40	0.8M	0.00	9.25	9.25	0.00	4.63	2.00	1.75	2.00	1.75	1.88	b	13.419	78.61	78.61	2714.1	78.19	61.898	1.55
2	2	35	6	7	10	1.270	1.27	0	1.75	12.88	10.10	10.88	8.60	0.8M	0.00	9.19	9.19	0.00	4.60	2.00	1.75	2.00	1.75	1.88	-	13.886	73.93	73.93	2274.49	72.82	58.213	1.44
2	3	36	7	1	10	1.270	1.27	6	1.75	14.88	11.70	12.81	10.10	0.9M	4.94	4.50	4.94	4.50	4.72	2.00	1.76	2.00	1.76	1.88	b	11.317	67.57	27.14	2140.04	67.56	53.205	1.14
2	3	37	7	2	10	1.270	1.27	6	1.75	15.06	11.90	13.00	10.20	0.9M	4.88	4.63	4.88	4.63	4.76	1.91	1.93	1.93	1.91	1.92	c	11.68	101.85	46.35	12258.45	99.01	80.193	1.69
2	3	38	7	3	10	1.270	1.27	6	1.75	14.75	11.60	12.69	10.00	0.9M	4.63	4.75	4.75	4.63	4.69	2.07	1.85	2.07	1.85	1.96	e	14.182	105.07	87.59	23837.1	104.44	82.732	1.78
2	3	39	7	4	10	1.270	1.27	6	1.75	14.88	11.70	12.81	10.10	0.9M	5.00	4.56	5.00	4.56	4.78	2.11	1.83	2.11	1.83	1.97	e,a	14.859	104.99	81.06	49632	104.47	82.669	1.76
2	3	40	7	5	10	1.270	1.27	0.00	1.75	15.06	11.90	12.94	10.20	0.9M	0.00	5.50	5.50	0.00	2.75	2.04	1.94	2.04	1.94	1.99	d	11.51	96.03	88.55	16704.36	95.65	75.614	1.59
2	3	41	7	6	10	1.270	1.27	0.00	1.75	14.81	11.70	12.63	9.90	0.9M	0.00	9.19	9.19	0.00	4.60	2.11	1.84	2.11	1.84	1.98	c	13.998	95.46	85.6	26410.94	94.719	75.165	1.61
2	3	42	7	7	10	1.270	1.27	0	1.75	14.88	11.70	12.69	10.00	0.9M	0.00	9.13	9.13	0.00	4.57	1.93	1.85	1.93	1.85	1.89	b	14.343	70.81	36.75	2211.965	70.8	55.756	1.19
2	4	43	8	1	10	1.270	1.27	6	3.75	10.17	8.00	7.89	6.20	0.8M	4.88	4.56	4.88	4.56	4.72	4.13	3.57	4.13	3.57	3.85	b	10.04	90.1	28.899	3056.812	90.01	70.945	2.22
2	4	44	8	2	10	1.270	1.27	6	3.75	10.00	7.90	7.50	5.90	0.8M	4.94	4.50	4.94	4.50	4.72	3.99	3.77	3.99	3.77	3.88	e	13.07	105.33	45.89	13860.88	103.93	82.937	2.63
2	4	45	8	3	10	1.270	1.27	6	3.75	9.94	7.80	7.53	5.90	0.8M	4.81	4.50	4.81	4.50	4.66	3.73	4.04	4.04	3.73	3.89	e	13.614	105.22	87.58	32609.7369	104.387	82.85	2.65
2	4	46	8	4	10	1.270	1.27	6	3.75	9.75	7.70	7.38	5.80	0.8M	4.69	4.81	4.81	4.69	4.75	3.72	4.03	4.03	3.72	3.88	e	14.284	105.38	86.85	25845.118	104.74	82.974	2.70
2	4	47	8	5	10	1.270	1.27	0.00	3.75	9.94	7.80	7.56	6.00	0.8M	0.31	5.19	5.19	0.31	2.75	3.57	4.16	4.16	3.57	3.87	b	10.249	101.72	92.01	11737.3855	100.085	80.096	2.56
2	4	48	8	6	10	1.270	1.27	0.00	3.75	9.81	7.70	7.56	6.00	0.8M	0.00	9.25	9.25	0.00	4.63	3.47	4.35	4.35	3.47	3.91	b	13.377	97.059	81.91	17335.0139	96.655	76.424	2.47
2	4	49	8	7	10	1.270	1.27	0	3.75	9.18	7.20	7.81	6.20	0.9M	0.00	9.44	9.44	0.00	4.72	3.39	4.34	4.34	3.39	3.87	b	14.103	95.932	91.25	13074.7103	95.47	75.537	2.61
3	2	50	9	1	11	1.410	1.56	6	3.75	13.75	9.80	10.97	7.80	0.8M	5.25	4.58	5.25	4.58	4.92	3.75	3.625	3.75	3.625	3.6875	e	9.345	120.63	52.76	19240.16	118.44	77.33	1.9824
3	2	51	9	2	11	1.410	1.56	6	3.75	13.50	9.60	10.48	7.40	0.8M	4.93	4.40	4.93	4.40	4.67	3.63	3.9375	3.9375	3.625	3.7813	e	14.728	118.23	51.09	26366.52	117.11	75.79	1.979
3	2	52	9	5	11	1.410	1.56	0.00	3.75	13.00	9.20	10.16	7.20	0.8M	0.00	5.26	5.26	0.00	2.63	3.50	3.6875	3.6875	3.5	3.5938	e	9.484	120.56	30.43	28026.51	119.35	77.28	2.0955
3	2	53	9	7	11	1.410	1.56	0	3.75	13.25	9.40	10.25	7.30	0.8M	0.00	9.25	9.25	0.00	4.63	3.63	3.75	3.75	3.625	3.6875	e	14.796	118.53	55.49	18655.83	117.55	75.98	2.0214
3	3	54	10	1	11	1.410	1.56	6	3.75	16.19	11.50	14.13	10.00	0.9M	4.59	4.72	4.72	4.59	4.655	3.562	3.75	3.75	3.56	3.66	e,b	8.208	136.24	69.075	44321.83	134.522	87.336	1.9012
3	3	55	10	2	11	1.410	1.56	6	3.75	15.76	11.20	13.88	9.80	0.9M	4.7	4.75	4.75	4.7	4.725	3.625	3.69	3.69	3.63	3.66	e	11.68	130.45	47.677	21460.0735	129.199	83.624	1.871

Test Records

3	3	56	10	3	11	1.410	1.56	6	3.75	15.75	11.20	14.25	10.10	0.9M	4.65	4.89	4.89	4.65	4.770	3.875	3.38	3.88	3.38	3.63	e	12.58	130.55	33.27	25613.7345	129.901	83.684	1.8729
3	3	57	10	5	11	1.410	1.56	0.00	3.75	15.31	10.90	13.88	9.80	0.9M	0.00	5.36	5.36	0.00	2.680	4.062	3.38	4.06	3.38	3.72	e	11.37	130.47	42.986	52389.6153	129.316	83.633	1.9252
3	3	58	10	6	11	1.410	1.56	0.00	3.75	15.25	10.80	13.56	9.60	0.9M	0.00	9.50	9.50	0.00	4.750	3.937	3.44	3.94	3.44	3.69	e	11.99	129.98	46.64	34599.1776	129.344	83.319	1.9259
3	1	59	11	1	11	1.41	1.56	6	1.75	18.625	13.2	15.406	10.9	0.8M	5.57	4.04	5.57	4.04	4.805	1.375	1.875	1.875	1.375	1.625	b	8.8262	116.21	58.704	24781.19	114.84	74.492	1.4098
3	1	60	11	2	11	1.41	1.56	6	1.75	18.625	13.2	15.563	11	0.8M	5.31	3.8	5.31	3.8	4.555	1.5	1.9375	1.9375	1.5	1.7188	e	10.38	130.06	50.297	23549.88	121.156	83.375	1.578
3	1	61	11	3	11	1.41	1.56	6	1.75	18.75	13.3	15.781	11.2	0.8M	4.8	4.3	4.8	4.3	4.55	1.4375	1.875	1.875	1.4375	1.6563	e	10.674	130.23	51.177	35677.54	129.22	83.481	1.5694
3	1	62	11	4	11	1.41	1.56	6	1.75	18.563	13.2	15.563	11	0.8M	4.9	4.63	4.9	4.63	4.765	1.875	1.75	1.875	1.75	1.8125	e	11.024	130.95	45.425	26685.53	127.419	83.941	1.594
3	1	63	11	5	11	1.41	1.56	0.00	1.75	18.75	13.3	15.687	11.1	0.8M	0	5.09	5.09	0	2.545	1.375	2.125	2.125	1.375	1.75	e	10.968	131.19	30.92	45529.73	101.139	84.095	1.581
3	1	64	11	6	11	1.41	1.56	0.00	1.75	18.438	13.1	15.531	11	0.8M	0	8.9375	8.9375	0	4.4688	1.5625	1.375	1.5625	1.375	1.4688	e	8.5322	130.4	30.208	32796.3	129.646	83.588	1.598
3	1	65	11	7	11	1.41	1.56	0	1.75	18.5	13.1	15.688	11.1	0.8M	0	8.875	8.875	0	4.4375	1.5	1.9375	1.9375	1.5	1.7188	e	10.926	130.35	57.003	36714.58	129.259	83.554	1.5921
3	4	66	12	1	11	1.41	1.56	6	1.75	17.563	12.5	14	9.9	0.8M	5	4.5	5	4.5	4.75	1.6875	1.875	1.875	1.6875	1.7813	b	8.89225	86.951	40.22	2150.602	86.95	55.738	1.1187
3	4	67	12	3	11	1.41	1.56	6	1.75	17.063	12.1	14.156	10	0.8M	4.75	4.25	4.75	4.25	4.5	1.75	1.8125	1.8125	1.75	1.7813	a,b	10.4254	142.52	100.95	73459.23	140.4	91.362	1.8875
3	4	68	12	5	11	1.41	1.56	0.00	1.75	16.875	12	14.063	10	0.8M	0	5.25	5.25	0	2.625	1.875	1.75	1.875	1.75	1.8125	b	9.48192	144.35	101.43	48609.25	142.976	92.531	1.9329
3	4	69	12	7	11	1.41	1.56	0	1.75	16.938	12	13.75	9.8	0.8M	0	9.25	9.25	0	4.625	1.8125	1.75	1.8125	1.75	1.7813	b	10.8382	117.87	101.12	20357.6	115.899	75.558	1.5725
4	1	70	13	1	10	1.27	1.27	6	1.75	14.938	11.8	13.03	10.3	0.9M	4.694	4.487	4.69	4.487	4.5905	1.755	1.805	1.805	1.755	1.78	b	13.596	122.55	79.09	32128.77	121.9	96.496	2.051
4	1	71	13	2	10	1.27	1.27	6	1.75	14.938	11.8	12.781	10.1	0.9M	4.89	4.488	4.89	4.488	4.689	1.779	1.805	1.805	1.779	1.792	c	13.638	136.47	93.7	76855.84	135.42	107.46	2.284
4	1	72	13	3	10	1.27	1.27	6	1.75	14.78	11.6	12.563	9.9	0.8M	4.846	4.462	4.85	4.462	4.654	1.882	1.725	1.882	1.725	1.8035	b	10.879	135.55	65.1	59200.09	130.19	106.73	2.2926
4	1	73	13	4	10	1.27	1.27	6	1.75	15.219	12	12.656	10	0.8M	4.702	4.617	4.70	4.617	4.6595	1.8595	1.738	1.8595	1.738	1.7988	-	13.626	139.16	71.4	101400.6	137.037	109.57	2.2859
4	1	74	13	5	10	1.27	1.27	0.00	1.75	15	11.8	12.469	9.8	0.8M	0.36	5.119	5.12	0.36	2.7395	2.1045	1.375	2.1045	1.375	1.7398	c	13.653	131.26	83.8	44837.78	130.352	103.36	2.1877
4	1	75	13	7	10	1.27	1.27	0	1.75	14.688	11.6	12.063	9.5	0.8M	0.22	8.9375	8.94	0.22	4.5788	1.742	1.8265	1.8265	1.742	1.7843	d	10.215	102.3	82.4	19493.06	102.105	80.551	1.7412
4	3	76	14	1	10	1.27	1.27	6	3.75	10.375	8.2	8.2188	6.5	0.8M	4.639	4.84	4.84	4.639	4.7395	3.75	3.875	3.875	3.75	3.8125	c	11.27	112.83	93.4	25318.5	111.74	88.843	2.7188
4	3	77	14	3	10	1.27	1.27	6	3.75	10.75	8.5	8.513	6.7	0.8M	4.621	4.868	4.87	4.621	4.7445	3.625	4	4	3.625	3.8125	e	14.08	133.5	89.3	61252.7	131.97	105.12	3.1047
4	3	78	14	4	10	1.27	1.27	6	3.75	10.938	8.6	8.4375	6.6	0.8M	4.688	4.908	4.91	4.688	4.798	3.875	3.6875	3.875	3.6875	3.7813	-	14.61	129.71	80	48164	127.82	102.13	2.9647
4	3	79	14	5	10	1.27	1.27	0.00	3.75	10.813	8.5	7.625	6	0.7M	5.281	0.19	5.28	0.19	2.7355	3.625	3.9375	3.9375	3.625	3.7813	-	13.84	131.13	79.5	55577	97.303	103.25	3.0318
4	3	80	14	7	10	1.27	1.27	0	3.75	10.938	8.6	7.6875	6.1	0.7M	9.1875	0.14	9.19	0.14	4.6638	3.75	3.875	3.875	3.75	3.8125	-	14.26	133.89	91.9	63043	133.19	105.43	3.0602
4	2	81	15	2	8	1	0.79	6	1.75	8.75	8.8	5.6875	5.7	0.7M	4.94	4.77	4.94	4.77	4.855	2	1.5	2	1.5	1.75	d	13.23	57.23	51.3	16520	57.15	72.443	2.0698
4	2	82	15	4	8	1	0.79	6	1.75	8.75	8.8	5.7813	5.8	0.7M	5.223	4.502	5.22	4.502	4.8625	1.75	1.75	1.75	1.75	1.75	d,b	15.62	70.36	51.5	47788	70.01	89.063	2.5447
4	2	83	15	5	8	1	0.79	0.00	1.75	8.8125	8.8	5.875	5.9	0.7M	5.576	0	5.58	0	2.788	1.75	1.875	1.875	1.75	1.8125	c	13.32	72.76	51.8	48801	72.34	92.101	2.6128
4	2	84	15	6	8	1	0.79	0.00	1.75	9	9	5.75	5.8	0.6M	9.4375	0	9.44	0	4.7188	1.8125	1.8125	1.8125	1.8125	1.8125	b	15.61	72.045	51.6	52006	71.385	91.196	2.5332
4	2	85	15	7	8	1	0.79	0	1.75	9.5625	9.6	6.5625	6.6	0.7M	9.5625	0	9.56	0	4.7813	1.5	2.0625	2.0625	1.5	1.7813	b	15.59	63.679	51.3	25381	63.286	80.606	2.1074
4	4	86	15	2	8	1	0.79	6	1.75	9.3125	9.3	6.9375	6.9	0.7M	4.978	4.807	4.98	4.807	4.8925	1.8125	1.75	1.8125	1.75	1.7813	b,d	13.19	64.575	50.4	34344.9	64.19	81.741	2.1944
4	4	87	15	4	8	1	0.79	6	1.75	8.8125	8.8	6.2813	6.3	0.7M	4.97	4.955	4.97	4.955	4.9625	1.8125	1.625	1.8125	1.625	1.7188	e	15.62	68.05	44.3	33075.4	67.797	86.139	2.4437
4	4	88	15	5	8	1	0.79	0.00	1.75	8.8125	8.8	5.875	5.9	0.7M	5.375	0.39	5.38	0.39	2.8825	1.75	1.8125	1.8125	1.75	1.7813	c	13.28	72.69	52.1	49990.7	72.25	92.013	2.6103
4	4	89	15	6	8	1	0.79	0.00	1.75	8.875	8.9	6.25	6.3	0.7M	9	0.43	9.00	0.43	4.715	1.6875	1.875	1.875	1.6875	1.7813	b,d,c	15.61	66.92	54	31143.3	66.5	84.709	2.3862
4	4	90	15	7	8	1	0.79	0	1.75	8.875	8.9	6	6	0.7M	9.375	0.4	9.38	0.4	4.8875	1.8125	1.75	1.8125	1.75	1.7813	b	15.59	60.67	51	19898	60.32	76.797	2.1633
5	1	91	16	1	11	1.41	1.56	6	1.75	15.188	10.8	12.969	9.2	0.9M	4.81	4.72	4.81	4.72	4.765	1.625	1.75	1.75	1.625	1.6875	b	13.931	125.86	102	31940.1	124.95	80.679	1.8725
5	1	92	16	2	11	1.41	1.56	6	1.75	15.875	11.3	13.703	9.7	0.9M	4.68	4.82	4.82	4.68	4.75	1.75	1.625	1.75	1.625	1.6875	b	10.0012	133.07	101	46620	131.96	85.301	1.8941
5	1	93	16	3	11	1.41	1.56	6	1.75	15.563	11	13.203	9.4	0.8M	4.77	4.75	4.77	4.75	4.76	1.8125	1.625	1.8125	1.625	1.7188	e	15.97	150.42	102.75	97178.87	146.75	96.422	2.1839
5	1	94	16	4	11	1.41	1.56	5	1.75	15.313	10.9	13.063	9.3	0.9M	4.75	4.69	4.75	4.69	4.72	1.8125	1.8125	1.8125	1.8125	1.8125	e	10.8604	142.79	100.5	98487.1	142.166	91.535	2.1071
5	1	95	16	5	11	1.41	1.56	0	1.75	15.375	10.9	13.219	9.4	0.9M	5.25	0	5.25	0	2.625	1.75	1.75	1.75	1.75	1.75	c	13.8764	150.07	101.9	98121.87	149.2	96.201	2.2056
5	1	96	16	6	11	1.41	1.56	0	1.75	15.125	10.7	12.75	9	0.8M	9.0625	0	9.06	0	4.5313	1.8125	1.75	1.8125	1.75	1.7813	b,d	15.97	138.76	99.5	73743.46	138	88.949	2.073
5	1	97	16	7	11	1.41	1.56	0	1.75	14.75	10.5	12.563	8.9	0.9M	9.25	0	9.25	0	4.625	1.75	1.8125	1.8125	1.75	1.7813	b	13.9977	123.58	100.5	19771.61	122.716	79.217	1.8931
5	2	98	16	1	11	1.41	1.56	6	1.75	16.125	11.4	13.125	9.3	0.8M	4.8	4.59	4.80	4.59	4.695	1.75	1.75	1.75	1.75	1.75	b	13.9635	123.14	100	24713	121.555	78.934	1.7255
5	2	99	16	2	11	1.41	1.56	6	1.75	15.875	11.3	12.844	9.1	0.8M	5.02	4.41	5.02	4.41	4.715	1.8125	1.75	1.8125	1.75	1.7813	b	10.4308	141.28	102.5	58648.11	139.899	90.565	2.011
5	2	100	16	3	11	1.41	1.56	6	1.75	16.125	11.4	13.031	9.2	0.8M	4.91	5.57	5.57	4.91	5.24	1.8125	1.75	1.8125	1.75	1.7813	e	15.97	144.46	102	102229.7	143	92.601	2.0243
5	2	101	16	4	11	1.41	1.56	6	1.75	16.438	11.7	13.406	9.5	0.8M	5.21	4.28	5.21	4.28	4.745	1.6875	1.8125	1.8125	1.6875	1.75	e	11.2041	142.26	99	91165.15	140.752	91.193	1.9556
5	2	102	16	5	11	1.41	1.56	0	1.75	16.688	11.8	13.625	9.7	0.8M	5.17	0	5.17	0	2.585	1.75	1.8125	1.8125	1.75	1.7813	e	13.9037	146.85	100.5	115369.4	145.411	94.132	1.9884
5	2	103	16	6	11	1.41	1.56	0	1.75	16.125	11.4	13	9.2	0.8M	9.1875	0	9.19	0	4.5938	1.6875	1.8125	1.8125	1.6875	1.75	e	15.97	150.76	102	78855.54	149.032	96.638	2.1126
5	2	104	16	7	11	1.41	1.56	0	1.75	16.063	11.4	13.125	9.3	0.8M	9.25	0	9.25	0	4.625	1.5625	1.875	1.875	1.5625	1.7188	b	14.0199	125.11	103	31877.18	123.3	80.196	1.7599
5	3	105	17	1	11	1.41	1.56	8.5	1.75	17.938	12.7	15.406	10.9	0.9M	6.9375	7.3125	7.31	6.9375	7.125	1.84	1.81	1.84	1.81	1.825	b,d	10.65	139.9	76.7	36697.9	138.9	89.679	1.7623
5	3	106	17	2	11	1.41	1.56	8.5	1.75	18.313	13	15.813	11.2	0.9M	7.375	6.9375	7.38	6.9375	7.1563	1.86	1.81	1.86	1.81	1.835	e	10.7456	144.21	83.24	58449.66	141.718	92.444	1.7794
5	3	107	17	3	11	1.41	1.56	8.5	1.75	18.188	12.9	15.513	11	0.9M	7.5	6.8125	7.50	6.8125	7.1563	1.76	1.82	1.82	1.76	1.79	e	10.8075	149.12	101.5	74409.82	147.834	95.587	1.8526
5	3	108	17	4	11	1.41	1.56	8.5	1.75	18.313	13	15.606	11.1	0.9M	7.375	6.8125	7.38	6.8125	7.0938	1.8	1.78	1.8	1.78	1.79	e	14.1768	143.06	88.1	103576.658	141.3	91.705	1.7652
5	4	109	18	1	11	1.41	1.56	8.5	3.75	15.594	11.1	12.344	8.8	0.8M	6.8125	7.3125	7.31	6.8125	7.0625	3.75	3.75	3.75	3.75	3.75	b,d	8.701	140.37	81.6	34560.42	139.2	89.978	2.0339
5	4	110	18	3	11	1.41	1.56	8.5	3.75	15	10.6	11.484	8.1	0.8M	7.0625	7.375	7.38	7.0625	7.2188	3.75	3.8125	3.8125	3.75	3.7813	e	12.568	149.74	NA	91581.74	148.591	95.987	2.2557
5	4	111	18	4	11	1.41	1.56	8.5	3.75	15.2	10.8	11.578	8.2	0.8M	7.125	7.0625	7.13	7.0625	7.0938	3.8125	3.625	3.8125	3.625	3.7188	e	12.568	149.58	101.7	83597.27	149.05	95.884	2.2236
6	1	112	19	1	11	1.41	1.56	6	2.75	16	11.3	13.641	9.7	0.9M	4.63	4.91	4.91	4.63	4.77	2.5625	2.875	2.875	2.5625	2.7188	b	9.548	123.62	56	27951	123.118	79.244	1.7458
6	1	113	19	2	11	1.41	1.56	6	2.75	16.156	11.5	13.797	9.8	0.9M	4.76	4.87	4.87	4.76	4.815	2.625	2.875	2.875	2.625	2.75	e	10.469	149.32	102.5	4916.6	148.386	95.715	2.0884
6	1	114	19	4	11	1.41	1.56	6	2.75	16	11.3	13.625	9.7	0.9M	4.64	5.27	5.27	4.64	4.955	2.875	2.75	2.875	2.75	2.8125	e	13.666	149.86	93	58059	141.77	96.062	2.1164
6	1	115	19	5	11	1.41	1.56	0	2.75	16.031	11.4	13.656	9.7	0.9M	0	5.23	5.23	0	2.615	2.875	2.6875	2.875	2.6875	2.7813	e	13.675	149.7	87	42552	148.578	95.962	2.1101
6	1	116	19	6	11	1.41	1.56	0	2.75	15.938	11.3	13.75	9.8	0.9M	0	9.125	9.13	0	4.5625	2.875	2.6875	2.875	2.6875	2.7813	b	10.035	137.58	87	32804	136.934	88.194	1.9506
6	1	117	19	7	11	1.41	1.56	0	2.75	15.625	11.1	13.438	9.5	0.9M	0	9.125	9.13	0	4.5625	2.6875	2.75	2.75	2.6875	2.7188	b	13.670	133.35	102	40946	132.496	85.482	1.9285
6	2	118	20	1	11	1.41	1.56	6	2.75	13.188	9.4	10.469	7.4	0.8M	4.89	4.601	4.89	4.601	4.7455	2.625	2.75	2.75	2.625	2.6875	b	10.865	96.99	43	2409	96.99	62.173	1.6619
6	2	119	20	2	11	1.41	1.56	6	2.75	13.438	9.5	10.578	7.5	0.8M	5.28	4.53	5.28	4.53	4.905	2.8125	2.625	2.8125	2.625	2.7188	c	11.426	143.51	101	49998	142.36	91.994	2.4132

Test Records

6	2	120	20	3	11	1.41	1.56	6	2.75	13.31	9.4	10.641	7.5	0.8M	4.73	4.745	4.75	4.73	4.7375	2.875	2.75	2.875	2.75	2.8125	e	12.222	148.7	102	57684	146.79	95.32	2.5245
6	2	121	20	4	11	1.41	1.56	6	2.75	13.313	9.4	10.625	7.5	0.8M	4.9485	4.5135	4.95	4.5135	4.731	2.8125	2.75	2.8125	2.75	2.7813	e	12.370	144.8	101	38996	141.264	92.819	2.4577
6	2	122	20	5	11	1.41	1.56	0	2.75	13.13	9.3	10.563	7.5	0.8M	0	5.0795	5.08	0	2.5398	2.875	2.875	2.875	2.875	2.875	c	11.190	120.47	103	27331	119.538	77.222	2.0732
6	2	123	20	7	11	1.41	1.56	0	2.75	13.19	9.4	10.531	7.5	0.8M	0	9.3125	9.31	0	4.6563	2.75	2.875	2.875	2.75	2.8125	c	11.691	96.9	43	2221	96.899	62.115	1.66
6	3	124	21	1	9	1.128	1	8.5	3.75	9.1563	8.1	6.6875	5.9	0.7M	7.375	7.375	7.38	7.375	7.375	3.5625	3.9375	3.9375	3.5625	3.75	b	12.330	86.277	69	27791	85.9193	86.277	2.6572
6	3	125	21	2	9	1.128	1	8.5	3.75	9.0938	8.1	6.8906	6.1	0.8M	7.25	7.25	7.25	7.25	7.25	3.625	3.875	3.875	3.625	3.75	b	13.193	98.55	68	51021	98.0975	98.55	3.056
6	3	126	21	3	9	1.128	1	8.5	3.75	9.25	8.2	6.9688	6.2	0.8M	7.25	7.625	7.63	7.25	7.4375	3.5625	4	4	3.5625	3.7813	-	12.602	96.172	66	75532	95.0493	96.172	2.9319
6	3	127	21	4	9	1.128	1	8.5	3.75	9.0625	8	6.7969	6	0.8M	7.25	7.25	7.25	7.25	7.25	3.5625	4	4	3.5625	3.7813	e	13.510	88.75	66	36815	88.2957	88.75	2.7617
6	4	128	22	1	9	1.128	1	8.5	1.75	11.125	9.9	8.2031	7.3	0.7M	7.1875	7.125	7.19	7.125	7.1563	1.75	1.8125	1.8125	1.75	1.7813	b	13.46	93.49	69	30905	93.36	93.49	2.3698
6	4	129	22	2	9	1.128	1	8.5	1.75	10.781	9.6	8.1094	7.2	0.8M	7.125	7.5	7.50	7.125	7.3125	1.75	1.8125	1.8125	1.75	1.7813	b	12.83	90.61	68	37038	90.265	90.61	2.37
6	4	130	22	3	9	1.128	1	8.5	1.75	11.13	9.9	8.44	7.5	0.8M	7	7.5	7.50	7	7.25	1.8125	1.8125	1.8125	1.8125	1.8125	d	12.77	89.24	69	25223	85.49	89.24	2.26